

**Similarities and variations of the enterobacterial chemotaxis
paradigm in *Sinorhizobium meliloti***

Alfred Agbekudzi

Dissertation submitted to the faculty of the Virginia Polytechnic Institute and State
University in partial fulfillment of the requirements for the degree of
Doctor of Philosophy
in
Biological Sciences

Birgit E. Scharf (Chair)

Clayton C. Caswell

Dorothea Tholl

Boris Vinatzer

December 7, 2023

Blacksburg, Virginia

Keywords: alfalfa, chemoattractant, chemoreceptor pentapeptide, chemotaxis
capillary assay, plant symbiont, sensory adaptation, two-component system

ABSTRACT

Sinorhizobium meliloti is a nitrogen-fixing endosymbiont of the legume *Medicago sativa* commonly known as alfalfa. It uses flagellar rotation and chemotaxis to seek roots of host plants to inhabit. This symbiosis serves as a great model system for studying biological nitrogen fixation and plant-microbe interactions. Since alfalfa brings enormous economic value to the USA, investments into the knowledge of the chemotaxis process that initiates symbiosis have the ability to mitigate deterioration of the environment and significantly increase food supply. The chemotaxis system in the enteric bacteria *Escherichia coli* is well studied and has been a great resource to understanding the process in other bacterial systems including our model organism *S. meliloti*.

This dissertation compares and contrasts the chemotaxis features in *E. coli* and *S. meliloti* and investigates their molecular functions. Based on the understanding gained so far, we attempt to offer plausible explanations for the underlying mechanisms of the *S. meliloti* chemotaxis pathway. Chapter 1 describes why biological nitrogen fixation is important for agriculture and the health of our environment. This chapter also sheds light on the symbiotic relationship between alfalfa and *S. meliloti*, which culminates in the formation of nitrogen fixing nodules. We expound on the chemotaxis systems in *E. coli* and other bacteria including *S. meliloti* and *Bacillus subtilis*.

In chapter 2, we compare the distribution of C-terminal pentapeptide-bearing receptors and the adaptation proteins that they tether in *E. coli* and *S. meliloti*. The stoichiometry data show that the ratio of pentapeptide-bearing chemoreceptors to chemotaxis protein (Che)R and CheB molecules are approximately 500- and 160-fold higher in *S. meliloti* than in *E. coli*, respectively. Since not all chemoreceptors in chemotactic bacteria have and utilize the pentapeptide moiety, we investigated the *S. meliloti* system and observed a strong interaction between CheR, activated

CheB and the isolated pentapeptides via *in-vitro* binding studies. On the contrary, unmodified CheB showed weak binding to the pentapeptide. Through *in-vivo* studies, we highlighted the physiological necessity of the pentapeptide for chemotaxis. *S. meliloti* strains with substitutions of the conserved tryptophan residue to alanine in one or all four pentapeptide-bearing Methyl-accepting Chemotaxis Proteins (MCPs) resulted in diminished or loss of chemotaxis to glycine betaine, lysine, and acetate, ligands sensed by pentapeptide-bearing McpX and pentapeptide-lacking McpU and McpV, respectively. The flexible linker connecting the pentapeptide to the MCPs together with the pentapeptide itself were shown to be functional on pentapeptide-lacking chemoreceptors and provided adaptational assistance to other chemoreceptors that lacked a functional pentapeptide. Based on these results, we concluded that *S. meliloti* employs a pentapeptide-dependent adaptation system with MCPs possessing a consensus pentapeptide motif (N/D)WE(E/N)F. Finally, we postulated that the higher abundance of CheR and CheB in *S. meliloti* compared to *E. coli* compensates for the lower number of pentapeptide-bearing chemoreceptors in the chemosensory array.

In chapter 3, we explored the putative phosphatase function of a novel protein, CheT, on phosphorylated *S. meliloti* response regulators. The kinase CheA phosphorylates both the sink response regulator, CheY1, and the flagellar motor interacting response regulator, CheY2. CheY1 competes with CheY2 for these phosphate groups, but we have discovered another layer of complexity to the story. Sequence comparison of *S. meliloti* CheT and the *E. coli* phosphatase CheZ shows little sequence homology. However, both proteins share a DXXXQ phosphatase motif. Phosphorylation assays performed using radiolabeled [γ - 32 P]-ATP revealed that CheT acts as a phosphatase of CheY1~P and accelerates dephosphorylation of CheY1~P by at least two-fold. Interestingly, we also discovered that CheT interacts with CheR, but this interaction did not affect

the enzymatic activity of either protein under the examined conditions. Unexpectedly, a *cheT* deletion strain and strains carrying mutations in the phosphatase motif exhibit an increased swimming speed, a phenotype that does not conform with the model that the absence of CheT or its activity results in increased CheY2~P levels and reduced swimming speed. We concluded that a revised *S. meliloti* signal termination pathway should include CheT enhancing dephosphorylation of CheY1~P and sensory adaptation involving the yet unknown function of CheT on CheR.

While the adaptation system in *S. meliloti* is unexplored, this work provides first insights into fascinating deviations and similarities to the known paradigm. We have also delivered evidence that the *S. meliloti* signal termination system requires a dedicated phosphatase. The knowledge gained here takes us a step closer to enhance the *S. meliloti* chemotaxis pathway towards improved symbiosis with alfalfa and to reduce our dependence on environmentally deleterious synthetic fertilizers.

GENERAL AUDIENCE ABSTRACT

Like all living things, bacteria inhabit a constantly changing environment, hence the need to take up and process this information. Bacterial cells have evolved sophisticated biological tools to tackle this challenge of detecting, responding and adapting to environmental signals like nutrients, toxins, temperature changes, light, metabolites, etc. Motile bacteria such as *Escherichia coli*, a gut resident microbe, and *Sinorhizobium meliloti*, a soil dwelling bacterium, direct their swimming behavior in response to chemical gradients within the milieu through a process termed chemotaxis. Generally, this vital process enables a bacterium to escape harmful chemicals and gravitate towards beneficial ones. However, *S. meliloti* specifically employs chemotaxis to locate the roots of its plant host (alfalfa) and to establish a symbiotic relationship through which the bacteria provide essential nitrogen for plant growth in exchange for nourishment. The biological tools employed by *S. meliloti* for chemotaxis include environmental sensing receptors called **Methyl-accepting Chemotaxis Proteins (MCPs)** and proteins inside the bacterial cell that transfer information from the sensors to long, helical rotating propeller structures, called flagella. Importantly, the efficiency of this process hinges on a timely termination of information flow and the ability to adapt to prevailing stimuli while maintaining sensitivity to increasing concentration gradients. This work investigates the function of the C-terminal five amino acid motif of MCPs known to be critical for adaptation in *E. coli* and the phosphatase activity of a novel protein, CheT, in signal termination of *S. meliloti* chemotaxis system.

DEDICATION

This work is dedicated to my family, especially the late Agbekudzi, and the first born of the Scharf lab, Seli Agbekudzi.

ACKNOWLEDGEMENTS

I celebrate this monumental achievement with all who have helped to lay the foundation for this moment. Thank you, mom, for finding the funds for my first-year college tuition. This feat wouldn't have been possible without that courageous decision you made. My mom always said, even though she could not make it far in your education, she would support her children as high as they wanted to go. I know you do not comprehend what I have been studying from college till date, but you have constantly encouraged me. Dad, I remember like yesterday, when you used to sit me on your lap and teach me grade school mathematics. At every stage of my education, you reminded me that there is a seat at the table for anyone who does their best. Your words have been proven true and will eternally remain with me even in your absence.

Ernesto, my brother, paving the way for you to follow has been a great motivation throughout my studies. I am impatiently waiting for you to enroll in a doctoral program soon. To Cecille Wendy Aboagye, thanks for the gift of Seli we share and the great care you and your family have given him. Seli, you are a delight to be with and I know you will do great things. To all my extended family, aunties, uncles, grandparents who chipped in resources here and there, I am very grateful! Dr. Scharf, can words truly describe my gratitude for the opportunity to be under your tutelage? From start to finish, you have believed in me and demonstrated genuine interest in my growth, well-being and academic progress. You knew when to push me out of my comfort zone and when to allow me to break my own shell. I have no regrets about choosing your lab, and I would do it all over again.

To Karl, Floricel, Tim, Richard, I am eternally indebted to you all since you guys taught me so much more than I gave back to you in the Scharf lab.

To my current lab members, Nate, Nisha, Foster (typical Ghanaian), Sharat, Abbey, Idella, past rotation students, thank you for your support and your kind words in difficult times. Your mere presence in the lab and at events we attended together made a big difference.

To my invaluable committee members, this feat is unachievable without your guidance, your attention to the details of my research. Boris, I won't be in Virginia Tech without you! I greatly appreciate your patience and disposition towards students. Indeed all TPSC students love you! Dr. Tholl, you gave me an opportunity to rotate in your lab and directed me to the Scharf lab. Thank you for constructive scrutiny of my research. Dr. Caswell, your exuberant spirit, your confidence and kindness I will emulate. Please keep checking in on us when you pass by LS1.

TABLE OF CONTENTS

Chapter 1: INTRODUCTION.....	1
REFERENCES.....	16
Chapter 2— Promiscuous but essential: The conserved C-terminal pentapeptide tether is required for <i>Sinorhizobium meliloti</i> chemotaxis regardless of chemoreceptor type	30
ABSTRACT	31
INTRODUCTION.....	32
RESULTS	36
DISCUSSION	43
MATERIALS AND METHODS.....	48
ACKNOWLEDGEMENTS	53
REFERENCES.....	54
Chapter 3— The novel <i>Sinorhizobium meliloti</i> chemotaxis protein CheT is a phosphatase for the sink response regulator and links signal termination and sensory adaptation.	71
ABSTRACT	72
INTRODUCTION.....	73
RESULTS	77
DISCUSSION	85
MATERIALS AND METHODS.....	89
ACKNOWLEDGMENTS.....	97
REFERENCES.....	112
Chapter 4— GENERAL DISCUSSION.....	119
REFERENCES.....	124

LIST OF FIGURES

Chapter 1

Fig. 1. 1 The various biological processes that constitute the nitrogen cycle.....	24
Fig. 1. 2 Initial signal exchange between the rhizobia and host legume.	25
Fig. 1. 3 A schematic of the symbiotic process between rhizobium bacteria and roots of legumes.	26
Fig. 1. 4 Two-component signal transduction pathways in bacteria.	27
Fig. 1. 5 An illustration of the architecture of an <i>E. coli</i> MCP.....	28
Fig. 1. 6 Signal transduction in <i>E. coli</i> from chemotaxis receptors (MCPs) to the flagellar motor.	29
Fig. 1. 7 Genetic organization of the <i>che1</i> operon in <i>S. meliloti</i>	29
Fig. 1. 1 The various biological processes that constitute the nitrogen cycle.....	24
Fig. 1. 2 Initial signal exchange between the rhizobia and host legume.	25
Fig. 1. 3 A schematic of the symbiotic process between rhizobium bacteria and roots of legumes.	26
Fig. 1. 4 Two-component signal transduction pathways in bacteria.	27
Fig. 1. 5 An illustration of the architecture of an <i>E. coli</i> MCP.....	28
Fig. 1. 6 Signal transduction in <i>E. coli</i> from chemotaxis receptors (MCPs) to the flagellar motor.	29
Fig. 1. 7 Genetic organization of the <i>che1</i> operon in <i>S. meliloti</i>	29

Chapter 2

Fig. 2. 1 Comparative features of the chemotaxis adaptation systems in <i>E. coli</i> (strain RP437 grown in minimal medium) and <i>S. meliloti</i>	62
Fig. 2. 2 An illustration of residues in the β -subdomain CheR that are important for the interaction with the MCP pentapeptide motif.	63
Fig. 2. 3 An illustration of residues in CheB that are important for the interaction with the MCP pentapeptide motif.	64
Fig. 2. 4 Binding of C-terminal MCP pentapeptides and their mutant variants to CheR.	66
Fig. 2. 5 Isothermal titration calorimetry of recombinant CheB and CheB-BeF ₃ ⁻ with pentapeptides.....	66
Fig. 2. 6 Chemotactic responses to 10 mM glycine betaine in the capillary assay for <i>S. meliloti</i> strains.	67
Fig. 2. 7 Chemotactic responses to 10 mM lysine in capillary assays for <i>S. meliloti</i> strains.	67
Fig. 2. 8 Chemotactic responses and relative abundance of McpU in mutant strains with C- terminal extensions.	68
Fig. 2. 9 Chemotactic responses to 1 mM acetate in capillary assays for <i>S. meliloti</i> strains.....	69
Fig. 2. 10 A summarized illustration of chemotaxis outcomes.	70

Chapter 3

Fig. 3. 1 Alignment of the amino acid sequence of <i>S. meliloti</i> CheT (NP_384751.1) with five paralogues from related alphaproteobacteria.	100
Fig. 3. 2 Structure prediction of <i>S. meliloti</i> CheT and comparison to <i>E. coli</i> CheZ.	101
Fig. 3. 3 Dephosphorylation of CheY1 and CheY2 in the presence of CheT.	102
Fig. 3. 4 Kinetics of CheY1~P dephosphorylation in the presence of CheT and its variants.	102
Fig. 3. 5 Isothermal titration calorimetry depicting the binding interaction.	103
Fig. 3. 6 Free swimming speeds of <i>S. meliloti</i> strains before and after the addition of the attractant proline.	104
Fig. 3. 7 . Biochemical analyses to assess the binding of <i>S. meliloti</i> CheT and CheR.	105
Fig. 3. 8 SEC-MALS analysis of CheT, CheR, CheT/CheR mixture and CheY1.	106
Fig. 3. 9 Kinetics of CheY1~P dephosphorylation in the presence of CheT and CheR in molar ratios of 1:1 and 1:3.	107
Fig. 3. 10 Time course of McpX methylation by CheR using [³ H]-S-adenosylmethionine (SAM[³ H]) as substrate.	108
Fig. 3. 11 McpX methylation by CheR using [³ H]-S-adenosylmethionine (SAM[³ H]) as substrate with various supplements.	109

LIST OF TABLES

Chapter 1

Table 1.1. Selected rhizobial species and their symbiotic hosts.	23
---	----

Chapter 2

Table 2.1. A comparison of MCPs with pentapeptide in <i>E. coli</i> and <i>S. meliloti</i>	60
Table 2.2. Bacterial strains and plasmids.....	60

Chapter 3

Table 3.1 Bacterial strains and plasmids.....	98
---	----

Chapter 1: INTRODUCTION

Nitrogen and nitrogen fixation in Rhizobia

Nitrogen is an indispensable chemical element that supports life on earth. Its necessity is evidenced by the need for nitrogen in the synthesis of essential biomolecules such as proteins and nucleic acids. Although nitrogen gas (N_2) is the most copious gas on earth, it is largely bio-unavailable because it is inert [1, 2]. The process of converting N_2 into biologically usable forms like ammonia (NH_3) is termed nitrogen fixation. Nitrogen fixation is fundamental to earth's nitrogen cycle as it enables organisms to transform nitrogen gas into many different forms for growth and energy needs. The major alterations of nitrogen are made possible via nitrification, nitrogen fixation, ammonification, anammox, and denitrification (Fig. 1.1) [3]. N_2 fixation mainly occurs in three different ways: through lightning, the industrial Haber–Bosch process, or the biological action of the nitrogenase enzyme in certain microorganisms [1]. Biological nitrogen fixation can happen in free-living or symbiotic diazotrophs [4]. The latter occurs via symbiosis between plants called legumes and nitrogen fixing bacteria called rhizobia [4]. This plant-microbe relationship is the focus of intense research due to its profound ecological, economic and agronomic benefits.

Ancient and modern agriculture has heavily relied on legumes for human nutrition, forage, and environmental and ecological needs. Legume cultivation occupies 12-15% of earth's arable land [5]. Legumes can be broadly categorized based on their use as grain and forage/pasture legumes [5]. Grain legumes include soybean, chickpea, and cowpea, while examples of forage legumes are red clover, sweet clover, and alfalfa.

***Medicago sativa* and *Sinorhizobium meliloti* symbiosis**

Alfalfa, also known as *Medicago sativa*, is a perennial herb characterized by compound leaves made up of three leaflets, tiny flowers that often are yellow, bluish-violet, or white and an extensive taproot [6]. In the US, 23 million acres of alfalfa are grown annually with Colorado, California, Nebraska South Dakota, Wisconsin, Minnesota, Montana, Idaho, Kansas, and Iowa, being the largest growers [7]. Alfalfa production in the US generates \$8 billion, making it third in revenue behind corn (first) and soybean (second), without accounting for its value in the production of dairy goods [7-9]. Alfalfa has broader benefits besides being mainly cultivated as a forage crop or harvested as hay bales to be used as animal feed. It is also included in crop rotation programs to replenish nitrogen that had been used up from the soil by other crops. The nitrogen replenishing ability and high protein content of alfalfa is conferred by its unique symbiotic interaction with rhizobia.

Rhizobia are rod-shaped gram-negative bacteria, that are motile using flagella for locomotion [10]. They can exist as free-living soil saprophytes or in a nitrogen-fixing symbiosis with most legumes [10]. When not in association with a host plant, they can be found on root surfaces or in the rhizosphere in response to nutrient excretions from the host plant [10]. On the other hand, a free-living rhizobium can infect a compatible host through a series of processes, which culminates in the bacteria inducing the production of and inhabiting specialized plant organs called nodules. Rhizobia belong to the genera *Azorhizobium*, *Rhizobium*, *Mesorhizobium*, *Sinorhizobium*, and *Bradyrhizobium*.

One rhizobial species of intensive research across the world is *Sinorhizobium meliloti* (previously *Rhizobium meliloti*), a soil-dwelling, Gram-negative α - proteobacterium that forms a symbiotic relationship with leguminous plants from the genera, *Melilotus*, *Trigonella* and *Medicago spp.* [11, 12] (Table 1). The sequenced genome of *S. meliloti* 1021 is composed of a 3.65 Mbp chromosome

and two symbiotic megaplasmids, pSymA (1.36 Mbp) and pSymB (1.68 Mbp) respectively [13]. Plasmids of diverse sizes known as non-pSym or cryptic plasmids, which are highly active in mediating conjugation, have been reported to be present in some strains [14, 15]. The symbiotic plasmids bear genes essential for the making a functioning symbiotic nodule in the host [16]. pSymA harbors *nod*, *nif*, and *fix* genes required for nodulation, nitrogenase synthesis, and nitrogen fixation, respectively. They also possess genes for transport of metabolites, carbon and nitrogen metabolism pathways, and stress and resistance responses that contribute to the viability of *S. meliloti* in natural and specialized habitats [17]. It is thought that pSymA might have been horizontally acquired due to its lower GC content (60.4%) compared to the chromosome and pSymB (62.4%) [13, 18].

Conversely, pSymB encodes enzymes involved in surface polysaccharide synthesis, interaction with the legume host, and uptake of various solutes and nutrients [16]. Unlike pSymA, pSymB has chromosomal features, which includes the presence of housekeeping genes like the asparagine-synthetic pathway genes, the arginine tRNA encoding gene, and the *minCDE* cell division genes [17].

Infection process upon interaction with cognate host

Plants, through exudates, influence the type, composition, and structure of the microbial community of the soil surrounding their roots [19]. The spectrum of plant root exudates may attract or ward off different microbial species. In the case of legume-rhizobia interactions, low bioavailable nitrogen in the soil results in legume rhizodeposition of phenolic compounds like flavonoids (2-phenyl-1,4-benzopyrone derivatives) [19, 20]. These chemical compounds serve as the initial signal that is sensed by the rhizobia and triggers the transcriptional regulator Nodulation

protein D (NodD), which activates the transcription of rhizobial nodulation genes. *S. meliloti* for example, has three *nodD* genes (*nodD1*, *nodD2*, *nodD3*) (Fig. 1.2) [20]. It has been found that the alfalfa-derived flavonoid luteolin causes the transcription of *S. meliloti nod* genes when bound to NodD1 [21]. This process serves as a first screen for compatibility between the symbiotic partners as non-host derived flavonoids cannot activate the transcription of *S. meliloti nod* genes [21].

A second phase of the legume-rhizobia interaction occurs when bacterial Nod proteins synthesize lipochitooligosaccharide Nod factors (Fig. 1.2) [22]. The backbone of Nod factors consist of β -1,4-linked N-acetyl-D-glucosamine residues and can be modified to influence host specificity [20]. Secreted bacterial Nod factors that bind to root cells receptors stimulate plant responses in preparation for bacterial invasion. These responses include reinitiation of mitosis in root cortex cells to eventually form the nodule primordium; a group of cells that houses the incoming bacteria [23]. Concomitant alteration of root hair cytoskeleton and spiking calcium levels lead to root hair curling, which confines the adhered rhizobia into a structure called the shepherd's crook [24].

Infection thread formation and life in the nodules

The production of Nod factors and symbiotically-active exopolysaccharide from the entrapped bacteria can stimulate the progressive extension of the root hair cell membrane resulting in the formation of the infection thread [24]. The bacteria invade the interior plant tissue through this thread (Fig. 1.3). In *S. meliloti*, exopolysaccharides (EPS), succinoglycan (EPSI) and galactoglucan (EPSII) have been implicated in facilitating the infection thread formation [25, 26]. The infection thread progressively grows through the cortical cells as rhizobia proliferate around the tip [19]. The infection thread eventually forms many branches to effectively colonize as many nodule cells as possible [23].

In developing indeterminate nodules, that have a continually dividing meristem, infection threads make their way past the meristematic region and invade the underlying cell that are no longer actively dividing [27]. The specific feature of these cells is their polyploidy nature due to genomic endoreduplication without cytokinesis [28, 29]. The higher transcription and metabolic rate in polyploid cells compared to cells with normal DNA content may be required for the nodule cells to host bacteria and support bacterial nitrogen fixation [23, 29]. At the inner plant cortex, a bacterial cell gets taken up by a cortical cell into a compartment consisting of the individual bacterium surrounded by a plant-derived endocytic membrane [30]. This unit is called the symbiosome [23].

The symbiosome of indeterminate nodules differs from determinate nodules. In the former the encapsulating plant membrane and the bacterium divide simultaneously prior to differentiation into nitrogen-fixing bacteroids, whereas in the latter, bacteria multiply inside the membrane compartment and form a group of cells [31]. Bacterial and host factors act in concert to ensure the survival and differentiation of the bacteroids. For example, the host plant imposes genome endoreduplication on the enclosed bacterial cells [27]. This enables bacteroids within indeterminate nodules to expand their cell size and genome content, for the purpose of sufficiently meeting the metabolic requirements of nitrogen fixation [27, 32]. In addition, the host provides nourishment and modulates the anaerobic environment required for nitrogen fixation through the action of leghemoglobin [23]. Leghemoglobins are plant-synthesized, oxygen-binding proteins, responsible for the red color of functional root nodules [33].

The bacteria, on the other hand, produce lipopolysaccharide (LPS), which is a key part of the outer membrane. It is made up of a membrane anchored lipid A attached to a sugar molecule and an O-antigen repeating unit [34]. The *bacA* gene in *S. meliloti* is required to produce the appropriate

lipid A moiety for survival inside the plant cell [35, 36]. *bacA* mutants have been shown to lyse after endocytosis and do not differentiate [35].

The anaerobic environment of the symbiosome activates the microaerobic respiratory enzymes and nitrogenase complex expression, which provide reductants and energy for nitrogen fixation [37]. During this process, other metabolic processes are downregulated while simultaneous expression of the genes involved in respiration and nitrogen fixation are elevated [37]. The nitrogenase enzyme catalyzes the respiratory activity below [38];



The NH_4^+ that is produced is secreted by bacteroids through NH_4^+ channels and then assimilated into host cells primarily via asparagine and glutamine synthetases [39]. Carbon is continuously provided by the plant to generate metabolites and energy for bacteroid differentiation and nitrogen fixation. Plant-derived dicarboxylic acids, such as malate, serve as fixed carbon that is transported into the bacterial cell via the Dct uptake system [38, 40]. This indicates that the production of acetyl-CoA from malate using malate synthase and pyruvate dehydrogenase is important for the provision of carbon into the citric acid cycle in bacteroids [38].

Signal transduction in bacterial chemotaxis

Chemotaxis is sensing chemical gradients and responding through directed movement towards beneficial environments and escaping harm. Its effectiveness hinges on recognition of environmental signals and signal transduction across the cell membrane to trigger the appropriate cellular response. The process of chemotaxis is carried out by a specialized two-component signaling system.

Bacterial, two-component systems (TCS) mediate the transduction of extracellular signals into intracellular output, mainly through differential gene expression or protein-protein interactions [41]. The key proteins involved in bacterial two-component systems include the transmembrane sensor histidine kinase and the cytosolic response regulator (RR) [41]. The transmembrane sensor kinase typically has a periplasmic or extracellular domain that detects remarkably diverse cues like temperature, toxins, nutrients, light, and cell density by direct ligand binding or indirectly via ligand bound proteins [42]. These interactions trigger the autophosphorylation of a conserved His residue of the HisKA domain and the subsequent phosphoryl group transfer to a conserved Asp residue within the conserved N-terminal receiver domain (REC) of the RR [42]. The effector domains of the RR show an enormous diversity in executing their output. While some bind DNA to regulate transcription, others are RNA-binding, enzymatically active, or protein-binding (Fig. 1.4) [41].

Chemotaxis in motile bacteria

Bacterial chemotaxis is a specialized example of a TCS pathway that allows movement of bacterial cells in response to a chemical gradient. It enables bacteria to move towards an attractant and move away from a repellent. In addition, chemotaxis provides bacteria with competitive fitness by allowing them to swim to, locate at, and colonize niches that best support their growth and survival. Bacterial locomotion occurs in different forms. While swimming and swarming motility is powered by flagella rotation through liquid or on surfaces, respectively, Type IV pili are typically used for twitching and gliding motility [43]. Swimming motility is animated via alternating ‘runs’ and ‘tumbles’ [44]. Runs are relatively long straight motions, while tumbles are short, random, reorienting turns. By regulating the incidence of runs and tumbles, the bacteria move towards the intended direction, termed as a ‘biased random walk’[44].

The chemotaxis machinery of *Escherichia coli* has been studied for its regulation of flagellar motility [42, 45-48]. In the *E. coli* chemotaxis system, a histidine kinase, CheA, is coupled by a scaffold protein, CheW, to transmembrane chemoreceptor proteins termed methyl-accepting chemotaxis proteins (MCPs). *E. coli* MCPs have a ligand binding domain that varies with its stimulatory ligand, two transmembrane domains, and a highly conserved cytoplasmic domain [49]. The cytoplasmic domain possesses three subdomains, namely, (1) the HAMP domain that links the transmembrane domain to the cytoplasmic domain, (2) the methylated helices 1 (MH1) and methylated helix 2 (MH2) domains, and (3) the signaling domain (Fig. 1.5) [50]. Input signals of the chemotaxis pathway are recognized through interaction with the ligand binding domain of the MCP and transduced through a conformational change to CheA, which interacts with the signaling domain [51]. CheA autophosphorylates and subsequently phosphorylates the chemotaxis response regulator, CheY. CheY dissociates from CheA upon phosphorylation and moves to the flagellar motors, where it triggers a switch from counterclockwise to clockwise rotation and tumbling (Fig. 1.6) [52-54]. Thus, an attractant binding represses tumbles by binding to chemoreceptors to inactivate CheA kinase activity, thus decreasing phosphorylated-CheY (CheY~P) [55]. The cellular level of CheY~P is regulated through three cytosolic enzymes: directly through the CheY-specific phosphatase CheZ and indirectly through two receptor-modifying enzymes CheR (methyltransferase) and CheB (methyl-esterase) [50]. While CheY possesses autophosphatase activity, CheZ enhances the rate of CheY~P dephosphorylation by about 10-fold to rapidly reset the system [56, 57]. Methylation changes on ligand-bound chemoreceptors by CheR and CheB adjust the signaling event and results in adaptation to an existing chemical stimulus [42].

Chemotaxis in *S. meliloti*

In the *S. meliloti*-alfalfa relationship, chemotaxis towards the appropriate host exudates is critical for establishing symbiosis. The molecular underpinnings of the chemotaxis pathway in *S. meliloti* parallels the *E. coli* chemotaxis pathway in many ways but also possesses some exceptions. In contrast to the enteric bacteria, *S. meliloti* has two response regulators, CheY1 and CheY2 but no CheZ phosphatase for signal termination. Here, CheY2~P serves as the motor response regulator that can retro-transfer phosphoryl groups to a CheA/CheS complex and passed on to CheY1, a phosphate sink [58-61]. Also, proteins unique to the *S. meliloti* chemotaxis system are encoded from the chemotaxis operon *cheI*. The *cheI* operon is part of the flagellar regulon, which is a long, contiguous cluster of chemotaxis (*che*), flagellar synthesis (*fla*), and motility (*mot*) genes in one 56-kb region of the chromosome [62, 63]. The *cheI* operon is made up of ten genes that express the core and auxiliary chemotaxis proteins such as CheD, a putative deamidase, CheS, a binding partner of CheA that mediates phosphate transfer from CheA to CheY1, and CheT, a protein of unknown function (Fig. 1.7) [13, 60, 64]. Lastly, *E. coli* possesses five MCPs, namely Tar, Tsr, Trg, Tap, and the cytosolic Aer, for detecting various signals through direct or indirect binding [65-67]. In comparison, *S. meliloti* has eight chemoreceptors, namely McpT through McpZ, and IcpA that transduce signals to chemotaxis proteins [68].

Chemoreceptors and their cognate ligands

The analysis of bacterial genomes with chemosensory signaling proteins shows that there are an average of 14 chemoreceptors and a maximum of 80 chemoreceptors, which are identifiable by the conserved cytosolic domain [69-71]. An increasing number of chemoreceptors correlates with complexity of bacteria lifestyles, the inhabited niche and metabolism needs for carbon and nitrogen resources [72, 73]. To sense a diverse array of environmental signals, bacteria have evolved

chemoreceptors with different ligand-binding domains (LBDs) that possess the ability to detect a wide spectrum of cues to enhance their survival. However, functional annotation of chemoreceptors have been severely hindered by the redundancy in multiple receptors binding the same ligand [70]. A crucial bioinformatics bottleneck is the difficulty in deducing the function of chemoreceptors as LBDs have high sequence divergence from their homologues. Amid these limitations, characterized LBDs of chemoreceptors across several species have been categorized into four structural families, namely, the 4-helix bundle (4HB) domain family, the single calcium channels and chemotaxis receptors (sCACHE) domain family, the double CACHE (dCACHE) domain family, and the helical bimodular (HBM) domain family [70]. The well-studied *E. coli* Tar and Tsr receptors, which directly sense aspartate and serine, respectively, typify the 4HB LBD [74-76]. Other 4HB-domain containing receptors involved in direct ligand binding include *S. meliloti* McpT, *P. aeruginosa* CtpH, *S. typhimurium* Tcp , and *Pseudomonas putida* PcaY, which recognize a broad range of carboxylates, inorganic phosphate, citrate and citrate/metal ion complexes, and carboxylic acids, respectively [76-79]. Indirect binding involving 4HB-domain containing chemoreceptors have been demonstrated in Trg attractant responses to sugars like ribose and galactose [80] and Tap perception of pyrimidines and dipeptides [81, 82]. The single Per/Arnt/Sim (PAS) domains of extracytosolic space are termed as sCACHE domains. These include TlpB-LBD of *Helicobacter pylori*, which directly senses gastric urea, and McpP of *P. putida* KT2440, which binds C2 and C3 carboxylic acids like acetate, propionate pyruvate, and L-lactate [83, 84]. Also, the periplasmic region of *S. meliloti* chemoreceptor McpV, which directly senses short-chain carboxylates, contains a sCACHE domain [85]. The helical bimodular (HBM) domain comprising two 4HBs was first identified in the McpS chemoreceptor of *P. putida* KT2440, while investigating its chemotaxis toward acetate and TCA cycle intermediates [71, 86]. The dCACHE domain is

thought to have originated from sCACHE domains as they are made up of two sCACHE domains; a ligand binding membrane distal and proximal module [87, 88]. The dCACHE domains make up the largest family of extracytoplasmic amino acids sensor domains in diverse species. This includes McpU and McpX in *S. meliloti*, McpA in *P. putida* KT2440, Tlp3 in *Campylobacter jejuni*, and Mlp37 in *Vibrio cholerae* [89-93]. Alternative classification by the size of chemoreceptor LBDs groups them into cluster 1 and cluster 2 with approximately 150 residues and 250 residues respectively [69].

The chemotaxis adaptation system in diverse bacterial species

The key players of the adaptation system in *E. coli* mainly involves CheR, CheB and the chemoreceptors. CheR and CheB are anchored to the receptor cluster by a conserved C-terminal pentapeptide (NWETF), preceded by a flexible linker, to enable access to the conserved glutamyl residues located at the methylation helices [94, 95] (Fig. 1.5) The sensory adaptation system re-establishes pre-stimulus CheA activity, after changes in ligand residency generate structural changes in receptor molecules [96-98]. This results in an equilibrium shift of the ternary complex (receptor-CheW-CheA dimer) from an ON to an OFF state or from an OFF to an ON state [99]. Thus, receptors are preferentially methylated by *E. coli* CheR in the OFF state in the presence of an attractant and preferentially demethylated and deamidated by CheB in the ON-state when an attractant is removed or a repellent is added [99]. CheB and CheR bound to the C-terminal pentapeptide are also mediating covalent modifications of the neighboring chemoreceptors [100]. Li and Hazelbauer further demonstrated that CheR- and CheB-catalyzed reactions on receptors lacking the pentapeptide (Trg) are significantly enhanced by the presence of receptor-bearing (Tar) or a variant Trg receptor with the C-terminal 19 amino acid residues of Tsr, including the flexible

linker and the pentapeptide, C-terminally fused to Trg [101, 102]. The adaptation assistance provided by Tar transcending to adjacent trimers of homodimers is modelled to aid the demethylation and methylation of five and seven bordering Trg dimers, respectively [101].

On the contrary, *B. subtilis* chemoreceptors lack the C-terminal pentapeptide tether. Instead, adaptation is achieved via three mechanisms that work in concert to ensure a robust chemotaxis system [100, 103]. Noticeably, methylation and demethylation of specific glutamyl sites on the same MCP modifies kinase activity without altering the net level of methylation [104]. While the functions of CheR and CheB are conserved, the MCPs are initially demethylated and then remethylated in the continued presence of an attractant or repellent [105]. *B. subtilis* possesses two CheY~P phosphatases, CheC and FliY [106]. CheC binds to CheY~P when concentrations are high and increases affinity for CheD resulting in the formation of CheD/CheC/CheY~P complex. Through this complex, CheC acts as an indirect regulator of adaptation by sequestering CheD, which binds to the receptors and promotes CheA autokinase activity. The CheC/CheD interaction decreases CheA activity in addition to reducing CheY~P concentration through its phosphatase activity [104]. *B. subtilis* CheV has an N-terminal CheW-like protein and a C-terminal REC domain for receiving phosphoryl groups from CheA~P [107]. CheV~P downregulates CheA autokinase function by an unknown mechanism, resulting in a feedback inhibition. CheV was shown to possess a dual role depending on the modification state of the receptors. When receptors are unmethylated, it functions to amplify the detected signal. On the other hand, when the receptors are methylated, CheV is involved in sensory adaptation [108].

Stoichiometry of bacterial chemotaxis proteins

Knowledge of stoichiometries of chemotaxis protein systems in *E. coli*, *B. subtilis*, and *S. meliloti* have shown great variations and have been vital to our understanding of the dynamics in bacterial chemotaxis. Quantification of chemotaxis proteins in *S. meliloti* displayed a lower number of molecules than in *E. coli* and *B. subtilis*. This has been attributed to the smaller cell size and the fact that less than half of the cell population expressed the chemotaxis molecules in the conditions tested. For instance, a *S. meliloti* cell possesses 423 chemoreceptors, while *E. coli* and *B. subtilis* expressed 59,960 and 26,000 chemoreceptor molecules, respectively [109-111]. However, the ratio of MCP to CheA dimer was observed to be 37:1 in *S. meliloti*, 24:1 in *B. subtilis*, and 3.4:1 in *E. coli*, suggesting that *S. meliloti* and *B. subtilis* have more features in common than with *E. coli*. Nonetheless, *B. subtilis* chemoreceptors do not have C-terminal pentapeptides for tethering CheR and CheB while 93% and 13% of receptors *E. coli* and *S. meliloti* bear the C-terminal pentapeptide motif, namely *E. coli* Tar and Tsr, and *S. meliloti* McpW, McpX, McpY, and McpT. The CheR to CheA dimer ratio in *S. meliloti* is 100-fold greater than in *B. subtilis* and 500-fold greater than in *E. coli* [112]. In addition, the ratio of CheB monomers to CheA dimer is 6-fold and 30-fold higher than in *B. subtilis* and *E. coli*, respectively. The receptor deamidase CheD is shared by *B. subtilis* and *S. meliloti* but not *E. coli* [62, 103]. The CheD ratio to a CheA dimer is approximately 50-fold greater in *S. meliloti* than in *B. subtilis*. Furthermore, the ratio of CheY2, the motor controlling response regulator, to the CheA dimer is approximately 20- and 40-fold higher in comparison to *B. subtilis* or *E. coli*, respectively [58, 112]. Comparison of signal termination proteins reveals that ratios of phosphatase to CheA dimer were similar for CheC in *B. subtilis* and CheZ dimer in *E. coli* (0.3 and 0.5), while *S. meliloti* CheY1 had a monomer to CheA dimer ratio of 90. Noticeably, ratios of each chemotaxis protein homologue per CheA dimer is higher in *S. meliloti* than in *E. coli* and *B. subtilis*, but the ratios of CheB to CheR in *S. meliloti* (0.4), *E. coli* (1.7), and *B. subtilis* (1.9)

are similar. Thus, these many variations attest to the deviation in mechanisms employed for adaptation and signal termination in these species.

Motivation

Every frontier of *S. meliloti* chemotaxis that has been explored revealed fascinating differences from known chemotaxis paradigms. Studies of chemoreceptor stoichiometry revealed that *S. meliloti* has fewer molecules than *B. subtilis* and *E. coli*, however, the chemotaxis proteins to CheA dimer ratio is higher in *S. meliloti*. The C-terminal pentapeptide tethering motif is localized to low and moderately expressed chemoreceptors in *S. meliloti* but located on high abundance chemoreceptors in *E. coli*. Signal termination mechanisms are vastly different as *S. meliloti* utilizes retrophosphorylation from the motor RR CheY2 to CheA and complexation of CheA and CheS to enhance phosphorylation of the sink RR CheY1. On the other hand, dedicated phosphatases directly contribute to the hydrolysis of active RR as demonstrated in *E. coli* and *B. subtilis*. Last but not least, the flagellar motors of *S. meliloti* operate differently from other species. While several research groups have made steady strides towards obtaining a holistic view of the *S. meliloti* chemotaxis, significant knowledge gaps still exist. These includes: 1. What is the function of the C-terminal pentapeptide situated on less abundant chemoreceptors? 2. How do the estimated stoichiometries of chemosensory proteins in *S. meliloti* influence chemotaxis? 3. What is the function of the novel protein CheT, which has no homology to any known chemotaxis protein? 4. What is the function of the putative CheD deamidase? 5. What is the role CheR and CheB in adaptation? In this work, new discoveries were made in our attempts to address these questions.

In chapter 2, we found that *S. meliloti* CheR and activated CheB had strong affinities to C-terminal pentapeptides of McpX, McpW, McpY and McpT while CheB binding is ten-fold weaker. Chemotaxis assays showed that mutations in the conserved tryptophan in one or all four MCP pentapeptides negatively affects chemotactic response to the chemoeffectors tested. More importantly, we discovered that the pentapeptide in conjunction with a flexible linker indiscriminately mediates chemotaxis when fused to the C-terminus of pentapeptide-lacking chemoreceptors such as McpU and McpV. In chapter 3 we discovered CheT functions in *S. meliloti* signal termination as a phosphatase of CheY1~P by binding and enhancing the dissipation of the sink phosphatase. In addition, CheT binds to CheR and exhibits a phenotype reminiscent of adaptation null mutants in swimming velocity assays.

We are highly encouraged by these findings as this gets our research a step closer to our translational goal of leveraging bacterial chemotaxis in a legume endosymbiont to make better inoculants for higher yields and a more sustainable environment.

REFERENCES

1. Hoffman, B.M. et al. 2014. Mechanism of nitrogen fixation by nitrogenase: the next stage. *Chemical Reviews*, 114(8): 4041-4062.
2. Jia, H.P., Quadrelli, E.A. 2014. Mechanistic aspects of dinitrogen cleavage and hydrogenation to produce ammonia in catalysis and organometallic chemistry: relevance of metal hydride bonds and dihydrogen. *Chemical Society Reviews*, 43(2): 547-564.
3. Bernhard, A. 2010. The nitrogen cycle: processes, players, and human impact. *Nature Education Knowledge*, 3(10): 25.
4. Smercina, D.N. et al. 2019. To fix or not to fix: controls on free-living nitrogen fixation in the rhizosphere. *Applied and Environmental Microbiology*, 85(6): e02546-18.
5. Graham, P.H., Vance, C.P. 2003. Legumes: importance and constraints to greater use. *Plant Physiology*, 131(3): 872-877.
6. Hanson, A. Alfalfa and alfalfa improvement. *Agronomy Monographs*, 1.
7. Fernandez, A.L., Sheaffer, C.C., Tautges, N.E., Putnam, D.H., and Hunter, M.C. 2019. Alfalfa, wildlife, and the environment. National Alfalfa and Forage Alliance.
8. Yost, M., Allen, N., Creech, E., Putnam, D., Gale, J. and Shewmaker, G., 2020. Ten Reasons Why Alfalfa is Highly Suitable for the West.
9. Putnam, D. and Meccage, E. 2022. Profitable alfalfa production sustains the environment. in *Proceedings. World Alfalfa Congress*.
10. Somasegaran, P. and Hoben, H.J., 2012. *Handbook for rhizobia: methods in legume-Rhizobium technology*. Springer Science & Business Media.
11. Hirsch, A.M., Lum, M.R., Downie, What makes the rhizobia-legume symbiosis so special? *Plant physiology*, 127(4): 1484-1492.
12. Stacey, G. The *Rhizobium*-legume nitrogen-fixing symbiosis. *Biology of the Nitrogen Cycle*. Elsevier. 147-163.
13. Galibert, F., Finan, T.M., Long, S.R., Pühler, A., Abola, P., Ampe, F., Barloy-Hubler, F., Barnett, M.J., Becker, A., Boistard, P. and Bothe, G., 2001. The composite genome of the legume symbiont *Sinorhizobium meliloti*. *Science*, 293(5530), 668-672.
14. Pistorio, M., Del Papa, M.F., Balagué, L.J. and Lagares, A., 2003. Identification of a transmissible plasmid from an Argentine *Sinorhizobium meliloti* strain which can be mobilised by conjugative helper functions of the European strain *S. meliloti* GR4. *FEMS Microbiology Letters*, 225(1), 15-21.
15. Pistorio, M., Giusti, M.A., Del Papa, M.F., Draghi, W.O., Lozano, M.J., Torres Tejerizo, G. and Lagares, A., 2008. Conjugal properties of the *Sinorhizobium meliloti* plasmid mobilome. *FEMS Microbiology Ecology*, 65(3), 372-382.
16. Schwartz, E. ed., 2009. *Microbial megaplasmids (Vol. 11)*. Springer Science & Business Media.
17. Barnett, M.J., Fisher, R.F., Jones, T., Komp, C., Abola, A.P., Barloy-Hubler, F., Bowser, L., Capela, D., Galibert, F., Gouzy, J. and Gurjal, M., 2001. Nucleotide sequence and predicted functions of the entire *Sinorhizobium meliloti* pSymA megaplasmid. *Proceedings of the National Academy of Sciences*, 98(17), 9883-9888.
18. Peixoto, L., Zavala, A., Romero, H. and Musto, H., 2003. The strength of translational selection for codon usage varies in the three replicons of *Sinorhizobium meliloti*. *Gene*, 320, 109-116.
19. Clúa, J., Roda, C., Zanetti, M.E. and Blanco, F.A., 2018. Compatibility between legumes and rhizobia for the establishment of a successful nitrogen-fixing symbiosis. *Genes*, 9(3), 125.

20. Perret, X., Staehelin, and Broughton, Molecular basis of symbiotic promiscuity. *Microbiology and Molecular Biology Reviews*, 64(1180-201).
21. Peck, M.C., Fisher, R.F. and Long, S.R., 2006. Diverse flavonoids stimulate NodD1 binding to nod gene promoters in *Sinorhizobium meliloti*. *Journal of Bacteriology*, 188(15), 5417-5427.
22. Oldroyd, G.E. and J.A Calcium, kinases and nodulation signalling in legumes. *Nature Reviews Molecular Cell Biology*, 5(7 566-576).
23. Jones, K.M., Kobayashi, H., Davies, B.W., Taga, M.E. and Walker, G.C., 2007. How rhizobial symbionts invade plants: the *Sinorhizobium*–*Medicago* model. *Nature Reviews Microbiology*, 5(8), 619-633.
24. Gage, D.J., 2004. Infection and invasion of roots by symbiotic, nitrogen-fixing rhizobia during nodulation of temperate legumes. *Microbiology and Molecular Biology Reviews*, 68(2), 280-300.
25. Glazebrook, J. and Walker, G.C., 1989. A novel exopolysaccharide can function in place of the calcofluor-binding exopolysaccharide in nodulation of alfalfa by *Rhizobium meliloti*. *Cell*, 56(4), 661-672.
26. Pellock, B.J., Cheng, H.P. and Walker, G.C., 2000. Alfalfa root nodule invasion efficiency is dependent on *Sinorhizobium meliloti* polysaccharides. *Journal of* , 182(15), 4310-4318
27. Mergaert, P., Uchiumi, T., Alunni, B., Evanno, G., Cheron, A., Catrice, O., Mausset, A.E., Barloy-Hubler, F., Galibert, F., Kondorosi, A. and Kondorosi, E., 2006. Eukaryotic control on bacterial cell cycle and differentiation in the *Rhizobium*–legume symbiosis. *Proceedings of the National Academy of Sciences*, 103(13), 5230-5235
28. Cebolla, A., Vinardell, J.M., Kiss, E., Olah, B., Roudier, F., Kondorosi, A. and Kondorosi, E., 1999. The mitotic inhibitor ccs52 is required for endoreduplication and ploidy-dependent cell enlargement in plants. *The EMBO journal*, 18(16), 4476-4484.
30. Brewin, N.J., 2004. Plant cell wall remodelling in the *Rhizobium*–legume symbiosis. *Critical Reviews in Plant Sciences*, 23(4), 293-316.
31. Prell, J. and P. Poole, Metabolic changes of rhizobia in legume nodules. *Trends in Microbiology*, 2006. 14(4), 161-168.
32. Galitski, T., Saldanha, A.J., Styles, C.A., Lander, E.S. and Fink, G.R., 1999. Ploidy regulation of gene expression. *Science*, 285(5425), 251-254.
33. Ott, T., van Dongen, J.T., Gu, C., Krusell, L., Desbrosses, G., Vigeolas, H., Bock, V., Czechowski, T., Geigenberger, P. and Udvardi, M.K., 2005. Symbiotic leghemoglobins are crucial for nitrogen fixation in legume root nodules but not for general plant growth and development. *Current biology*, 15(6), 531-535.
34. Campbell, G.R., Reuhs, and G.C Chronic intracellular infection of alfalfa nodules by *Sinorhizobium meliloti* requires correct lipopolysaccharide core. *Proceedings of the National Academy of Sciences*, 99(6 3938-3943).
35. Glazebrook, J., Ichige, A. and Walker, G.C., 1993. A *Rhizobium meliloti* homolog of the *Escherichia coli* peptide-antibiotic transport protein SbmA is essential for bacteroid development. *Genes & Development*, 7(8), 1485-1497.
36. Ferguson, G.P., Datta, A., Baumgartner, J., Roop, R.M., Carlson, R.W. and Walker, G.C., 2004. Similarity to peroxisomal-membrane protein family reveals that *Sinorhizobium* and *Brucella* BacA affect lipid-A fatty acids. *Proceedings of the National Academy of Sciences*, 101(14), 5012-5017.

37. Cebolla, A. and A. Palomares, genetic regulation of nitrogen fixation in *Rhizobium meliloti*. *Microbiologia* (Madrid, Spain), 1994. 10(4), 371-384.
38. Day D.A., Poole, P.S., Tyerman, S.D. and Rosendahl, L., 2001. Ammonia and amino acid transport across symbiotic membranes in nitrogen-fixing legume nodules. *Cellular and Molecular Life Sciences CMLS*, 58, 61-71.
39. Barsch, A., Carvalho, H.G., Cullimore, J.V. and Niehaus, K., 2006. GC-MS based metabolite profiling implies three interdependent ways of ammonium assimilation in *Medicago truncatula* root nodules. *Journal of Biotechnology*, 127(1), 79-83.
40. Ronson, C.W., P. Lyttleton, and J.G. Robertson, C4-dicarboxylate transport mutants of *Rhizobium trifolii* form ineffective nodules on *Trifolium repens*. *Proceedings of the National Academy of Sciences*, 1981. 78(7), 4284-4288.
41. Zschiedrich, C.P., Keidel, V. and Szurmant, H., 2016. Molecular mechanisms of two-component signal transduction. *Journal of Molecular Biology*, 428(19), 3752-3775.
42. Kirby, J.R., 2009. Chemotaxis-like regulatory systems: unique roles in diverse bacteria. *Annual Review of Microbiology*, 63, 45-59.
43. Harshey, R.M., 2003. Bacterial motility on a surface: many ways to a common goal. *Annual Reviews in Microbiology*, 57(1), 249-273.
44. Berg, H.C., 1993. *Random walks in biology*. Princeton University Press.
45. Parkinson, J.S., 1974. Data processing by the chemotaxis machinery of *Escherichia coli*. *Nature*, 252(5481), 317-319.
46. Colin, R., Ni, B., Laganenka, L., Sourjik, V., 2021. Multiple functions of flagellar motility and chemotaxis in bacterial physiology. *FEMS Microbiology Reviews*, 45(6), 38.
47. Hazelbauer, G.L. and Lai, W.C., 2010. Bacterial chemoreceptors: providing enhanced features to two-component signaling. *Current Opinion in Microbiology*, 13(2), 124-132.
48. Hazelbauer, G.L., Falke, J.J. and Parkinson, J.S., 2008. Bacterial chemoreceptors: high-performance signaling in networked arrays. *Trends in Biochemical Sciences*, 33(1), 9-19.
49. Wadhams, G.H. and Armitage, J.P., 2004. Making sense of it all: bacterial chemotaxis. *Nature reviews Molecular cell biology*, 5(12), 1024-1037.
50. Baker, M.D., Wolanin, P.M. and Stock, J.B., 2006. Signal transduction in bacterial chemotaxis. *Bioessays*, 28(1), 9-22.
51. Surette, M.G. and Stock, J.B., 1996. Role of α -helical coiled-coil interactions in receptor dimerization, signaling, and adaptation during bacterial chemotaxis. *Journal of Biological Chemistry*, 271(30), 17966-17973.

52. Li, J., Swanson, R.V., Simon, M.I. and Weis, R.M., 1995. Response regulators CheB and CheY exhibit competitive binding to the kinase CheA. *Biochemistry*, 34(45), 14626-14636.
53. Scharf, B.E., Fahrner, K.A., Turner, L. and Berg, H.C., 1998. Control of direction of flagellar rotation in bacterial chemotaxis. *Proceedings of the National Academy of Sciences*, 95(1), 201-206.
54. Alon, U., Camarena, L., Surette, M.G., y Arcas, B.A., Liu, Y., Leibler, S. and Stock, J.B., 1998. Response regulator output in bacterial chemotaxis. *The EMBO journal*, 17(15), 4238-4248.

55. Borkovich, K.A., Kaplan, N., Hess, J.F. and Simon, M.I., 1989. Transmembrane signal transduction in bacterial chemotaxis involves ligand-dependent activation of phosphate group transfer. *Proceedings of the National Academy of Sciences*, 86(4), 1208-1212.
56. Stock, A.M., Stock, J.B., 1987. Purification and characterization of the CheZ protein of bacterial chemotaxis. *Journal of Bacteriology*, 169(7), 3301-3311.
57. Segall, J.E., Manson, M.D., Berg, H.C., 1982. Signal processing times in bacterial chemotaxis. *Nature*, 296(5860), 855-857.
58. Sourjik, V., Schmitt, R., 1996. Different roles of CheY1 and CheY2 in the chemotaxis of *Rhizobium meliloti*. *Molecular Microbiology*, 22(3), 427-436.
59. Sourjik, V. and Schmitt, R., 1998. Phosphotransfer between CheA, CheY1, and CheY2 in the chemotaxis signal transduction chain of *Rhizobium meliloti*. *Biochemistry*, 37(8), 2327-2335.
60. Dogra, G., Purschke, F.G., Wagner, V., Haslbeck, M., Kriehuber, T., Hughes, J.G., Van Tassel, M.L., Gilbert, C., Niemeyer, M., Ray, W.K., Helm, R.F., 2012. *Sinorhizobium meliloti* CheA complexed with CheS exhibits enhanced binding to CheY1, resulting in accelerated CheY1 dephosphorylation. *Journal of Bacteriology*, 194(5), 1075-1087.
61. Schmitt, R., 2002. Sinorhizobial chemotaxis: a departure from the enterobacterial paradigm. *Microbiology*, 148(3), 627-631.
62. Sourjik, V., Sterr, W., Platzer, J., Bos, I., Haslbeck, M. and Schmitt, R., 1998. Mapping of 41 chemotaxis, flagellar and motility genes to a single region of the *Sinorhizobium meliloti* chromosome. *Gene*, 223(1-2), 283-290.
63. Capela, D., Barloy-Hubler, F., Gouzy, J., Bothe, G., Ampe, F., Batut, J., Boistard, P., Becker, A., Boutry, M., Cadieu, E. and Dréano, S., 2001. Analysis of the chromosome sequence of the legume symbiont *Sinorhizobium meliloti* strain 1021. *Proceedings of the National Academy of Sciences*, 98(17), 9877-9882.
64. Ulrich, L.E. and Zhulin, I.B., 2010. The MiST2 database: a comprehensive genomics resource on microbial signal transduction. *Nucleic Acids Research*, 38, D401-D407.
65. Bibikov, S.I., Biran, R., Rudd, K.E., Parkinson, J.S., 1997. A signal transducer for aerotaxis in *Escherichia coli*. *Journal of Bacteriology*, 179(12), 4075-4079.
66. Falke, J.J., Hazelbauer, G.L., 2001. Transmembrane signaling in bacterial chemoreceptors. *Trends in Biochemical Sciences*, 26(4), 257-265.
67. Ortega, Á., Zhulin, I.B., Krell, T., 2017. Sensory repertoire of bacterial chemoreceptors. *Microbiology and Molecular Biology Reviews*, 81(4), 10-1128.
69. Lacal, J., García-Fontana, C., Muñoz-Martínez, F., Ramos, J.L. Krell, T., 2010. Sensing of environmental signals: classification of chemoreceptors according to the size of their ligand binding regions. *Environmental Microbiology*, 12(11), 2873-2884.
70. Matilla, M.A. and Krell, T., 2017. Chemoreceptor-based signal sensing. *Current Opinion in Biotechnology*, 45, 8-14.
71. Pineda-Molina, E., Reyes-Darias, J.A., Lacal, J., Ramos, J.L., García-Ruiz, J.M., Gavira, J.A. and Krell, T., 2012. Evidence for chemoreceptors with bimodular ligand-binding regions harboring two signal-binding sites. *Proceedings of the National Academy of Sciences*, 109(46), 18926-18931.
72. Krell, T., Lacal, J., Muñoz-Martínez, F., Reyes-Darias, J.A., Cadirci, B.H., García-Fontana, C. and Ramos, J.L., 2011. Diversity at its best: bacterial taxis. *Environmental Microbiology*, 13(5), 1115-1124.
73. Miller, L.D., Russell, M.H., Alexandre, G., 2009. Diversity in bacterial chemotactic responses and niche adaptation. *Advances in Applied Microbiology*, 66, 53-75.

74. Milburn, M.V., Privé, G.G., Milligan, D.L., Scott, W.G., Yeh, J., Jancarik, J., Koshland Jr, D.E. and Kim, S.H., 1991. Three-dimensional structures of the ligand-binding domain of the bacterial aspartate receptor with and without a ligand. *Science*, 254(5036), 1342-1347.
75. Tajima, H., Imada, K., Sakuma, M., Hattori, F., Nara, T., Kamo, N., Homma, M. and Kawagishi, I., 2011. Ligand specificity determined by differentially arranged common ligand-binding residues in bacterial amino acid chemoreceptors Tsr and Tar. *Journal of Biological Chemistry*, 286(49), 42200-42210.
76. Neumann, S., Hansen, C.H., Wingreen, N.S. and Sourjik, V., 2010. Differences in signalling by directly and indirectly binding ligands in bacterial chemotaxis. *The EMBO Journal*, 29(20), 3484-3495.
77. Iwama, T., Ito, Y., Aoki, H., Sakamoto, H., Yamagata, S., Kawai, K. and Kawagishi, I., 2006. Differential recognition of citrate and a metal-citrate complex by the bacterial chemoreceptor Tcp. *Journal of Biological Chemistry*, 281(26), 17727-17735.
78. Luu, R.A., Kootstra, J.D., Nesteryuk, V., Brunton, C.N., Parales, J.V., Ditty, J.L. and Parales, R.E., 2015. Integration of chemotaxis, transport and catabolism in *Pseudomonas putida* and identification of the aromatic acid chemoreceptor PcaY. *Molecular Microbiology*, 96(1), 134-147.
79. Baaziz, H., Compton, K.K., Hildreth, S.B., Helm, R.F. and Scharf, B.E., 2021. McpT, a broad-range carboxylate chemoreceptor in *Sinorhizobium meliloti*. *Journal of Bacteriology*, 203(17), 10-1128.
80. Harayama, S., Palva, E.T. and Hazelbauer, G.L., 1979. Transposon-insertion mutants of *Escherichia coli* K12 defective in a component common to galactose and ribose chemotaxis. *Molecular and General Genetics MGG*, 171, 193-203.
81. Manson, M.D., Blank, V., Brade, G. and Higgins, C.F., 1986. Peptide chemotaxis in *E. coli* involves the Tap signal transducer and the dipeptide permease. *Nature*, 321(6067), 253-256.
82. Liu, X. and Parales, R.E., 2008. Chemotaxis of *Escherichia coli* to pyrimidines: a new role for the signal transducer tap. *Journal of Bacteriology*, 190(3), 972-979.
83. Huang, J.Y., Sweeney, E.G., Sigal, M., Zhang, H.C., Remington, S.J., Cantrell, M.A., Kuo, C.J., Guillemin, K. and Amieva, M.R., 2015. Chemodetection and destruction of host urea allows *Helicobacter pylori* to locate the epithelium. *Cell Host & Microbe*, 18(2), 147-156.
84. García, V., Reyes-Darias, J.A., Martín-Mora, D., Morel, B., Matilla, M.A. and Krell, T., 2015. Identification of a chemoreceptor for C2 and C3 carboxylic acids. *Applied and Environmental Microbiology*, 81(16), 5449-5457.
85. Compton, K.K., Hildreth, S.B., Helm, R.F. and Scharf, B.E., 2018. *Sinorhizobium meliloti* chemoreceptor McpV senses short-chain carboxylates via direct binding. *Journal of Bacteriology*, 200(23), 10-1128.
86. Lacal, J., Alfonso, C., Liu, X., Parales, R.E., Morel, B., Conejero-Lara, F., Rivas, G., Duque, E., Ramos, J.L. and Krell, T., 2010. Identification of a chemoreceptor for tricarboxylic acid cycle intermediates: differential chemotactic response towards receptor ligands. *Journal of Biological Chemistry*, 285(30), 23126-23136.
87. Liu, Y.C., Machuca, M.A., Beckham, S.A., Gunzburg, M.J. and Roujeinikova, A., 2015. Structural basis for amino-acid recognition and transmembrane signalling by tandem Per-Arnt-Sim (tandem PAS) chemoreceptor sensory domains. *Acta Crystallographica Section D: Biological Crystallography*, 71(10), 2127-2136.
88. Rico-Jiménez, M., Muñoz-Martínez, F., García-Fontana, C., Fernández, M., Morel, B., Ortega, Á., Ramos, J.L. and Krell, T., 2013. Paralogous chemoreceptors mediate chemotaxis

- towards protein amino acids and the non-protein amino acid gamma-aminobutyrate (GABA). *Molecular Microbiology*, 88(6), 1230-1243.
89. Webb, B.A., Karl Compton, K., Castañeda Saldaña, R., Arapov, T.D., Keith Ray, W., Helm, R.F. and Scharf, B.E., 2017. *Sinorhizobium meliloti* chemotaxis to quaternary ammonium compounds is mediated by the chemoreceptor McpX. *Molecular Microbiology*, 103(2), 333-346.
 90. Corral-Lugo, A., De la Torre, J., Matilla, M.A., Fernández, M., Morel, B., Espinosa-Urgel, M. and Krell, T., 2016. Assessment of the contribution of chemoreceptor-based signalling to biofilm formation. *Environmental Microbiology*, 18(10), 3355-3372.
 91. Nishiyama, S.I., Takahashi, Y., Yamamoto, K., Suzuki, D., Itoh, Y., Sumita, K., Uchida, Y., Homma, M., Imada, K. and Kawagishi, I., 2016. Identification of a *Vibrio cholerae* chemoreceptor that senses taurine and amino acids as attractants. *Scientific Reports*, 6(1), 20866.
 92. Rahman, H., King, R.M., Shewell, L.K., Semchenko, E.A., Hartley-Tassell, L.E., Wilson, J.C., Day, C.J. and Korolik, V., 2014. Characterisation of a multi-ligand binding chemoreceptor CcmL (Tlp3) of *Campylobacter jejuni*. *PLoS pathogens*, 10(1), e1003822.
 93. Shrestha, M., Compton, K.K., Mancl, J.M., Webb, B.A., Brown, A.M., Scharf, B.E. and Schubot, F.D., 2018. Structure of the sensory domain of McpX from *Sinorhizobium meliloti*, the first known bacterial chemotactic sensor for quaternary ammonium compounds. *Biochemical Journal*, 475(24), 3949-3962.
 94. Wu, J., Li, J., Li, G., Long, D.G. and Weis, R.M., 1996. The receptor binding site for the methyltransferase of bacterial chemotaxis is distinct from the sites of methylation. *Biochemistry*, 35(15), 4984-4993.
 95. Barnakov, A.N., Barnakova, L.A., Hazelbauer, G.L., 1999. Efficient adaptational demethylation of chemoreceptors requires the same enzyme-docking site as efficient methylation. *Proceedings of the National Academy of Sciences*, 96(19), 10667-10672.
 96. Borkovich, K.A., Alex, L.A., Simon, M.I., 1992. Attenuation of sensory receptor signaling by covalent modification. *Proceedings of the National Academy of Sciences*, 89(15), 6756-6760.
 97. Danielson, M.A., Biemann, H.P., Koshland Jr, D.E., Falke, J.J., 1994. Attractant-and disulfide-induced conformational changes in the ligand binding domain of the chemotaxis aspartate receptor: a 19F NMR study. *Biochemistry*, 33(20), 6100-6109.
 98. Milligan, D.L. and Koshland, D.E., 1988. Site-directed cross-linking. Establishing the dimeric structure of the aspartate receptor of bacterial chemotaxis. *Journal of Biological Chemistry*, 263(13), 6268-6275.
 99. Parkinson, J.S., Hazelbauer, G.L., Falke, J.J., 2015. Signaling and sensory adaptation in *Escherichia coli* chemoreceptors: 2015 update. *Trends in Microbiology*, 23(5), 257-266.
 100. Le Moual, H., Quang, T. and Koshland, D.E., 1997. Methylation of the *Escherichia coli* chemotaxis receptors: intra-and interdimer mechanisms. *Biochemistry*, 36(43), 13441-13448.
 101. Li, M. and Hazelbauer, G.L., 2005. Adaptational assistance in clusters of bacterial chemoreceptors. *Molecular Microbiology*, 56(6), 1617-1626.
 102. Feng, X., Lilly, A.A. and Hazelbauer, G.L., 1999. Enhanced function conferred on low-abundance chemoreceptor Trg by a methyltransferase-docking site. *Journal of Bacteriology*, 181(10), 3164-3171.
 103. Rao, C.V., Glekas, G.D. and Ordal, G.W., 2008. The three adaptation systems of *Bacillus subtilis* chemotaxis. *Trends in Microbiology*, 16(10), 480-487.

104. Glekas, G.D., Cates, J.R., Cohen, T.M., Rao, C.V. and Ordal, G.W., 2011. Site-specific methylation in *Bacillus subtilis* chemotaxis: effect of covalent modifications to the chemotaxis receptor McpB. *Microbiology*, 157, 56.
105. Thoelke, M.S., Kirby, J.R. and Ordal, G.W., 1989. Novel methyl transfer during chemotaxis in *Bacillus subtilis*. *Biochemistry*, 28(13), 5585-5589.
106. Szurmant, H., Muff, T.J. and Ordal, G.W., 2004. *Bacillus subtilis* CheC and FliY are members of a novel class of CheY-P-hydrolyzing proteins in the chemotactic signal transduction cascade. *Journal of Biological Chemistry*, 279(21), 21787-21792.
107. Fredrick, K.L. and Helmann, J.D., 1994. Dual chemotaxis signaling pathways in *Bacillus subtilis*: a sigma D-dependent gene encodes a novel protein with both CheW and CheY homologous domains. *Journal of Bacteriology*, 176(9), 2727-2735.
108. Walukiewicz, H.E., Tohidifar, P., Ordal, G.W. and Rao, C.V., 2014. Interactions among the three adaptation systems of *Bacillus subtilis* chemotaxis as revealed by an in vitro receptor-kinase assay. *Molecular Microbiology*, 93(6), 1104-1118.
109. Li, M. and Hazelbauer, G.L., 2004. Cellular stoichiometry of the components of the chemotaxis signaling complex. *Journal of Bacteriology*, 186(12), 3687-3694.
110. Cannistraro, V.J., Glekas, G.D., Rao, C.V. and Ordal, G.W., 2011. Cellular stoichiometry of the chemotaxis proteins in *Bacillus subtilis*. *Journal of Bacteriology*, 193(13), 3220-3227.
111. Zatakia, H.M., Arapov, T.D., Meier, V.M., Scharf, B.E., 2018. Cellular stoichiometry of methyl-accepting chemotaxis proteins in *Sinorhizobium meliloti*. *Journal of Bacteriology*, 200(6), 10-1128.
112. Arapov, T.D., Saldaña, R.C., Sebastian, A.L., Ray, W.K., Helm, R.F. and Scharf, B.E., 2020. Cellular stoichiometry of chemotaxis proteins in *Sinorhizobium meliloti*. *Journal of Bacteriology*, 202(14), 10-1128.
113. Barton, N.H., et al., *Evolution*. 2007.

TABLE

Table 1.1. Selected rhizobial species and their symbiotic hosts.

Species	Host Range
<i>Azorhizobium caulinodans</i>	<i>Sesbania rostrata</i>
<i>Bradyrhizobium japonicum</i>	<i>Glycine max</i> (Soybean), <i>Vigna unguiculata</i> (cowpea)
<i>Mesorhizobium loti</i>	<i>Lotus japonicus</i> (Gifu)
<i>Rhizobium etli</i>	<i>Phaseolus vulgaris</i> (Common bean)
<i>Rhizobium leguminosarum</i> bv. <i>phaseoli</i>	<i>Phaseolus vulgaris</i> (Common bean)
<i>Rhizobium leguminosarum</i> bv. <i>trifolii</i>	<i>Trifolium spp.</i> (Clover)
<i>Rhizobium leguminosarum</i> bv. <i>viciae</i>	<i>Pisum sativum</i> (Pea), <i>Vicia faba</i> (vetch)
<i>Rhizobium tropici</i>	<i>Phaseolus vulgaris</i> (Common bean)
<i>Sinorhizobium fredii</i>	<i>Glycine max</i> (Soybean)
<i>Sinorhizobium meliloti</i>	<i>Medicago sativa</i> (Alfalfa)

FIGURES

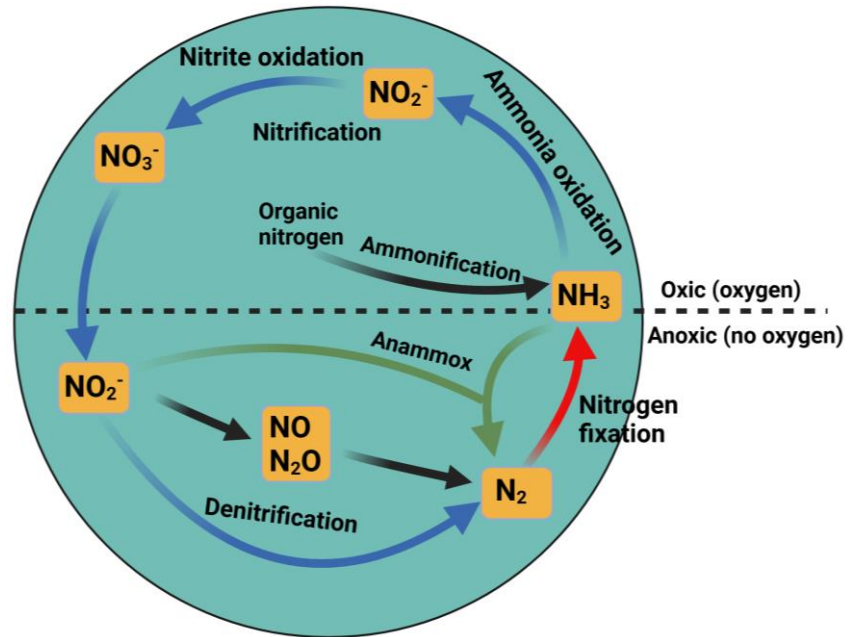


Fig. 1. 1 The various biological processes that constitute the nitrogen cycle.

Nitrification, which converts ammonia into nitrate (NO₃⁻), and ammonification, which releases organic nitrogen (e.g., amino acids, DNA) from dead cells, are oxygen dependent processes. Contrarily, denitrification and anammox, which return bioavailable nitrogen to N₂, as well as nitrogen fixation are anaerobic processes. Image was reproduced from [3].

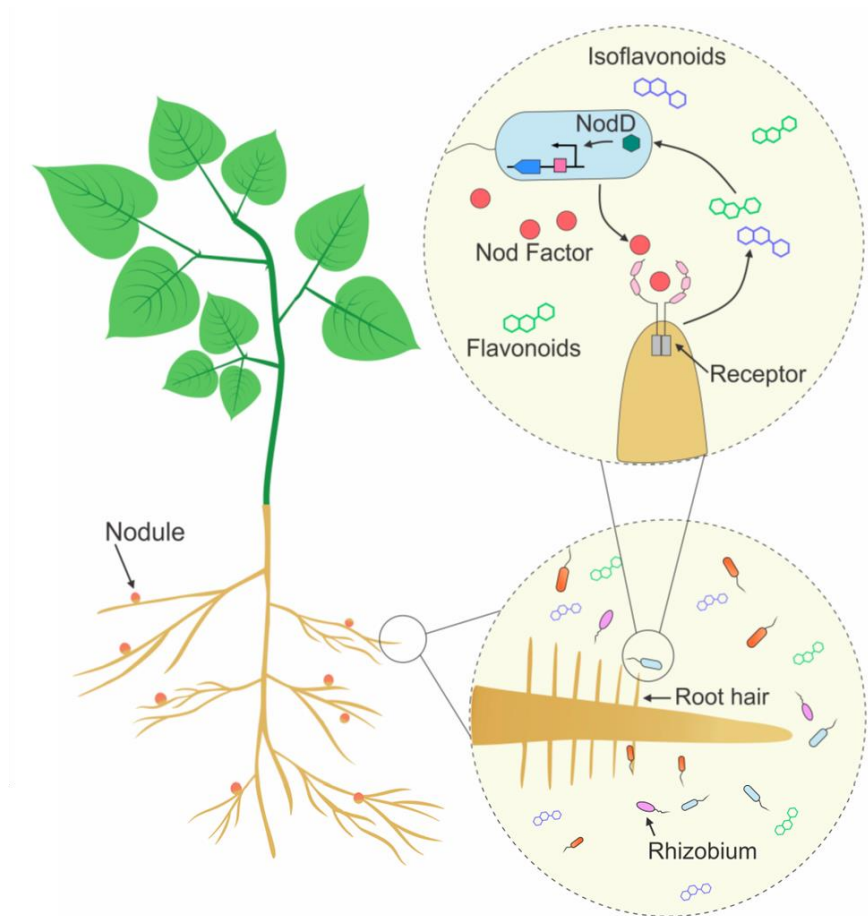


Fig. 1. 2 Initial signal exchange between the rhizobia and host legume. Legume root exudates recruit compatible rhizobia, which in turn release Nod factors. This tightly regulated recognition event is a vital initial step for the success of symbiotic relationships. Image used with permission from [19].

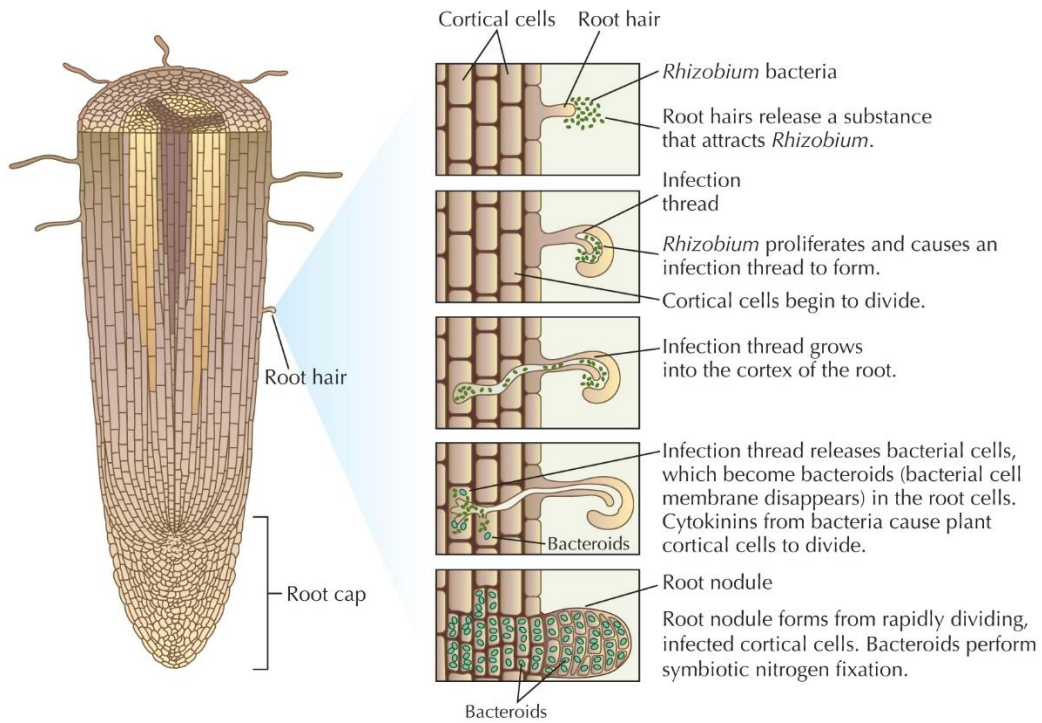


Fig. 1. 3 A schematic of the symbiotic process between rhizobium bacteria and roots of legumes. The process outlines the sequence of events between the symbiotic partners that culminate in nodule formation and nitrogen fixation in indeterminate legumes. Image used with permission from [113] and copyright to Cold Spring Harbor Laboratory Press.

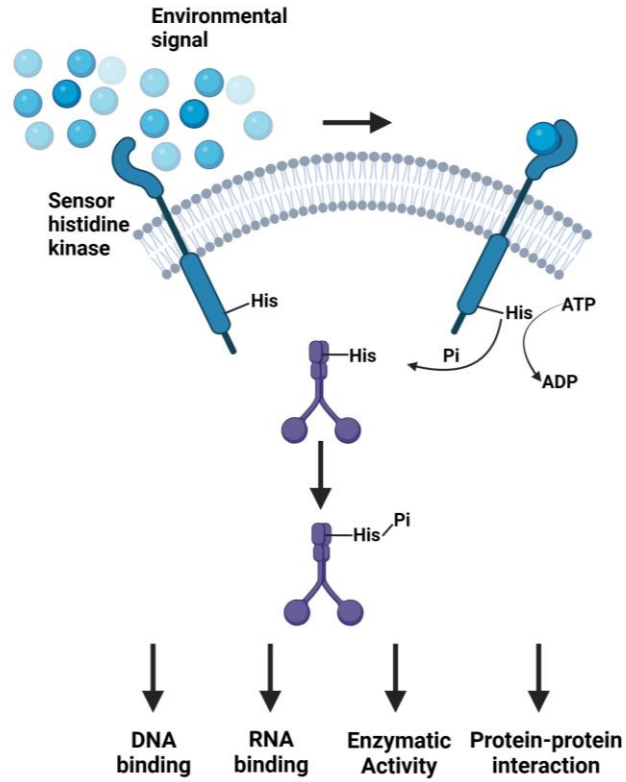


Fig. 1. 4 Two-component signal transduction pathways in bacteria. A transduced environmental stimulus from the membrane receptor triggers a cascade of phosphorylation and phosphate transfer events that results in several possible outputs [41].

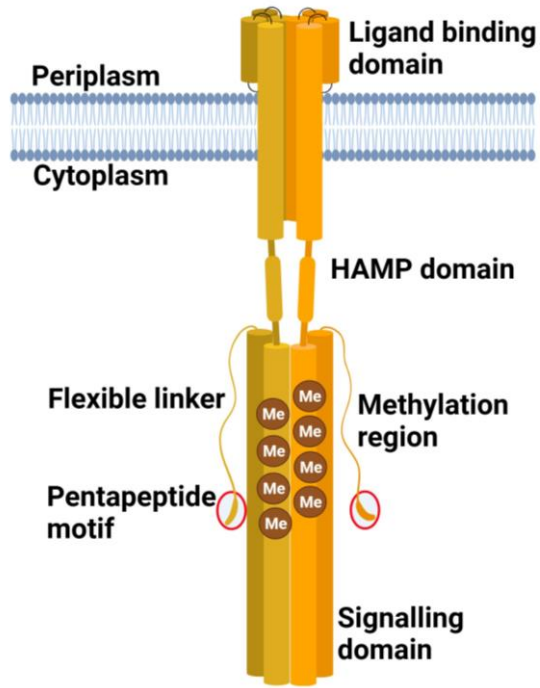


Fig. 1. 5 An illustration of the architecture of an *E. coli* MCP. The cytoplasmic domain is made up of the HAMP region, the methylated helices that interact with CheR and CheB, and the signaling domain that interacts with CheA.

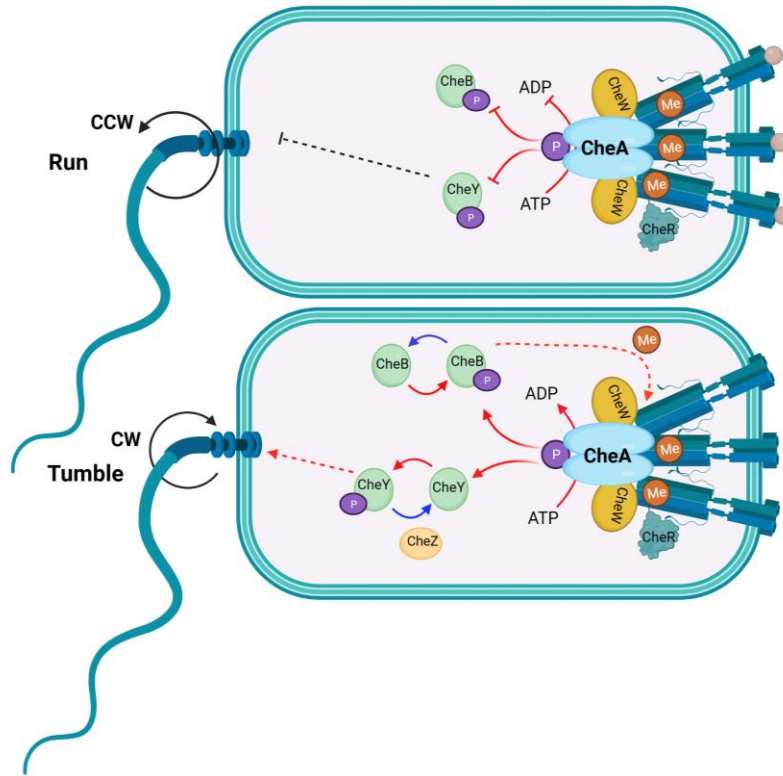


Fig. 1. 6 Signal transduction in *E. coli* from chemotaxis receptors (MCPs) to the flagellar motor. Ligand binding (top image) inactivates the CheA kinase and subsequent phosphorylation events result in default counterclockwise rotation and run behavior. In the absence of ligand (bottom image), CheA activation promotes a downstream phosphorylation of CheY that causes a switch in flagellar rotation and cell tumbling.

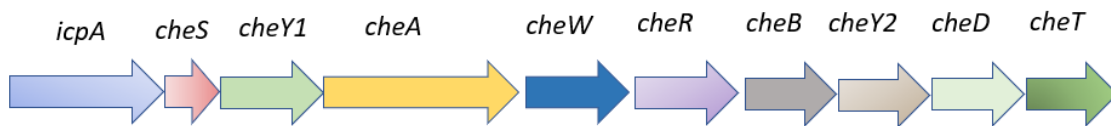


Fig. 1. 7 Genetic organization of the *che1* operon in *S. meliloti*. The *che1* operon regulates motility in response to chemical gradients. The *che1* operon also contains genes coding for an internal chemoreceptor, IcpA, a receptor-modifying deamidase CheD, the CheA-adaptor protein CheS, and CheT, a protein of unknown function[13].

Chapter 2— Promiscuous but essential: The conserved C-terminal pentapeptide tether is required for *Sinorhizobium meliloti* chemotaxis regardless of chemoreceptor type

ALFRED AGBEKUDZI & BIRGIT E. SCHARF

Virginia Tech, Department of Biological Sciences, Life Sciences I, Blacksburg, VA 24061

Running title: Chemoreceptor pentapeptide is critical for chemotaxis

For correspondence:

E-mail bscharf@vt.edu

Tel (+1) 540 231 0757

Fax (+1) 540 231 4043

Biological Sciences, Life Sciences I

Virginia Tech

Blacksburg, VA 24061, USA

ABSTRACT

Sensory adaptation in chemotaxis is mediated by posttranslational modifications of Methyl-accepting Chemotaxis Proteins (MCPs). In *Escherichia coli*, the adaptation proteins CheR and CheB tether to a conserved C-terminal receptor pentapeptide. Here, we investigated the function of the similarly conserved pentapeptide motif (N/D)WE(E/N)F in *S. meliloti* chemotaxis. Isothermal titration calorimetry revealed tight binding of the pentapeptides to CheR ($K_D = 10\text{-}15\ \mu\text{M}$) and activated CheB ($K_D = 27\text{-}46\ \mu\text{M}$). Strains with mutations of the conserved tryptophan in one or all four MCP pentapeptides resulted in a significant decrease or loss of chemotaxis to glycine betaine, lysine, and acetate, chemoattractants sensed by pentapeptide-bearing McpX and pentapeptide-lacking McpU and McpV, respectively. Importantly, we discovered that the pentapeptide indiscriminately mediates chemotaxis when fused to the C-terminus of pentapeptide-lacking chemoreceptors via a flexible linker. We propose that proximity and a threshold number of available sites enable the efficient docking of adaptation proteins to the chemosensory array. Altogether, these results demonstrate that *S. meliloti* effectively utilizes a pentapeptide-dependent adaptation system with a minimal number of tethering units and we hypothesize that the higher abundance of CheR and CheB in *S. meliloti* compared to *E. coli* allows for ample recruitment of adaptation proteins to the chemosensory array.

Key words: chemoattractant, plant microbe interaction, protein methylation, two-component system.

INTRODUCTION

Bacteria use one component, two component, chemotaxis and chemotaxis-like systems to sense and respond to environmental signals [1]. Chemotaxis and chemotaxis-like systems are variations of two component systems that employ the binding of signaling molecules to transmembrane receptors, which form a ternary complex with a histidine kinase (CheA) and a scaffold protein (CheW) for the transmission of external signals to a cytoplasmic response regulator [2]. More importantly, chemotaxis and chemotaxis-like systems have evolved an adaptation module that enhances sensitivity to a wide stimuli gradient through reversible methylation of chemoreceptors named methyl-accepting chemotaxis proteins (MCPs) [3, 4].

The well-studied *Escherichia coli* chemotaxis pathway consists of signal sensing, intracellular signal transduction, and sensory adaptation [3, 5]. The binding of external ligands to the periplasmic domain of chemoreceptors triggers sequential conformational changes of the two transmembrane helices, which is transduced to the cytoplasmic domain [6, 7]. Chemoreceptors assemble as a signaling unit of trimers of dimers with their associated CheA and CheW partners. Trimers of different chemoreceptor types form highly ordered chemosensory clusters, linked through shared CheA and CheW proteins, to enhance signaling [8-11]. These receptor clusters provide adaptational assistance and enhance signal amplification and sensitivity. Chemoreceptors modulate the activity of the associated CheA kinase, which changes the level of response regulator (CheY) phosphorylation [7, 12]. CheY-P diffuses and binds to the cytoplasmic surface of the flagellar motor, which controls the directionality of motor rotation [13, 14]. To terminate the signaling pathway, a phosphatase (CheZ) accelerates CheY-P dephosphorylation [15-17].

E. coli chemoreceptors in the kinase-off state are preferably methylated at signature glutamyl residues in the cytoplasmic methylation helices by the methyltransferase CheR, which uses S-adenosylmethionine as substrate [18, 19]. Conversely, the methylesterase CheB, when activated

via phosphorylation by CheA, removes methyl groups from the glutamyl-methyl esters in the kinase-on state of chemoreceptors [20] and also generates some methyl-accepting sites by deamidation of conserved glutamyl side chains [21]. In *E. coli*, CheR and CheB are recruited to the methylation sites by binding to a conserved pentapeptide (NWETF) connected to the C-terminus of the high-abundance receptors (Tar and Tsr) via a structureless but flexible linkers [22, 23]. This unique tether enables CheR and CheB to directly dock to the receptor clusters providing a locally increased enzyme concentration. This feature also enables the covalent modification of low-abundance receptors, which lack the pentapeptide tether [24, 25].

Sinorhizobium meliloti is the endosymbiont of alfalfa (*Medicago sativa*), an economically important forage legume with over 54 million tons being grown in the United States in 2019 [26]. Like other legumes, alfalfa naturally obtains nitrogen through the nitrogen-fixing symbiosis with diazotrophs [27]. This beneficial interaction provides a source of biological nitrogen, which avoids the use of costly and environmentally polluting nitrogenous fertilizers in agriculture. The chromosome of *S. meliloti* encodes motility-regulating chemotaxis proteins from the *che1* operon on the chromosome [28, 29], as well as chemoreceptors from separate loci. Its chemotaxis signaling pathway exhibits similarities in the basic design but also deviations from the *E. coli* system.

S. meliloti employs a phosphate sink mechanism with an additional response regulator CheY1 to inactivate the motor response regulator, CheY2-P [15, 30, 31]. It also possesses additional chemotaxis proteins namely CheD, a putative deamidase, CheS, a protein that enhances binding of CheY1 to CheA, and CheT, a protein of unknown function [32, 33].

MCPs in *E. coli* and *S. meliloti* differ in number, abundance, and their ligand spectrum. *E. coli* possesses five MCPs, namely Tar, Tsr, Trg, Tap, and the cytosolic Aer, for detecting various

signals through direct binding or indirectly via periplasmic binding proteins [34-36]. Tar mediates positive responses to aspartate and indirectly to maltose, and negative responses to metal ions [37-41]. Tsr responds to serine, 3,4-dihydroxymandelic acid, and indirectly to autoinducer 2 [42-45]. In addition, Tsr and Aer sense intracellular oxygen, redox, and energy signals [44]. Trg indirectly mediates attractant responses to ribose and galactose [46], while Tap senses pyrimidines and indirectly dipeptides [47, 48]. In *S. meliloti*, eight chemoreceptors, namely McpT through McpZ, and IcpA contribute to the chemotactic behavior [49]. McpV and McpT mediate a positive response to carboxylates [50, 51], while McpU and McpX mediate chemotaxis to amino acids and quaternary ammonium compounds, respectively [52, 53]. The ligands of McpW, McpY, McpZ, and IcpA have not been characterized [54].

E. coli Tar and Tsr, which constitute 93% of the total chemoreceptor population, have a conserved NWETF pentapeptide sequence at their C-terminus [55]. In contrast, four of the eight *S. meliloti* MCPs (McpT, McpY, McpW, and McpX) bear a conserved pentapeptide motif, but these chemoreceptors only represent 13% of the receptor population (Table 1) [56, 57]. The sequences exhibit slight variations from the *E. coli* pentapeptide, however, critical residues involved in the binding of adaptation proteins in *E. coli* and other bacterial species are well conserved [58-60], with a consensus sequence of (N/D)WE(E/N)F [49, 56]. While the total cellular number of chemoreceptor molecules and the number of chemoreceptors with a C-terminal pentapeptide differ between *E. coli* and *S. meliloti*, [55, 56], an even more relevant parameter is the ratio of MCPs to adaptation proteins [61]. *E. coli* has approximately 0.007 CheR and 0.01 CheB molecules, respectively, per pentapeptide-bearing MCP monomer (PP_{MCPs}) (Fig. 1). In contrast, *S. meliloti* possesses 3.8 CheR and 1.6 CheB molecules, respectively, per monomer of PP_{MCPs}. It is postulated that the high number of *E. coli* PP_{MCPs} increases the local concentration of moderately expressed

CheR and CheB proteins recruited to the chemosensory cluster [24, 25]. Other species, such as *Bacillus subtilis* and *Thermotoga maritima*, are completely devoid of pentapeptide-bearing chemoreceptors and yet efficiently methylate their chemoreceptors [59]. Thus, bacteria employ pentapeptide-dependent or pentapeptide-independent mechanisms to recruit adaptation proteins to chemoreceptor clusters [60]. These differences highlight the varied strategies used by different bacterial species to achieve efficient chemosensory adaptation. At this point, it is unknown whether *S. meliloti* utilizes the pentapeptide in a similar manner as the *E. coli* tether, or whether the pentapeptide motif is obsolete as shown for CheB function in *Pectobacterium atrosepticum* where none of the nine different C-terminal pentapeptides of 19 MCPs bind to CheB [62]. In this study, we investigated the importance of the conserved C-terminal pentapeptide in *S. meliloti* chemoreceptors.

RESULTS

The chemoreceptor pentapeptide-binding site in *S. meliloti* CheR is weakly conserved.

Structural analysis of *S. enterica* CheR identified residues within its β -subdomain that interact with the chemoreceptor pentapeptide [18]. A bioinformatics analysis identified residues Q182, R187, G188, G190, G194, and R197 within a 16 amino acid long sequence that are highly conserved in CheR proteins from organisms containing one CheR and at least one MCP with a putative pentapeptide motif (Fig. 2A & B) [18, 59]. The sequence identity between *E. coli* and *S. meliloti* CheR and the β -subdomain are rather low with 37% and 24%, respectively. Furthermore, amino acid residues involved in MCP binding in other bacterial species are not conserved in *S. meliloti* (Fig. 2B; highlighted in gray). In addition, the participating residues in the β -subdomain of *E. coli* and *S. typhimurium* CheR are located in a region that has an α -helix and a short, antiparallel three β -sheet strands (Fig. 2A, C) [63], while the AlphaFold structure of the β -subdomain of *S. meliloti* CheR predicts one α -helix and two relatively long antiparallel β -strands (Fig. 2B, C). In addition, García-Fontana et al. (2014) reported that pentapeptide-binding CheR proteins possess an insertion of a tripeptide motif (GPX; Fig. 2A & B) that forms a loop to link strands 2 and 3 of the CheR pentapeptide-binding site. Although residues that interact with the MCP pentapeptide motif are not conserved in *S. meliloti* CheR, it possesses a tripeptide insertion (AGG) that similarly links the two strands (Fig. 2C). In conclusion, the sequence analysis provided some weak evidence that *S. meliloti* CheR might bind to chemoreceptors in a pentapeptide-dependent manner.

The chemoreceptor pentapeptide-binding site in *S. meliloti* CheB is conserved.

CheB is a two-domain protein comprised of a regulatory REC domain and a methyltransferase effector domain connected by a linker region [64]. Biochemical studies of *E. coli* CheB identified

eleven residues (aa 130 to 140) in the C-terminal extension of the REC domain and N-terminal region of the linker as the pentapeptide-binding region (Fig. 3A) [65]. An alignment of CheB from 107 bacterial species generated a sequence logo for this region, containing signature residues with positively charged side chains at positions 128, 132, and 134, hydrophobic side chains at position 135, and bulky side chains at position 138 (Fig. 3A and 3B) [21]. Especially residues with positively charged side chains are conserved in the *S. meliloti* CheB sequence (Fig. 3A and 3C). Thus, we predict that the receptor binding of CheB in *S. meliloti* is pentapeptide dependent.

CheR binds to the conserved C-terminal pentapeptides of *S. meliloti* chemoreceptors.

The sequence analysis of *S. meliloti* CheR failed to identify a clear consensus sequence for pentapeptide binding. Therefore, CheR was overexpressed in *E. coli* and purified in its native form via affinity and size exclusion chromatography. The purified protein was subjected to microcalorimetric titrations with the three different chemoreceptor pentapeptides, as well as pentapeptides carrying an Ala mutation in the position of the essential Trp and Phe residue, respectively [58]. During the titrations of CheR with the wild-type peptides, exothermic binding heats were observed, with derived dissociation constants (K_D) of 15 μM , 12 μM , and 10 μM for the pentapeptides of McpX/W, McpY, and McpT, respectively (Fig. 4). In contrast, small and uniform heat changes resulting from titrations of CheR with both mutant pentapeptides indicated that there was no binding (Fig. 4). The measured affinities were slightly weaker than for the pentapeptide NWETF and *E. coli* CheR (2.5 μM and 10 μM) [22, 66] and considerably weaker than observed for *P. aeruginosa* CheR2 and the pentapeptide GWEEF (0.5 μM) [67]. These results demonstrate binding of *S. meliloti* CheR to the C-terminal pentapeptides of McpT, McpW, McpX,

and McpY and emphasize the essential role of the conserved Trp and Phe in the second and fifth position.

Inactive and activated CheB present differential binding to the pentapeptide of *S. meliloti* chemoreceptors.

The sequence analysis of *S. meliloti* CheB clearly identified a consensus sequence for pentapeptide binding. To experimentally analyze this binding, CheB was overexpressed in *E. coli* and purified in its native form via affinity and size exclusion chromatography. The purified protein was subjected to microcalorimetric titrations with chemoreceptor pentapeptides. However, no K_D was derived from the small and even heat changes (Fig. 5A). This result is different from *E. coli* and *P. aeruginosa* CheB, which exhibited a relatively low but measurable affinity to the conserved pentapeptide with K_{DS} of 160 μM and 93 μM , respectively [21], [62].

Next, we investigated whether CheB phosphorylation alters the affinity for pentapeptide. As the half-life of phosphorylated CheB is typically only a few seconds, we generated a stable BeF_3^- analogue that mimics phosphorylation representing the active form of the protein [68-70]. We then investigated CheB- BeF_3^- for its interaction with the *S. meliloti* wild-type and mutant pentapeptides. These titrations produced exothermic binding heats with derived K_{DS} of 46 μM , 42 μM , and 27 μM for the McpX/W, McpY and McpT pentapeptides, respectively (Fig. 5 B, C & D). Similar to CheR, both non-functional mutant pentapeptides lacked binding, confirming the essential role of the Trp and Phe residues in position two and five, respectively (Fig. 5 B, C & D). The derived K_D for the activated *E. coli* CheB and the pentapeptide-bearing receptor (Tar) was in a similar range (13 μM) [21]. In conclusion, *S. meliloti* CheB exhibits a pentapeptide-dependent receptor binding, which is reliant on CheB activation.

The C-terminal pentapeptide is critical for chemotaxis mediated by pentapeptide-bearing and pentapeptide-lacking receptors.

McpX constitutes 9% of the total chemoreceptor population but 68% of the pentapeptide-bearing chemoreceptor population in *S. meliloti*. To establish the importance of the C-terminal pentapeptide in McpX-mediated chemotaxis, we constructed a mutant in which the essential Trp residue in the pentapeptide was substituted by Ala (McpX-PP_{W-A}), as we have shown, that CheR and activated CheB have no affinity to the mutant pentapeptide (Figs. 4 & 5). We performed quantitative Adler capillary assays to analyze the chemotactic proficiency of this mutant towards one of its strongest ligands, glycine betaine [53]. Compared to the *mcpX* deletion strain, which produced an 80% reduced response when compared to wild type, the response of the McpX-PP_{W-A} strain was significantly reduced by 60% (Fig. 6). To assess whether the loss of functional pentapeptides in all pentapeptide-bearing receptors had an additional effect on McpX-mediated chemotaxis, a quadruple strain with mutations in all four essential Trp residues was constructed (McpX/W/Y/T-PP_{W-A}). This strain exhibited an 80% reduction in its response to glycine betaine, comparable to that of the *mcpX* deletion strain and significantly lower than that of the McpX-PP_{W/A} strain. These results infer that the C-terminal pentapeptide sequence is critical for McpX-mediated chemotaxis in *S. meliloti*. In addition, the response to lysine in the McpX-PP_{W-A} strain, which lacks approximately two thirds of the pentapeptide population, was reduced by 50%. The quadruple strain with mutations in all four essential Trp residues, McpX/W/Y/T-PP_{W-A}, exhibited an 80% reduction in its response to the McpU-specific attractant lysine, a similar reduction as observed for the *mcpU* deletion strain (Fig. 7). This result suggests that a loss-of function mutation in the pentapeptide motif negatively affects chemotaxis in both pentapeptide-bearing and

pentapeptide-lacking chemoreceptors, and that this effect seems to correlate with the number of available pentapeptide sites.

Addition of the pentapeptide to a pentapeptide-lacking receptor abolishes its function unless it is fused with the preceding flexible linker.

Next, we asked the question whether the pentapeptide can be moved from a pentapeptide-bearing receptor type to a pentapeptide-lacking receptor type. We focused our studies on McpX and McpU as previous findings from our lab determined that these receptors have similar cellular expression levels [56]. First, we tested the effect of pentapeptide addition on McpU-mediated chemotaxis (McpU+McpX₇₈₄₋₇₈₈). Interestingly, fusion of the McpX pentapeptide to the C-terminus of McpU abolished chemotaxis to lysine (Fig. 8A). However, when the C-terminal 55 amino acid residues, including the flexible linker of McpX (McpU+McpX₇₃₄₋₇₈₈) (Fig. S1), were fused to the C-terminus of McpU the chemotactic response of the resulting strain to lysine was equivalent to wild type (Fig. 8A). This finding demonstrates that fusion of the flexible linker in conjunction with the pentapeptide motif of McpX maintains McpU's functionality. Our group had discovered previously that the addition of amino acid residues to the C-terminus of McpU increased its abundance, likely by interfering with its controlled proteolysis [71]. To test whether this is the case for McpU+McpX₇₈₄₋₇₈₈ and McpU+McpX₇₃₄₋₇₈₈, we determined their cellular abundance using semi-quantitative immunoblots (Fig. 8B). The addition of the McpX pentapeptide sequence led to an 8-fold increased abundance, compared to a 6-fold increased abundance as previously determined for the 6XHis fusion mutant [71] (Fig. 8C). In contrast, the fusion of the flexible tail region in addition to the pentapeptide resulted in a statistically insignificant increase in McpU abundance. This result together with the capillary assay data supports our previous interpretation

that strains with increased McpU stability are negatively affected in McpU function. However, we had observed only a small reduction of chemotactic proficiency on soft agar swim plates for a strain with a C-terminal 3X-FLAG fusion to McpU, whereas a strain with a 6XHis fusion to McpU displayed wild-type behavior [71]. Thus, we tested the chemotactic behavior of the mutant with a 6XHis fusion to McpU in the capillary assay and observed a 60% reduction compared to wild type (Fig. 8A). This outcome provides evidence that strains with increased abundance exhibit impaired McpU-mediated chemotaxis and that the capillary assay is superior and more sensitive than the indirect swim plate assay.

The C-terminal pentapeptide in conjunction with the flexible linker is functional regardless of the receptor type it is attached to.

As we established conditions that allowed the addition of a functional pentapeptide tether to a non-pentapeptide-bearing receptor (Fig. 6-8A), we sought to evaluate if the pentapeptide tether on receptors lacking this motif can substitute the McpX pentapeptide. In addition to McpU, we also fused the linker and pentapeptide of McpX to the C-terminus of the small carboxylate sensor (McpV+McpX₇₃₄₋₇₈₈) in a strain that bears a non-functional McpX pentapeptide (McpX-PP_{W-A}). Based on previously determined receptor stoichiometries [56], the resulting strains had a pentapeptide-bearing receptor population of 15% (McpX-PP_{W-A}/McpU+McpX₇₃₄₋₇₈₈) and 74% (McpX-PP_{W-A}/McpV+McpX₇₃₄₋₇₈₈), respectively, compared to 13% in wild type. Next, we performed capillary assays and observed an elevated chemotactic response from 40% to 91% for glycine betaine and from 50% to 85% for lysine for the McpX-PP_{W-A} strain compared to the McpX-PP_{W-A}/McpU+McpX₇₃₄₋₇₈₈ strain (Figs. 6 & 7). Similarly, we noticed an increase in glycine betaine and lysine chemotaxis to 90% and 104%, respectively, for the McpX-PP_{W-A}/McpV+McpX₇₃₄₋₇₈₈

strain (Figs. 6 & 7). This finding suggests that the presence of the pentapeptide motif, regardless of the chemoreceptor type, is sufficient to support effective chemotaxis. Next, we tested the behavior of a strain that only possesses a native McpX pentapeptide (McpW/Y/T-PP_{W-A}), which results in a one-third reduction of functional pentapeptides. This strain exhibited wild-type chemotaxis to glycine betaine, however, chemotaxis to lysine was significantly lower than wild type but significantly higher than in the strain without functional pentapeptides (Figs. 7 & 8). This result implies that the pentapeptide in McpX is sufficient to promote McpX-mediated chemotaxis, but not fully sufficient to support chemotaxis mediated by a pentapeptide-lacking receptor such as McpU. Finally, we tested the behavior of a strain with the linker and pentapeptide extension on McpV with non-functional pentapeptides in all four native pentapeptide-bearing receptors (McpX/W/Y/T-PP_{W-A}/McpV+McpX₇₃₄₋₇₈₈). This strain was fully functional in glycine betaine and lysine chemotaxis (Figs. 6 & 7). We also assayed the chemotactic reaction of this strain to acetate, which is an McpV ligand, to ascertain that McpV function has not been compromised by the C-terminal fusion. Indeed, all three strains exhibited wild-type behavior towards acetate (Fig. 9). Furthermore, a strain without any functional pentapeptide motifs (McpX/W/Y/T-PP_{W-A}) was unable to react towards acetate. This result shows that chemotaxis mediated by McpV is pentapeptide dependent regardless of the high abundance of McpV in the receptor population (71%). (Fig. 9). Taken together, these data provide information about the essentiality of the pentapeptide for chemotaxis, but also infer promiscuity regarding the location of the pentapeptide tether.

DISCUSSION

The chemotaxis signaling pathway in *E. coli* and *S. enterica* has served as a model system for studying sensory adaptation, and interactions between the adaptation enzymes and chemoreceptors have been defined on a molecular level. However, the chemotaxis systems of other bacterial species deviate from this well-established scheme. In particular, work in *B. subtilis*, *T. maritima*, *P. aeruginosa*, and *P. atrosepticum* revealed that the recruitment of CheR and CheB through the C-terminal chemoreceptor pentapeptide motif is not a commonly shared function. Here, we show that adaptation in the chemotaxis system of the symbiotic alpha-proteobacterium *S. meliloti* is pentapeptide-dependent and discuss similarities and differences to other bacterial species.

The antagonistic effect of CheR and CheB on specific chemoreceptor glutamyl residues modulates sensitivity to concentration gradients of signaling molecules. The interaction mode of both adaptation enzymes can be categorized as pentapeptide-dependent or pentapeptide-independent binding. Pentapeptide-dependent enzymes require binding to a C-terminal, conserved five amino acid motif separated from the receptor body by a 30-35 amino acid long linker that enables flexible movement to the neighboring receptors in the array [72], while pentapeptide-independent enzymes directly bind to the methylation region [73]. Although it may seem plausible that the presence of the C-terminal pentapeptide corresponds to the utilization of this moiety, studies in *P. atrosepticum* refute this correlation, as none of the eight different C-terminal chemoreceptor pentapeptides bind to any of the adaptation proteins [62]. Another unique occurrence is the specificity of one pentapeptide-bearing receptor (McpB) for one of four CheR and CheB paralogs (CheR2 and CheB2) in *P. aeruginosa*. Additionally, the presence of signature residues in CheR and CheB that are involved in pentapeptide binding are not providing clear evidence about the binding mechanism because they can be found in both, pentapeptide-dependent and pentapeptide-independent proteins [73]. Four of eight *S. meliloti* chemoreceptors harbor a C-terminal

pentapeptide motif with the consensus (N/D)WE(E/N)F (Table 1). While sequence analysis of *S. meliloti* CheR only gave weak indication of pentapeptide-dependent binding, the sequence logo predicted in pentapeptide binding is conserved in CheB (Figs. 2 & 3). Using biochemical and behavioral assays, we generated experimental proof that *S. meliloti* CheR and CheB utilize a pentapeptide-dependent binding mechanism for both, pentapeptide-bearing and pentapeptide-lacking chemoreceptors.

The dissociation constant (K_D) for the binding of CheR to the three *S. meliloti* chemoreceptor pentapeptides ranged between 10 and 15 μM (Fig. 4), which is comparable to that observed for *E. coli* CheR [66]. *E. coli* CheB and *P. aeruginosa* CheB2 have been demonstrated to bind the respective pentapeptide motif with a K_D of 160 and 93 μM , respectively [62, 74]. In *E. coli*, this binding is activation dependent, as a functional synthetic mimic of activated CheB, generated by substitution of the phosphoryl-accepting aspartyl with a cysteinyl residue exhibited a K_D of 13 μM for binding of pentapeptide-bearing receptors. [21]. We did not observe binding of non-activated CheB to the *S. meliloti* pentapeptides (Fig. 5A). However, with the stable aspartyl phosphate mimic of CheB, which was produced by modification with BeF_3^- , pentapeptides bound with K_D s between 27 and 46 μM (Fig. 5 B, C & D). This result allows the conclusion that *S. meliloti* chemoreceptors utilize the pentapeptide as high-affinity and selective tether to recruit the activated enzyme, as has been proposed for *E. coli* [21-24].

The Trp residue in position two of the pentapeptide is essential for adaptation protein binding (Figs. 4 & 5) and effective chemotaxis (Figs. 6 & 7), similar to *E. coli* Tar [58]. Quantitative capillary assays demonstrated that the McpX-specific chemotaxis response is dependent on the presence of its pentapeptide tether (Fig. 6). In addition, the chemotaxis response to a compound that is sensed by a receptor natively lacking a pentapeptide is greatly diminished or abolished when two thirds

or the entire population of pentapeptides are inactivated, respectively, as demonstrated for the McpU-mediated response to lysine (Fig. 7). We can rule out that the observed reduction in lysine chemotaxis is an artifact due to a direct recognition of lysine by McpX because we have shown previously that McpX senses proline but none of the other proteinogenic amino acids [53]. The diminished chemotaxis responses to glycine betaine and lysine in the McpX-PP_{W-A} strain suggests that the conserved pentapeptide is necessary for chemotaxis controlled by pentapeptide-bearing and pentapeptide-lacking MCPs.

The binding affinities of *S. meliloti* CheR or activated CheB are similar or 2- to 3.5-fold weaker, respectively, than their *E. coli* counterparts. However, *S. meliloti* uses only 13% of its chemoreceptor population to tether its adaptation enzymes, while 93% of *E. coli* chemoreceptors are equipped with a pentapeptide tether (Table 1). This raises the question how *S. meliloti* achieves a sufficiently high local concentration of adaptation proteins to execute their function on the remaining 87% of chemoreceptors that are devoid of the pentapeptide. We previously reported the cellular stoichiometries of chemotaxis proteins in *S. meliloti*, which concludes a ratio of pentapeptide-bearing chemoreceptor monomers to CheR to CheB equaling 1 : 3.8 : 1.6 (Fig. 1) [56, 61]. In comparison, the ratio in *E. coli* RP437 grown in minimal medium has been measured to be 1 : 0.007 : 0.01 (Fig. 1) [55]. We hypothesize that the increased levels of CheR and CheB in *S. meliloti* allow for ample recruitment of adaptation proteins to the chemosensory array regardless of the low number of pentapeptide bearing receptors (Fig. 1).

The C-terminal fusion of the pentapeptide and 6XHis tag to McpU increased its stability and negatively affected its function by interfering with controlled proteolysis (Fig. 8; [71]). In contrast, the addition of the flexible linker with the pentapeptide resulted in chemotactic responses similar to wild type. This finding implies that the flexible linker between the receptor body and the C-

terminal pentapeptide is important for chemoreceptor function. A result that is in line with studies by Li and Hazelbauer, who discovered that nested deletions of more than 20 residues in the linker sequence of Tar abolished receptor methylation, demethylation, deamidation, and chemotaxis [72]. Consequently, we manipulated the *S. meliloti* chemotaxis system by transforming natively pentapeptide-lacking chemoreceptors into pentapeptide-bearing receptors through fusion of the McpX pentapeptide in conjunction with the flexible linker to McpU and McpV. These two receptors were chosen because (i) their ligand spectrum is known, and (ii) they represent different receptor abundance levels [51, 52, 56]. Pentapeptide-hybrid receptor strains were then additionally equipped with a combination of non-functional pentapeptide mutations in the four natively pentapeptide-bearing receptors.

Our main findings and conclusions are summarized in the graphical representations of the *S. meliloti* chemosensory array in Fig. 10. The wild-type arrangement of pentapeptide abundance and location mediates wild-type chemotaxis (Fig. 10A), while absence of any functional pentapeptides leads to a complete loss of chemotaxis (Fig. 10B). Moving the pentapeptide from McpX to McpU (two receptors with similar cellular abundance) and keeping the three remaining pentapeptide-bearing receptors unchanged, results in wild-type responses to McpU, McpV, and McpX ligands (Fig. 10C). Finally, adding the McpX pentapeptide to McpV (a high-abundance receptor) in the absence of functional pentapeptides in any other receptor type, also results in wild-type responses to McpU, McpV, and McpX ligands (Fig. 10D). Moreover, the additional introduction of pentapeptide sites in the chemosensory array (71% compared to 13%) did not enhance chemotaxis beyond the wild type response. This implies that *S. meliloti* evolved to use a minimum number of pentapeptide sites to achieve efficient chemotaxis. The discovery that the pentapeptide tether can be promiscuously moved to different receptor types without compromising the robustness of the

chemotaxis system is interesting and requires further analysis. It is conceivable that the answer lays in the composition of the chemosensory array. This assumption is supported by the differential chemotaxis responses in the McpW/Y/T-PP_{W-A} strain, which constitutes two thirds of functional pentapeptides. While its McpX-mediated response to glycine betaine was unaffected, the McpU-mediated response to lysine was reduced by about one third (Figs. 6 & 7). A non-uniform arrangement of chemoreceptors across the array may lead to a differential recruitment of adaptation proteins by pentapeptide-bearing receptors and consequently, variations in chemotaxis responses.

Pentapeptide-containing chemoreceptors represent about a quarter of chemoreceptors among Rhizobiales and are abundant in bacteria establishing host interactions [60]. We determined that the *S. meliloti* chemotaxis system is pentapeptide dependent, a phenomenon that may present itself in other nitrogen-fixing plant symbionts. It remains to be solved how the significant differences in *E. coli* and *S. meliloti* chemotaxis result in efficient responses of both organisms to their environment. This work opens opportunities to unravel the adaptation system in *S. meliloti* and closely related bacteria.

MATERIALS AND METHODS

Strains and plasmids

E. coli K-12 and *S. meliloti* MV II-I derivatives are listed in Table 2. The wild-type strain, RU11/001, used in this study is a spontaneous streptomycin-resistant derivative of MVII-1 [75].

Media and growth conditions

E. coli cells were grown using lysogeny broth (LB) at 37 °C [76] while *S. meliloti* cells were grown at 30 °C in TYC medium containing 0.5 % tryptone, 0.3 % yeast extract (BD, Sparks, MD), and 6 mM CaCl₂ (Fisher, Fairlawn, NJ) with 600 µg/ml streptomycin. Minimal medium used for *S. meliloti* was Rhizobium Basal (RB) medium [0.1 mM NaCl, 0.01 Na₂MoO₄, 6.1 mM K₂HPO₄, 3.9 mM KH₂PO₄, 1 mM (NH₄)₂SO₄, 1 µM FeSO₄, 1 mM MgSO₄, 0.1 mM CaCl₂, 20 µg/l D-biotin, and 10 µg/l thiamin] [77]. Low nutrient Bromfield plates (0.04% tryptone, 0.01% yeast extract, 0.01% CaCl₂·2H₂O) were prepared as outlined by Sourjik and Schmitt [78]. Ampicillin and kanamycin concentrations were 100 µg/ml and 25 µg/ml, respectively.

Proteins purification via the IMPACT™ system

Purification of *S. meliloti* CheR and CheB using the IMPACT protocol was performed as follows. CheR and CheB were expressed in *E. coli* ER2566 from plasmids pBS450 and pBS93, respectively. Cells were grown in LB containing 100 µg/ml ampicillin at 37 °C to an OD₆₀₀ of 0.7-0.9 and gene expression was induced with 0.3 mM isopropyl-β-d-thiogalactopyranoside. Cultures were grown for 16-20 h at 16 °C before cells were harvested by centrifugation. The cell pellet was suspended in IMPACT buffer (20 mM Tris/HCl [pH 8.0], 500 mM NaCl, 1 mM EDTA, 1 mM PMSF). Cells were lysed by three passages through a French pressure cell (SLM Aminco, Silver Spring, MD) at 20,000 psi and centrifuged 48,000 x g at 4 °C for 1 h to remove insoluble portion

and unlysed cells. The soluble fraction was passed through a 0.2 μm filter and loaded on a chitin agarose (NE Biolabs, Beverly MA, USA) column (2.6 x 5.0 cm) equilibrated with IMPACT buffer at 4 °C. The column was washed with 10-20 bed volumes of IMPACT buffer containing PMSF at 4 °C. Intein-mediated cleavage was initiated by equilibration of the column with two bed volumes of IMPACT buffer containing 50 mM dithiothreitol, followed by incubation for 12-36 h at 4 °C. The protein was eluted with IMPACT buffer, and fractions were collected and analyzed using SDS polyacrylamide gel electrophoresis (SDS-PAGE). Protein-containing fractions were pooled, concentrated to 10 ml, and subjected to size exclusion chromatography (SEC) on a HiPrep™ 26/60 Sephacryl™ S-200 HR column (Cytiva) in SEC buffer (125 mM NaCl, 25 mM Tris/HCl pH 7.5). After SEC, protein-containing fractions were analyzed by SDS-PAGE and appropriate fractions pooled and concentrated to 5 ml. The protein concentration was determined using Bradford assay (BioRad) and adjusted to 50 μM .

Preparation of peptides

The acetylated pentapeptides of McpX/W (NWEEF), McpY (DWENF) and McpT (DWEEF) and the mutant variants of McpX/W (NAEEF & NWEEA), McpY (DAENF & DWENA) and McpT (DAEEF & DWEEA) were purchased from Genscript (Piscataway NJ, USA). Peptides (2-3 mg) were dissolved in 1 ml of SEC buffer, and stock solutions were titrated to pH 7.5 with 4 N NaOH. Peptide concentrations were adjusted to 1.5 mM prior to isothermal titration calorimetry measurements.

Isothermal titration calorimetry (ITC)

Direct binding analysis was performed with a MicroCal PEAQ-ITC (Malvern Panalytical Ltd). Three hundred microliters of 50 μM CheR or CheB were loaded into the sample cell and titrated with 1.5 mM pentapeptide solution from the syringe. To produce the CheB-BeF₃⁻ complex, 7 mM MgCl₂, 5 mM BeSO₄, and 30 mM NaF were mixed with 130 μM CheB for 5 min at room temperature. All ITC experiments were performed at 25 °C. Protein and ligand solutions were degassed at 27 °C before loading them into the MicroCal PEAQ-ITC. To obtain baseline titrations and for reference subtraction, pentapeptides were titrated into the buffer without protein. The dissociation constant (K_D) was determined from heat changes during titration of the ligand with the protein using the MicroCal PEAQ-ITC analysis software “one binding sites” model.

Mutant construction and genetic manipulation

S. meliloti DNA was isolated and purified as described previously, and PCR amplification of chromosomal DNA was performed according to published protocols [78]. Plasmid DNA, DNA fragments, and PCR products were purified according to the manufacturers’ instructions. Genetic mutations in *S. meliloti* were made using *in vitro* overlap-extension PCR [79]. PCR products containing the mutations were cloned into the mobilizable suicide vector pK18*mobsacB* used to transform *E. coli* S17-1, and conjugally transferred to *S. meliloti* via filter mating. Allelic replacement was achieved by consecutive selections on neomycin and 10% sucrose plates as described previously [78]. Confirmation of allelic replacement and elimination of the vector was obtained by Sanger sequencing.

Capillary assay

Capillary assays were performed as described by Adler [80] with some modifications for *S. meliloti* [53]. Motile *S. meliloti* cells were obtained by diluting stationary phase TYC cultures into 10 ml of RB overlaid onto Bromfield agar plates at a final OD₆₀₀ of 0.004 and incubating at 30 °C for 16 h. Cells were harvested at an OD₆₀₀ of 0.16 to 0.18 and sedimented by centrifugation at 3,000 × g for 5 min before being suspended to a final OD₆₀₀ of 0.15. A culture amount of 350 µl was dispensed into a U-shaped glass tube between two glass plates. One-µl Microcaps glass capillaries (Drummond Scientific, Broomall, PA) were sealed at one end over a flame and filled with ligand solution or RB for controls. Filled capillaries were placed into the bacterial ponds and incubated at room temperature for 2 h. The capillaries were then removed, broken at the sealed tip, and their contents expelled into RB. Serial dilutions were plated in triplicates onto TYC agar plates containing streptomycin, and colonies were counted after three days. The colony counts of RB control capillaries were subtracted from all ligand capillaries to account for accumulation due to random movement of bacteria into the capillary. Three technical replicates were performed for each of three biological replicates.

Immunoblotting

Polyclonal antibodies raised against the ligand binding domain of McpU were purified as described by Scharf *et al.* [81]. Briefly, 1 mg of purified protein was separated by SDS-PAGE and transferred to a nitrocellulose membrane (Amersham Protran, 0.45µm; Cytiva). A 1% Ponceau S solution was used to visualize blotted proteins, and protein-containing blot paper was cut into smaller pieces (1 cm²). Membrane pieces were transferred into a tube containing 2 ml crude serum and incubated under slow rotation at 4°C for 16 h. Next, the blots were washed three times with Phosphate-buffered saline (10 mM Na₂HPO₄, 23 mM NaH₂PO₄, 100 mM NaCl) containing 0.1% Bovine

Serum Albumin (BSA), twice with PBS containing 0.1% BSA and 0.1% Nonidet P-40, and three times with PBS containing 0.1% BSA for 5 min per wash step. Bound antibodies were eluted from the membrane by incubating with 750 μ l of 0.2 M glycine/HCl (pH 2.5) for 1 min, immediately followed by neutralization with 375 μ l of prechilled 1 M potassium phosphate (pH 9.0). The elution step was repeated, and the pooled fractions were dialyzed three times against PBS at 4 °C. Whole-cell extracts for immunoblots were prepared as follows. Wild-type and mutant strains were grown in 20 ml of *S. meliloti* motility medium to an OD₆₀₀ of 0.25. Aliquots (1 ml) were then sedimented by centrifugation at 13,000 x g for 10 min and suspended in approximately 20 μ l of the supernatant and 20 μ l of Laemmli buffer (4.5% SDS, 18.7 mM Tris/HCl [pH 6.5], 43.5% glycerol, 0.0125% bromophenol blue, and 5% β -mercaptoethanol). Samples were boiled for 10 min and stored at -20 °C. Immunoblots were performed in the same manner as described by Zatakia *et al.* [56]. Cell extracts were separated by SDS-PAGE and transferred onto a 0.45- μ m nitrocellulose membrane in transfer buffer (20% [vol/vol] methanol, 50 mM Tris, 40 mM glycine, pH 8.3). Blot membranes were blocked overnight in PBS containing 5% nonfat dry milk and 0.1% Tween 20. Blots were probed for 90 min with a 1:200 dilution of affinity-purified antibodies in PBS containing 5% nonfat dry milk and 0.1% Tween 20. Blots were washed for 30 min with PBS containing 0.1% Tween 20 with four buffer changes and then probed with a 1:10,000 dilution of donkey anti-rabbit horseradish peroxidase-conjugated antibodies. The blots were then washed for 30 min with PBS containing 0.1% Tween 20 with four buffer changes. Detection was performed by chemiluminescence (Amersham ECL Western blotting detection kit; Cytiva) using Amersham Hyperfilm ECL (Cytiva).

ACKNOWLEDGEMENTS

This study was supported by NSF grants MCB-1253234 and MCB-1817652 to B.E.S. Illustrations were created with BioRender. The authors declare no conflict of interest.

AUTHOR CONTRIBUTIONS

AA and BES conceived and designed this study, performed experiments, wrote, and edited the manuscript.

ABBREVIATED SUMMARY

The *Escherichia coli* system achieves chemotaxis adaptation by using a significantly greater number of pentapeptide-bearing MCPs (PP_{MCPs}) to tether and localize the small number of the available adaptation proteins, CheR and CheB. Conversely, *Sinorhizobium meliloti* has comparatively fewer PP_{MCPs} and greater number of CheR and CheB proteins. Investigating the role of the conserved pentapeptide in *S. meliloti* revealed that it is promiscuous but critical for chemotaxis via its binding to CheR and activated CheB.

REFERENCES

1. Kirby J.R., 2009. Chemotaxis-like regulatory systems: unique roles in diverse bacteria. *Annual Review of Microbiology*, 63:45-59.
2. Porter, S.L., Wadhams, G.H., and Armitage, J.P., 2011. Signal processing in complex chemotaxis pathways. *Nature Reviews Microbiology*, 9(3), 153-165.
3. Colin, R., Sourjik V., 2017. Emergent properties of bacterial chemotaxis pathway. *Current Opinion in Microbiology*, 39:24-33.
4. Jurica, M.S. and Stoddard, B.L., 1998. Mind your B's and R's: bacterial chemotaxis, signal transduction and protein recognition. *Structure*, 6:809-813.
5. Sourjik, V. and Wingreen, N.S., 2012. Responding to chemical gradients: bacterial chemotaxis. *Current Opinion in Cell Biology*, 24:262-268.
6. Parkinson, J.S., and Hazelbauer, G.L., Falke, J.J., 2015. Signaling and sensory adaptation in *Escherichia coli* chemoreceptors: 2015 update. *Trends in Microbiology*, 23:257-266.
7. Hazelbauer, G.L., Falke, J.J., Parkinson, J.S., 2008. Bacterial chemoreceptors: high-performance signaling in networked arrays. *Trends in Biochemical Sciences*, 33:9-19.
8. Hazelbauer, G.L., Lai, W.C. 2010. Bacterial chemoreceptors: providing enhanced features to two-component signaling. *Current Opinion in Microbiology*, 13:124-132.
9. Zhang, P., Khursigara, C.M., Hartnell, L.M., Subramaniam, S., 2007. Direct visualization of *Escherichia coli* chemotaxis receptor arrays using cryo-electron microscopy. *Proceedings of the National Academy of Sciences*, 104:3777-3781.
10. Khursigara, C.M., Wu, X., Subramaniam, S., 2008. Chemoreceptors in *Caulobacter crescentus*: trimers of receptor dimers in a partially ordered hexagonally packed array. *Journal of Bacteriology*, 190:6805-6810.
11. Greenfield, D., McEvoy, A.L., Shroff, H., Crooks, G.E., Wingreen, N.S., Betzig, E., Liphardt, J., 2009. Self-organization of the *Escherichia coli* chemotaxis network imaged with super-resolution light microscopy. *PLoS biology*, 7:e1000137.
12. Stewart R.C., 1997. Kinetic characterization of phosphotransfer between CheA and CheY in the bacterial chemotaxis signal transduction pathway. *Biochemistry*, 36:2030-2040.
13. Bren, A., and Eisenbach, M., 1998. The N terminus of the flagellar switch protein, FliM, is the binding domain for the chemotactic response regulator, CheY. *Elsevier*, vol 278, 507-514.
14. Toker, A.S., Macnab, R.M., 1997. Distinct regions of bacterial flagellar switch protein FliM interact with FliG, FliN and CheY. *Journal of Molecular Biology*, 273:623-634.
15. Zhao, R., Collins, E.J., Bourret, R.B., Silversmith, R.E., 2002. Structure and catalytic mechanism of the *E. coli* chemotaxis phosphatase CheZ. *Nature Structural Biology*, 9:570-575.
16. Blat, Y. and Eisenbach, M., 1994. Phosphorylation-dependent binding of the chemotaxis signal molecule CheY to its phosphatase, CheZ. *Biochemistry*, 33:902-906.

17. Silversmith, R.E., 2010. Auxiliary phosphatases in two-component signal transduction. *Current Opinion in Microbiology*, 13:177-183.
18. Djordjevic, S., Stock, A.M., 1998. Chemotaxis receptor recognition by protein methyltransferase CheR. *Nature Structural Biology*, 5:446-450.
19. Li M Hazelbauer 2020. Methyltransferase CheR binds to its chemoreceptor substrates independent of their signaling conformation yet modifies them differentially. *Protein Science* 29:443-454.
20. Yonekawa H Hayashi H Parkinson J 1983. Requirement of the CheB function for sensory adaptation in *Escherichia coli*. *Journal of Bacteriology* 156:1228-1235.
21. Li M Xu X Zou X Hazelbauer 2021. A selective tether recruits activated response regulator CheB to its chemoreceptor substrate. *Mbio* 12:e03106-21.
22. Wu J Li J Li G Long Weis 1996. The receptor binding site for the methyltransferase of bacterial chemotaxis is distinct from the sites of methylation. *Biochemistry* 35:4984-4993.
23. Barnakov Barnakova Hazelbauer 1999. Efficient adaptational demethylation of chemoreceptors requires the same enzyme-docking site as efficient methylation. *Proceedings of the National Academy of Sciences* 96:10667-10672.
24. Li M Hazelbauer 2005. Adaptational assistance in clusters of bacterial chemoreceptors. *Molecular Microbiology* 56:1617-1626.
25. Feng X, Lilly AA, Hazelbauer GL. 1999. Enhanced function conferred on low-abundance chemoreceptor Trg by a methyltransferase-docking site. *Journal of Bacteriology* 181:3164-3171.
26. Crop Production 2020 Summary United States Department of Agriculture.
27. Biró, B., Köves-Péchy, K., Vörös, I., Takács, T., Eggenberger, P., Strasser, R., 2000. Interrelations between *Azospirillum* and *Rhizobium* nitrogen-fixers and arbuscular mycorrhizal fungi in the rhizosphere of alfalfa in sterile, AMF-free or normal soil conditions. *Applied Soil Ecology* 15:159-168.
28. Galibert, F., Finan, T.M., Long, S.R., Pühler, A., Abola, P., Ampe, F., Barloy-Hubler, F., Barnett, M.J., Becker, A., Boistard, P., 2001. The composite genome of the legume symbiont *Sinorhizobium meliloti*. *Science*. 293:668-672.
29. Scharf BE, Hynes MF, Alexandre GM. 2016. Chemotaxis signaling systems in model beneficial plant–bacteria associations. *Plant Molecular Biology* 90:549-559.
30. Sourjik V, Schmitt R. 1998. Phosphotransfer between CheA, CheY1, and CheY2 in the chemotaxis signal transduction chain of *Rhizobium meliloti*. *Biochemistry* 37:2327-2335.
31. Kuo SC, Koshland Jr DE. 1987. Roles of cheY and cheZ gene products in controlling flagellar rotation in bacterial chemotaxis of *Escherichia coli*. *Journal of Bacteriology* 169:1307-1314.
32. Dogra G, Purschke FG, Wagner V, Haslbeck M, Kriehuber T, Hughes JG, Van Tassell ML, Gilbert C, Niemeyer M, Ray WK. 2012. *Sinorhizobium meliloti* CheA complexed with CheS

exhibits enhanced binding to CheY1, resulting in accelerated CheY1 dephosphorylation. *Journal of Bacteriology* 194:1075-1087.

33. Ulrich LE, Zhulin IB. 2010. The MiST2 database: a comprehensive genomics resource on microbial signal transduction. *Nucleic Acids Research* 38:D401-D407.

34. Bibikov SI, Biran R, Rudd KE, Parkinson JS. 1997. A signal transducer for aerotaxis in *Escherichia coli*. *Journal of Bacteriology* 179:4075-4079.

35. Falke JJ, Hazelbauer GL. 2001. Transmembrane signaling in bacterial chemoreceptors. *Trends in Biochemical Sciences* 26:257-265.

36. Ortega Á, Zhulin IB, Krell T. 2017. Sensory repertoire of bacterial chemoreceptors. *Microbiology and Molecular Biology Reviews* 81:e00033-17.

37. Springer MS, Goy MF, Adler J. 1977. Sensory transduction in *Escherichia coli*: two complementary pathways of information processing that involve methylated proteins. *Proceedings of the National Academy of Sciences* 74:3312-3316.

38. Milburn MV, Prive GG, Milligan DL, Scott WG, Yeh J, Jancarik J, Koshland Jr DE, Kim S-H. 1991. Three-dimensional structures of the ligand-binding domain of the bacterial aspartate receptor with and without a ligand. *Science* 254:1342-1347.

39. Gardina P, Conway C, Kossman M, Manson M. 1992. Aspartate and maltose-binding protein interact with adjacent sites in the Tar chemotactic signal transducer of *Escherichia coli*. *Journal of bacteriology* 174:1528-1536.

40. Hazelbauer GL. 1975. Maltose chemoreceptor of *Escherichia coli*. *Journal of Bacteriology* 122:206-214.

41. Tso W-W, Adler J. 1974. Negative chemotaxis in *Escherichia coli*. *Journal of Bacteriology* 118:560-576.

42. Lin L-N, Li J, Brandts JF, Weis RM. 1994. The serine receptor of bacterial chemotaxis exhibits half-site saturation for serine binding. *Biochemistry* 33:6564-6570.

43. Hegde M, Englert DL, Schrock S, Cohn WB, Vogt C, Wood TK, Manson MD, Jayaraman A. 2011. Chemotaxis to the quorum-sensing signal AI-2 requires the Tsr chemoreceptor and the periplasmic LsrB AI-2-binding protein. *Journal of Bacteriology* 193:768-773.

44. Rebbapragada A, Johnson MS, Harding GP, Zuccarelli AJ, Fletcher HM, Zhulin IB, Taylor BL. 1997. The Aer protein and the serine chemoreceptor Tsr independently sense intracellular energy levels and transduce oxygen, redox, and energy signals for *Escherichia coli* behavior. *Proceedings of the National Academy of Sciences* 94:10541-10546.

45. Pasupuleti S, Sule N, Cohn WB, MacKenzie DS, Jayaraman A, Manson MD. 2014. Chemotaxis of *Escherichia coli* to norepinephrine (NE) requires conversion of NE to 3, 4-dihydroxymandelic acid. *Journal of Bacteriology* 196:3992-4000.

46. Harayama S, Palva ET, Hazelbauer GL. 1979. Transposon-insertion mutants of *Escherichia coli* K12 defective in a component common to galactose and ribose chemotaxis. *Molecular and General Genetics* 171:193-203.

47. Manson MD, Blank V, Brade G, Higgins CF. 1986. Peptide chemotaxis in *E. coli* involves the Tap signal transducer and the dipeptide permease. *Nature* 321:253-256.
48. Liu X, Parales RE. 2008. Chemotaxis of *Escherichia coli* to pyrimidines: a new role for the signal transducer tap. *Journal of bacteriology* 190:972-979.
49. Meier VM, Muschler P, Scharf BE. 2007. Functional analysis of nine putative chemoreceptor proteins in *Sinorhizobium meliloti*. *Journal of bacteriology* 189:1816-1826.
50. Baaziz H, Compton KK, Hildreth SB, Helm RF, Scharf BE. 2021. McpT, a broad-range carboxylate chemoreceptor in *Sinorhizobium meliloti*. *Journal of Bacteriology* 203:e00216-21.
51. Compton KK, Hildreth SB, Helm RF, Scharf BE. 2018. *Sinorhizobium meliloti* chemoreceptor McpV senses short-chain carboxylates via direct binding. *Journal of Bacteriology* 200:e00519-18.
52. Webb BA, Compton KK, Del Campo JSM, Taylor D, Sobrado P, Scharf BE. 2017. *Sinorhizobium meliloti* chemotaxis to multiple amino acids is mediated by the chemoreceptor McpU. *Molecular Plant-Microbe Interactions* 30:770-777.
53. Webb BA, Karl Compton K, Castañeda Saldaña R, Arapov TD, Keith Ray W, Helm RF, Scharf BE. 2017. *Sinorhizobium meliloti* chemotaxis to quaternary ammonium compounds is mediated by the chemoreceptor McpX. *Molecular Microbiology* 103:333-346.
54. Salar S, Ball NE, Baaziz H, Nix JC, Sobe RC, Compton KK, Zhulin IB, Brown AM, Scharf BE, Schubot FD. 2023. The structural analysis of the periplasmic domain of *Sinorhizobium meliloti* chemoreceptor McpZ reveals a novel fold and suggests a complex mechanism of transmembrane signaling. *Proteins: Structure, Function, and Bioinformatics*.
55. Li M, Hazelbauer GL. 2004. Cellular stoichiometry of the components of the chemotaxis signaling complex. *Journal of bacteriology* 186:3687-3694.
56. Zatakia HM, Arapov TD, Meier VM, Scharf BE. 2018. Cellular stoichiometry of methyl-accepting chemotaxis proteins in *Sinorhizobium meliloti*. *Journal of Bacteriology* 200:e00614-17.
57. Meier VM, Scharf BE. 2009. Cellular localization of predicted transmembrane and soluble chemoreceptors in *Sinorhizobium meliloti*. *Journal of bacteriology* 191:5724-5733.
58. Shiomi D, Okumura H, Homma M, Kawagishi I. 2000. The aspartate chemoreceptor Tar is effectively methylated by binding to the methyltransferase mainly through hydrophobic interaction. *Molecular Microbiology* 36:132-140.
59. Perez E, Stock AM. 2007. Characterization of the *Thermotoga maritima* chemotaxis methylation system that lacks pentapeptide-dependent methyltransferase CheR: MCP tethering. *Molecular Microbiology* 63:363-378.
60. Ortega Á, Krell T. 2020. Chemoreceptors with C-terminal pentapeptides for CheR and CheB binding are abundant in bacteria that maintain host interactions. *Computational and structural biotechnology journal* 18:1947-1955.

61. Arapov TD, Saldaña RC, Sebastian AL, Ray WK, Helm RF, Scharf BE. 2020. Cellular stoichiometry of chemotaxis proteins in *Sinorhizobium meliloti*. *Journal of Bacteriology* 202:e00141-20.
62. Velando F, Gavira JA, Rico-Jiménez M, Matilla MA, Krell T. 2020. Evidence for pentapeptide-dependent and independent CheB methylesterases. *International Journal of Molecular Sciences* 21:8459.
63. Djordjevic S, Stock AM. 1997. Crystal structure of the chemotaxis receptor methyltransferase CheR suggests a conserved structural motif for binding S-adenosylmethionine. *Structure* 5:545-558.
64. Djordjevic S, Goudreau PN, Xu Q, Stock AM, West AH. 1998. Structural basis for methylesterase CheB regulation by a phosphorylation-activated domain. *Proceedings of the National Academy of Sciences* 95:1381-1386.
65. Barnakov AN, Barnakova LA, Hazelbauer GL. 2001. Location of the receptor-interaction site on CheB, the methylesterase response regulator of bacterial chemotaxis. *Journal of Biological Chemistry* 276:32984-32989.
66. Yi X, Weis R. 2002. The receptor docking segment and S-adenosyl-L-homocysteine bind independently to the methyltransferase of bacterial chemotaxis. *Biochimica et Biophysica Acta (BBA)-Protein Structure and Molecular Enzymology* 1596:28-35.
67. García-Fontana C, Corral Lugo A, Krell T. 2014. Specificity of the CheR2 methyltransferase in *Pseudomonas aeruginosa* is directed by a C-terminal pentapeptide in the McpB chemoreceptor. *Science Signaling* 7:ra34-ra34.
68. Lupas A, Stock J. 1989. Phosphorylation of an N-terminal regulatory domain activates the CheB methylesterase in bacterial chemotaxis. *Journal of Biological Chemistry* 264:17337-17342.
69. Anand GS, Goudreau PN, Stock AM. 1998. Activation of methylesterase CheB: evidence of a dual role for the regulatory domain. *Biochemistry* 37:14038-14047.
70. Stewart RC. 1993. Activating and inhibitory mutations in the regulatory domain of CheB, the methylesterase in bacterial chemotaxis. *Journal of Biological Chemistry* 268:1921-1930.
71. Arapov TD, Kim J, Cronin RM, Pahima M, Scharf BE. 2020. Programmed proteolysis of chemotaxis proteins in *Sinorhizobium meliloti*: features in the C-terminal region control McpU degradation. *Journal of Bacteriology* 202:e00124-20.
72. Li M, Hazelbauer GL. 2006. The carboxyl-terminal linker is important for chemoreceptor function. *Molecular microbiology* 60:469-479.
73. Shiomi D, Zhulin IB, Homma M, Kawagishi I. 2002. Dual recognition of the bacterial chemoreceptor by chemotaxis-specific domains of the CheR methyltransferase. *Journal of Biological Chemistry* 277:42325-42333.
74. Barnakov AN, Barnakova LA, Hazelbauer GL. 2002. Allosteric enhancement of adaptational demethylation by a carboxyl-terminal sequence on chemoreceptors. *Journal of Biological Chemistry* 277:42151-42156.

75. Krupski G, Götz R, Ober K, Pleier E, Schmitt R. 1985. Structure of complex flagellar filaments in *Rhizobium meliloti*. *Journal of Bacteriology* 162:361-366.
76. Bertani G. 1951. Studies on lysogenesis I: the mode of phage liberation by lysogenic *Escherichia coli*. *Journal of bacteriology* 62:293-300.
77. Götz R, Limmer N, Ober K, Schmitt R. 1982. Motility and chemotaxis in two strains of *Rhizobium* with complex flagella. *Microbiology* 128:789-798.
78. Sourjik V, Schmitt R. 1996. Different roles of CheY1 and CheY2 in the chemotaxis of *Rhizobium meliloti*. *Molecular Microbiology* 22:427-436.
79. Bryksin AV, Matsumura I. 2010. Overlap extension PCR cloning: a simple and reliable way to create recombinant plasmids. *Biotechniques* 48:463-465.
80. Adler J. 1973. A method for measuring chemotaxis and use of the method to determine optimum conditions for chemotaxis by *Escherichia coli*. *Microbiology* 74:77-91.
81. Scharf B, Schuster-Wolff-Bühning H, Rachel R, Schmitt Rd. 2001. Mutational analysis of the *Rhizobium lupini* H13-3 and *Sinorhizobium meliloti* flagellin genes: importance of flagellin A for flagellar filament structure and transcriptional regulation. *Journal of Bacteriology* 183:5334-5342.
82. Hanahan D, Meselson M. 1983. [24] Plasmid screening at high colony density, p 333-342, *Methods in Enzymology*, vol 100. Elsevier.
83. Simon R, O'Connell M, Labes M, Pühler A. 1986. Plasmid vectors for the genetic analysis and manipulation of rhizobia and other gram-negative bacteria. *Methods in enzymology* 118:640-659.
84. Pleier E, Schmitt R. 1991. Expression of two *Rhizobium meliloti* flagellin genes and their contribution to the complex filament structure. *Journal of bacteriology* 173:2077-2085.

TABLES

Table 2.1. A comparison of MCPs with pentapeptide in *E. coli* and *S. meliloti*

	<i>E. coli</i>	<i>S. meliloti</i>
MCPs with pentapeptide (PP _{MCPs})	Tar, Tsr	McpT, McpW, McpX McpY,
PP sequence of each MCP	NWETF, NWETF	DWEEF, NWEWF, NWEWF, DWENF
Cellular abundance of PP _{MCPs} in total MCP population	93%	13%

Table 2.2. Bacterial strains and plasmids

Strain/Plasmid	Relevant characteristics	Source or Reference
<i>E. coli</i>		
DH5 α	<i>recA1 endA1</i>	[82]
ER2566	<i>ion ompT lacZ::T7</i>	New England Biolabs
S17-1	Sm ^r Tp ^r ; <i>recA endA thi hsdR</i> RP4-2 Tc::Mu::Tn7	[83]
<i>S. meliloti</i>		
RU11/001	Sm ^r ; Spontaneous streptomycin-resistant wild-type strain	[84]
RU11/805	$\Delta mcpX$	[56]
RU11/828	$\Delta mcpU$	[56]
BS220	Sm ^r , McpU+6X His	[71]
BS285	Sm ^r , McpX-W785A (McpX-PP _{W-A})	This work

BS308	Sm ^r , McpX-W785A, McpW-W686A, McpY-W590A, McpT-W662A (McpX/W/Y/T-PP _{W-A})	This work
BS290	Sm ^r , McpU+McpX ₇₈₄₋₇₈₈ (PP)	This work
BS327	Sm ^r , McpU+McpX ₇₃₄₋₇₈₈	This work
BS344	Sm ^r , McpX-PP _{W-A} /McpU+McpX ₇₃₄₋₇₈₈	This work
BS345	Sm ^r , WT /McpV+McpX ₇₃₄₋₇₈₈	This work
BS346	Sm ^r , McpX-PP _{W-A} /McpV+McpX ₇₃₄₋₇₈₈	This work
BS347	Sm ^r , McpX/W/Y/T-PP _{W-A} /McpV+McpX ₇₃₄₋₇₈₈	This work
BS348	Sm ^r , McpX/W/Y/T-PP _{W-A} /McpX	This work
Plasmids		This work
pTYB1	Ap ^r ; expression vector for IMPACT system	New England Biolabs
pBS93	Ap ^r ; pTYB1- <i>cheB</i>	[61]
pBS450	Ap ^r ; pTYB1- <i>cheR</i>	[61]

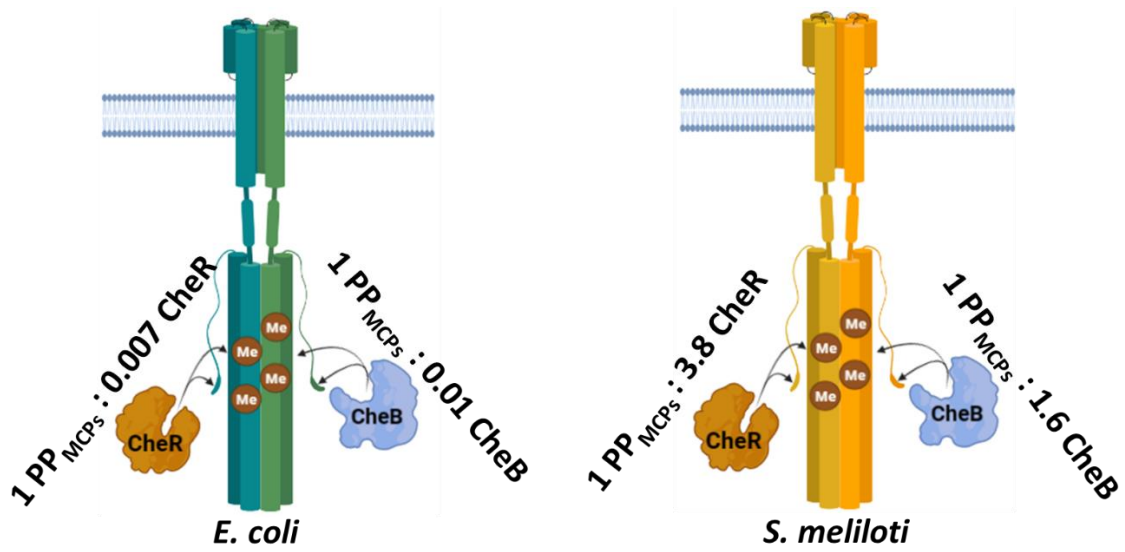


Fig. 2. 1 Comparative features of the chemotaxis adaptation systems in *E. coli* (strain RP437 grown in minimal medium) and *S. meliloti*.

The cellular ratios of CheR and CheB proteins to the pentapeptide-bearing chemoreceptor monomers (PP_{MCPs}) were obtained by dividing the number of PP_{MCPs} by the number of CheR or CheB proteins reported in [55, 56, 61].

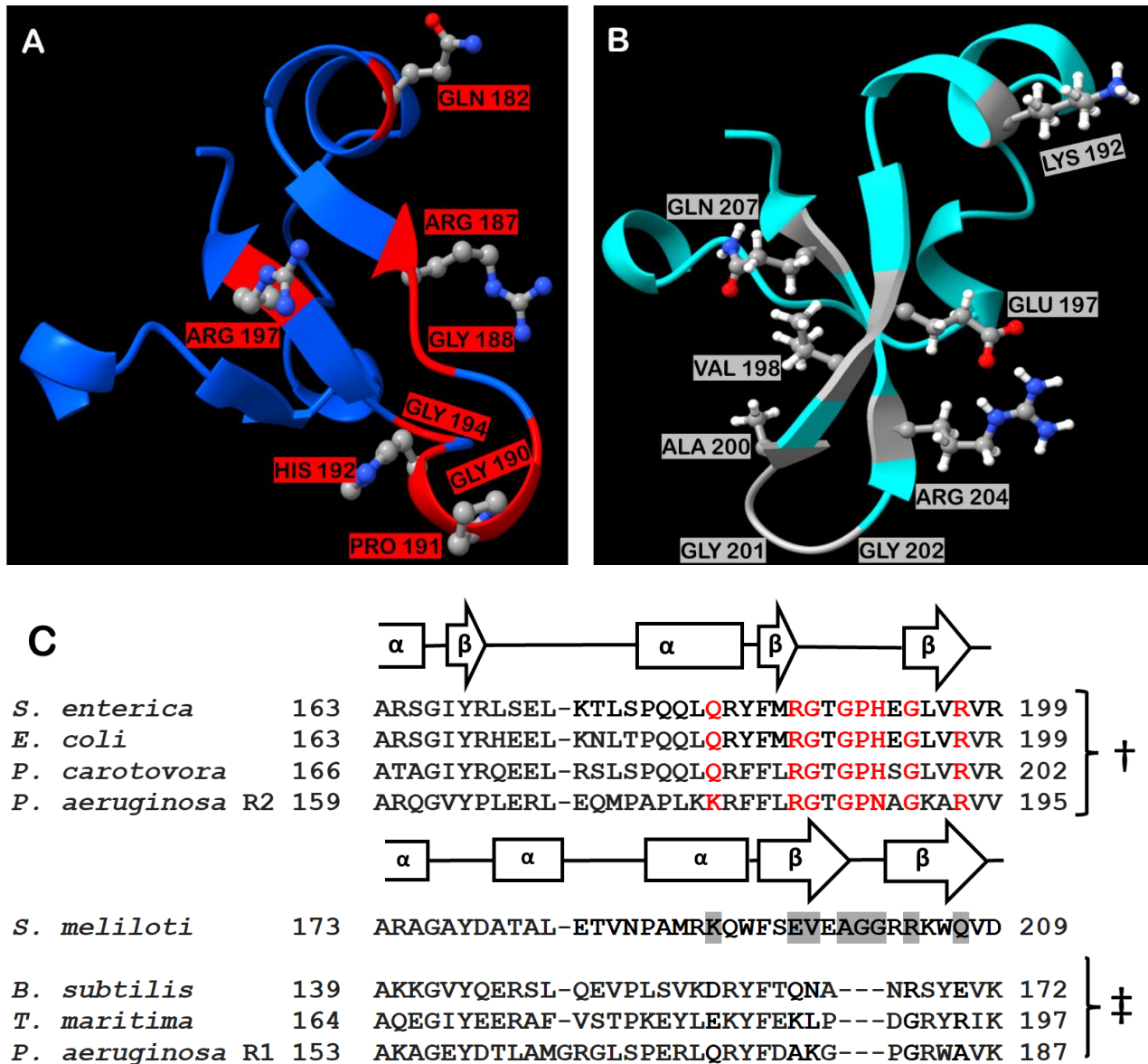


Fig. 2. 2 An illustration of residues in the β -subdomain CheR that are important for the interaction with the MCP pentapeptide motif.

A. Ribbon diagram of a segment of the *S. enterica* CheR β -subdomain. The colors represent carbon (gray), nitrogen (blue), and oxygen (red). Residues in *S. enterica* CheR shown to interact with the pentapeptide motif are labelled in red. Image was generated from ChimeraX using PDB ID 1BC5 B. Ribbon diagram of the predicted *S. meliloti* CheR β -subdomain. Shown in the diagram are the corresponding residues of *S. meliloti* CheR (highlighted in gray) in the same position as *S. enterica* CheR. The colors represent carbon (gray), nitrogen (blue), hydrogen (white), and oxygen (red). The image was generated from ChimeraX using an AlphaFold predicted structure. C. Sequence alignment and the accompanying secondary structure map of a segment of the β -subdomain of pentapeptide-dependent and pentapeptide-independent CheR proteins. The secondary structure maps are that of *S. enterica* and *S. meliloti* CheR. Species were selected based on known pentapeptide-dependent and pentapeptide-independent CheR proteins [18, 22, 59, 67]. The alignment was performed using CLUSTAL OMEGA with the default gap opening penalty of 6 bits, gap

extension of 1 bit. The symbols † and ‡ represent bacterial CheR β -subdomains that bind or do not bind to the C-terminal pentapeptide, respectively.

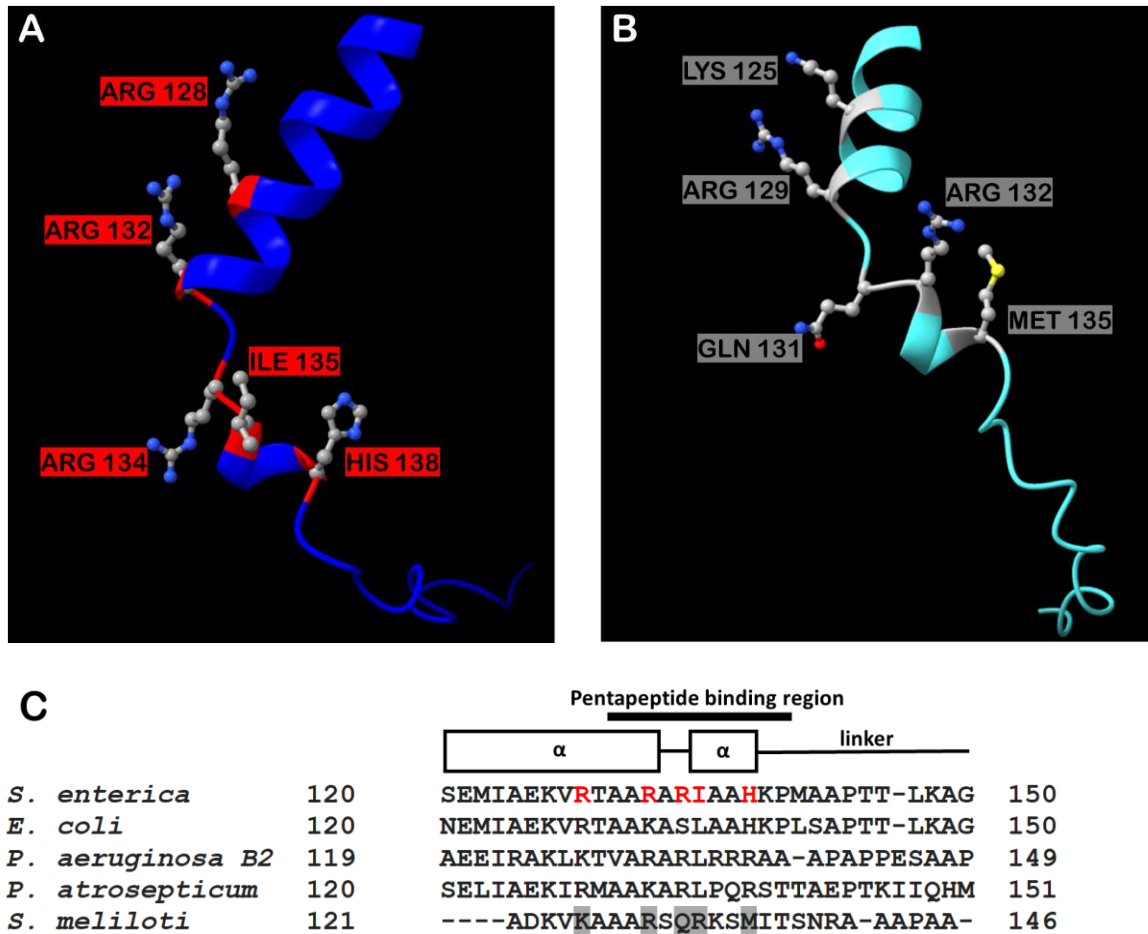


Fig. 2. 3 An illustration of residues in CheB that are important for the interaction with the MCP pentapeptide motif.

A. Ribbon diagram of a region of *S. enterica* CheB that binds the pentapeptide motif. The colors represent carbon (gray) and nitrogen (blue). Residues in *S. enterica* CheB shown to interact with the pentapeptide motif are labelled in red. Image was generated from ChimeraX using PDB ID 1A2O B. A ribbon diagram of the *S. meliloti* CheB region predicted to bind to the pentapeptide motif. Shown in the diagram are the corresponding residues of *S. meliloti* CheB (highlighted in gray) in the same position as *S. enterica* CheB. The colors represent carbon (gray), nitrogen (blue), oxygen (red), and sulfur (yellow). The image was generated from ChimeraX using an AlphaFold predicted structure. C. Sequence alignment of *S. enterica*, *E. coli*, *P. aeruginosa*, *P. atrosepticum*, and *S. meliloti* CheB. Species were selected based on published research of known pentapeptide-dependent and pentapeptide-independent CheB proteins. The alignment was performed using CLUSTAL OMEGA with the default gap opening penalty of 6 bits, gap extension of 1 bit.

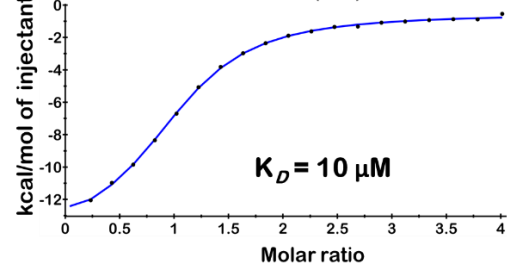
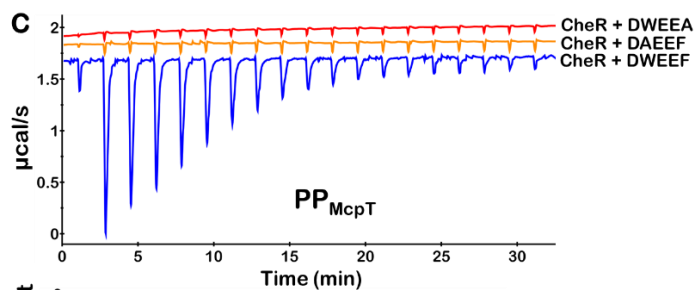
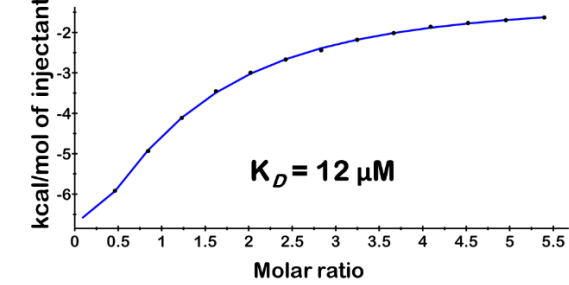
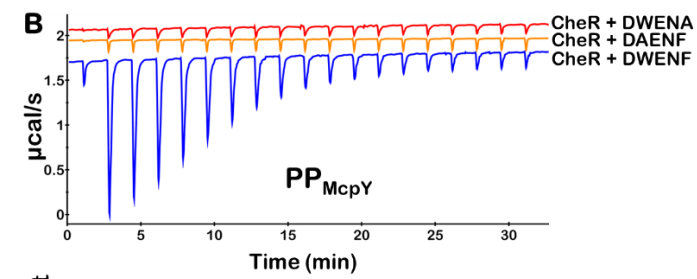
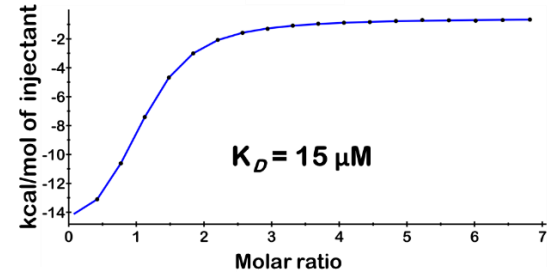
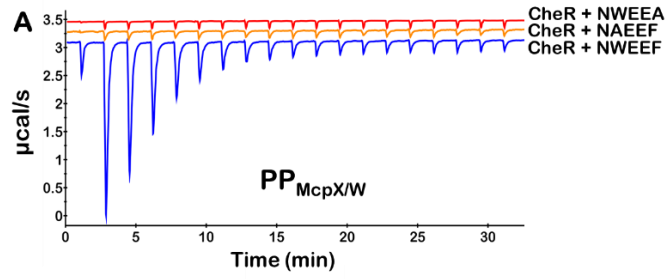


Fig. 2. 4 Binding of C-terminal MCP pentapeptides and their mutant variants to CheR.

A. McpX/W ($PP_{McpX/W}$), B. McpY (PP_{McpY}), C. McpT (PP_{McpT}). Upper panels: Representative isothermal titration calorimetry (ITC) raw titration data of 50 μ M recombinant CheR with 1.5 mM of WT (blue), pentapeptide with Trp-Ala substitution (orange), and pentapeptide with Phe-Ala substitution (red). Lower panels: Integrated raw data to obtain K_D s of 15 μ M, 12 μ M, and 10 μ M were performed using 3- μ L aliquots of the pentapeptides. Data were fitted using the “one binding site model” of the Malvern MicroCal PEAQ-ITC Analysis Software.

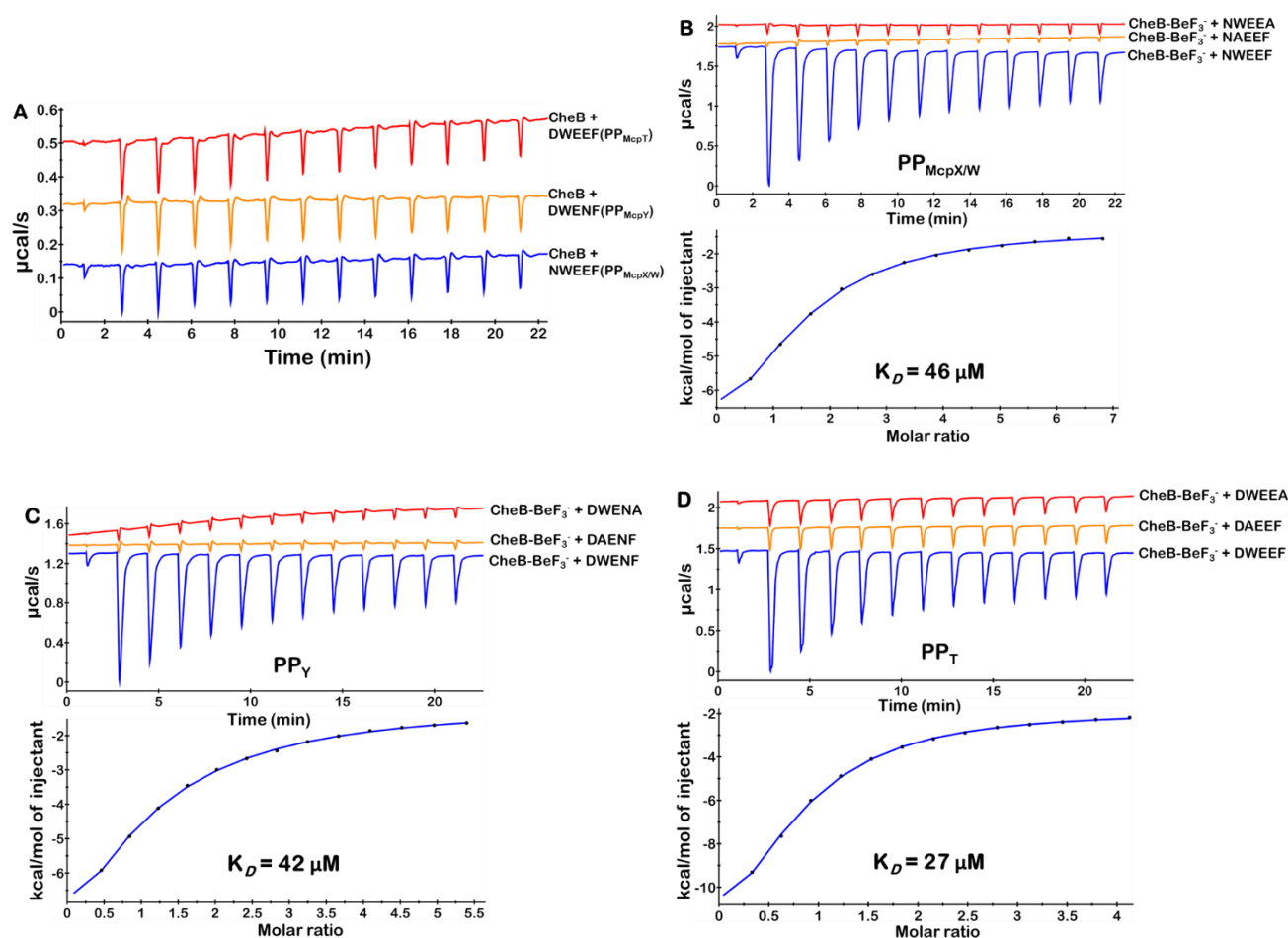


Fig. 2. 5 Isothermal titration calorimetry of recombinant CheB and CheB-BeF₃⁻ with pentapeptides.

A. Representative isothermal titration calorimetry (ITC) raw titration data of 50 μ M CheB with 1.8 mM pentapeptide of McpX/W (blue), McpY (orange), and McpT (red). Binding of 50 μ M CheB-BeF₃⁻ complex with the 1.8 mM pentapeptide of B. McpX/W ($PP_{McpX/W}$), C. McpY (PP_{McpY}), and D. McpT (PP_{McpT}). WT pentapeptide (blue), Trp-Ala substitution (orange) and Phe-Ala substitution (red). Upper panels: Representative isothermal titration calorimetry (ITC) raw titration data. Lower panels: Integrated raw data to obtain K_D s of 46 μ M, 42 μ M, and 27 μ M for the binding of the CheB-BeF₃⁻ complex to $PP_{McpX/W}$, PP_{McpY} and PP_{McpT} , respectively. Data were fitted using the “one binding site model” of the Malvern MicroCal PEAQ-ITC Analysis Software.

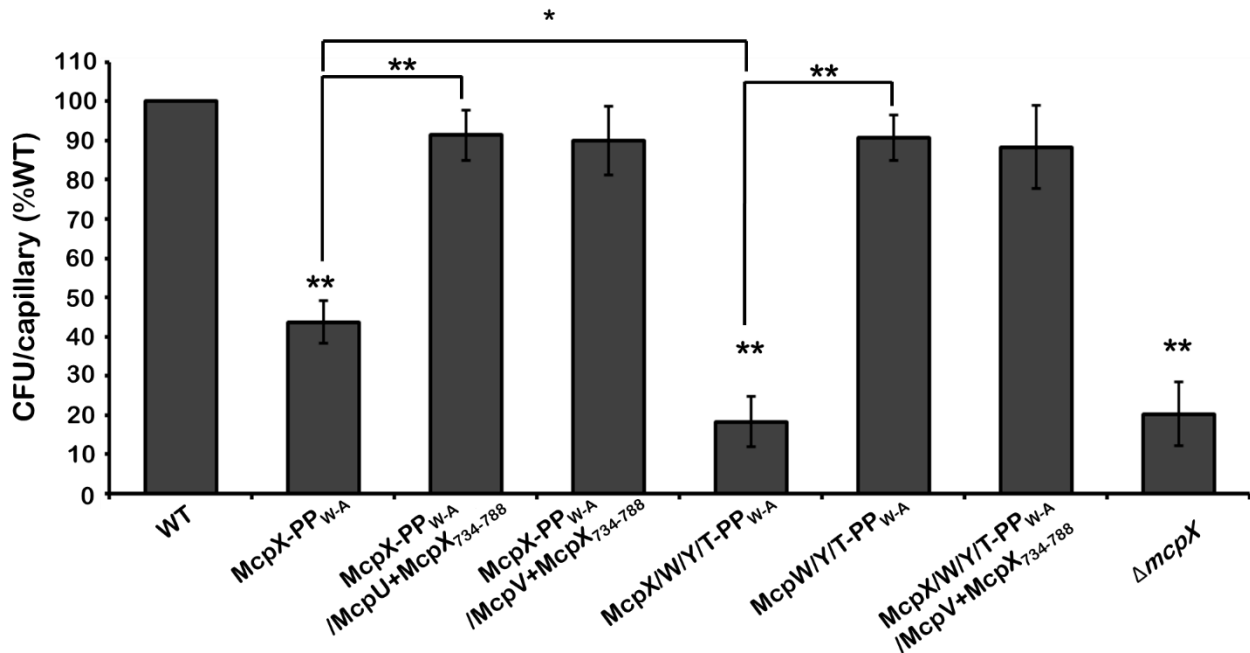


Fig. 2. 6 Chemotactic responses to 10 mM glycine betaine in the capillary assay for *S. meliloti* strains. WT (RU11/001), McpX-PP_{W-A} (BS285), McpX-PP_{W-A}/McpU+McpX₇₃₄₋₇₈₈ (BS344), McpX-PP_{W-A}/McpV+McpX₇₃₄₋₇₈₈ (BS346), McpX/W/Y/T-PP_{W-A} (BS308), McpW/Y/T-PP_{W-A} (BS348), McpX/W/Y/T-PP_{W-A}/McpV+McpX₇₃₄₋₇₈₈ (BS347) and ΔmcpX (RU11/805). Data are the means and standard deviations from three biological replicates. Asterisks denotes *P* values determined by two-tailed student t-test; *, *P* < 0.005; **, *P* < 0.0001. Unless otherwise indicated, *P* values represent significant differences compared to wild type.

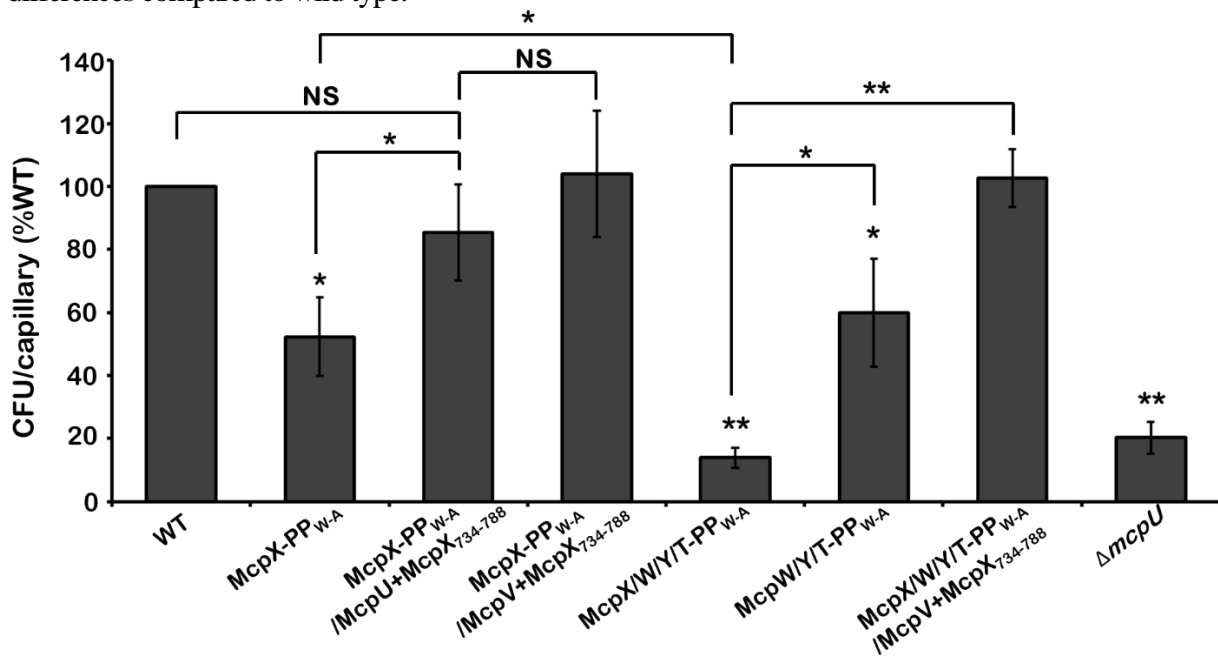


Fig. 2. 7 Chemotactic responses to 10 mM lysine in capillary assays for *S. meliloti* strains. WT (RU11/001), McpX-PP_{W-A} (BS285), McpX-PP_{W-A}/McpU+McpX₇₃₄₋₇₈₈ (BS344), McpX-PP_{W-A}/McpV+McpX₇₃₄₋₇₈₈ (BS346), McpX/W/Y/T-PP_{W-A} (BS308), McpW/Y/T-PP_{W-A} (BS348),

McpX/W/Y/T-PP_{W-Δ}/McpV+McpX₇₃₄₋₇₈₈ (BS347) and $\Delta mcpU$ (RU11/828). Data are the means and standard deviations from three biological replicates. Statistical significance was determined by a two-tailed Student t-test *, $P < 0.05$; **, $P < 0.0005$ NS, not significant ($P > 0.05$). Unless otherwise indicated, P values represent significant differences compared to wild type.

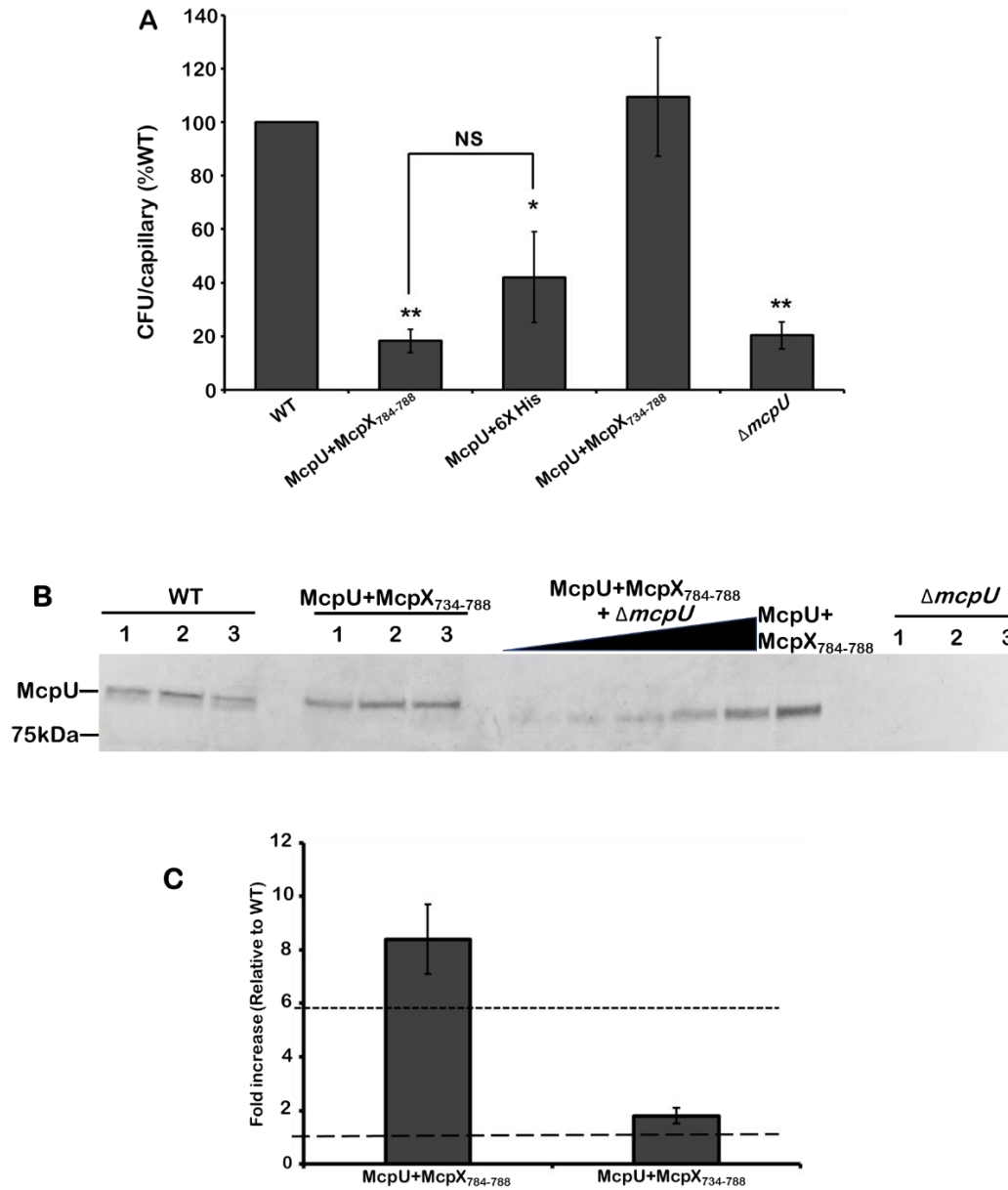


Fig. 2. 8 Chemotactic responses and relative abundance of McpU in mutant strains with C-terminal extensions.

A. Chemotaxis of *S. meliloti* WT (RU11/001), McpU+McpX₇₈₄₋₇₈₈ (BS290), McpU+6XHis (BS220), McpU+McpX₇₃₄₋₇₈₈ (BS327), and $\Delta mcpU$ (RU11/828) to 10 mM lysine in the capillary assay. Data are the means and standard deviations from three biological replicates. Asterisks denote P values determined by two-tailed student t-test; *, $P < 0.005$; **, $P < 0.00005$ NS, not significant ($P > 0.05$). Unless otherwise indicated, P values represent significant differences compared to wild type. B. Representative immunoblot used to quantify the relative abundance of McpU in cell lysates of the wild type compared to mutant strains.

The first three lanes contain WT lysates (RU11/001) from 1 ml of culture at an OD₆₀₀ of 0.25. The next three lanes contain McpU+McpX₇₃₄₋₇₈₈ (BS327) lysates from 1 ml of culture at an OD₆₀₀ of 0.25. A standard curve was made using lanes denoted by a wedge shape containing a mix of McpU+McpX₇₈₄₋₇₈₈ (BS290) and $\Delta mcpU$ (RU11/828) at volume ratios of 100 μ l + 900 μ l, 150 μ l + 850 μ l, 250 μ l + 750 μ l, 500 μ l + 500 μ l, and 750 μ l + 250 μ l, yielding a total volume of 1 ml of culture at an OD₆₀₀ of 0.25. The next lane contains lysate from 1 ml BS290, and the last three lanes contain $\Delta mcpU$ (RU11/828) lysates from 1 ml of culture at an OD₆₀₀ of 0.25. C. Relative abundance of McpU in mutant strains with C-terminal extensions compared to wild type and BS220 (McpU+6X His; [71]). The long and short dashed lines represent abundance of McpU in wild type and BS220, respectively. Values and error bars are the means and standard deviations from three biological replicates with statistical significance determined by a two-tailed student t-test ($P < 0.05$).

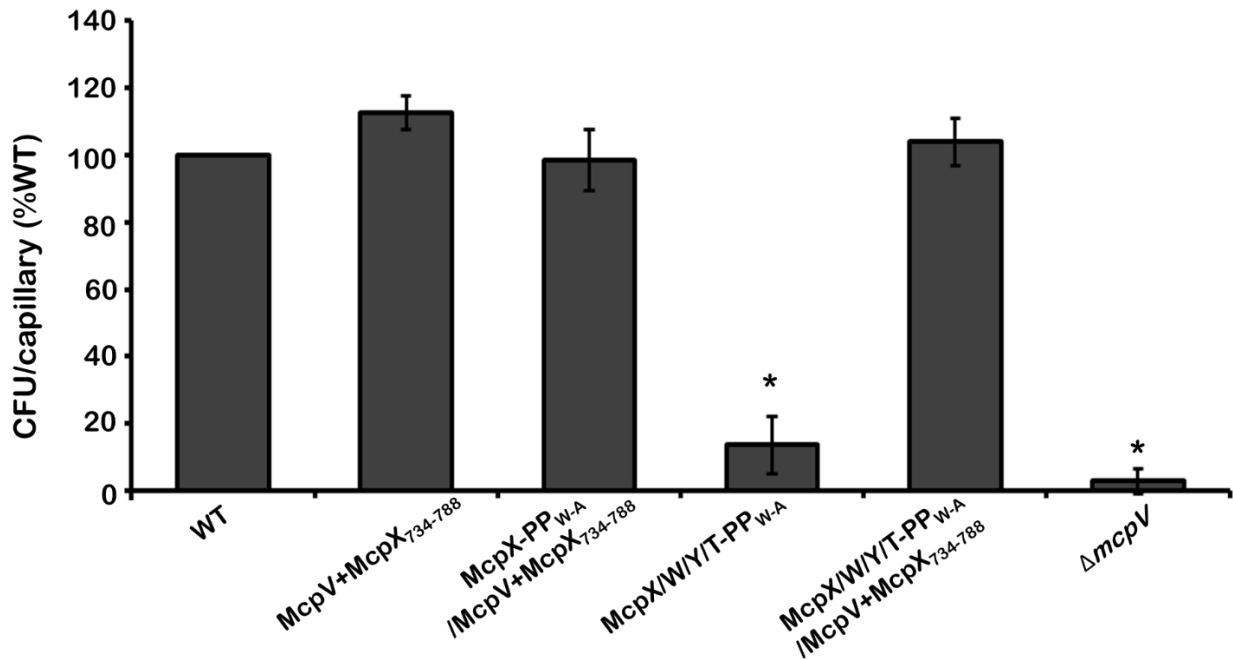


Fig. 2. 9 Chemotactic responses to 1 mM acetate in capillary assays for *S. meliloti* strains. WT (RU11/001), McpV+McpX₇₃₄₋₇₈₈ (BS345), McpX-PP_{w-A}/McpV+McpX₇₃₄₋₇₈₈ (BS346), McpX/W/Y/T-PP_{w-A} (BS308), McpX/W/Y/T-PP_{w-A}/McpV+McpX₇₃₄₋₇₈₈ (BS347) and $\Delta mcpV$ (RU11/830). Data are the means and standard deviations from three biological replicates. Statistical significance was determined by a two-tailed Student t-test *, $P < 0.005$; **, $P < 0.0005$ NS, not significant ($P > 0.05$). Unless otherwise indicated, P values represent significant differences compared to wild type.

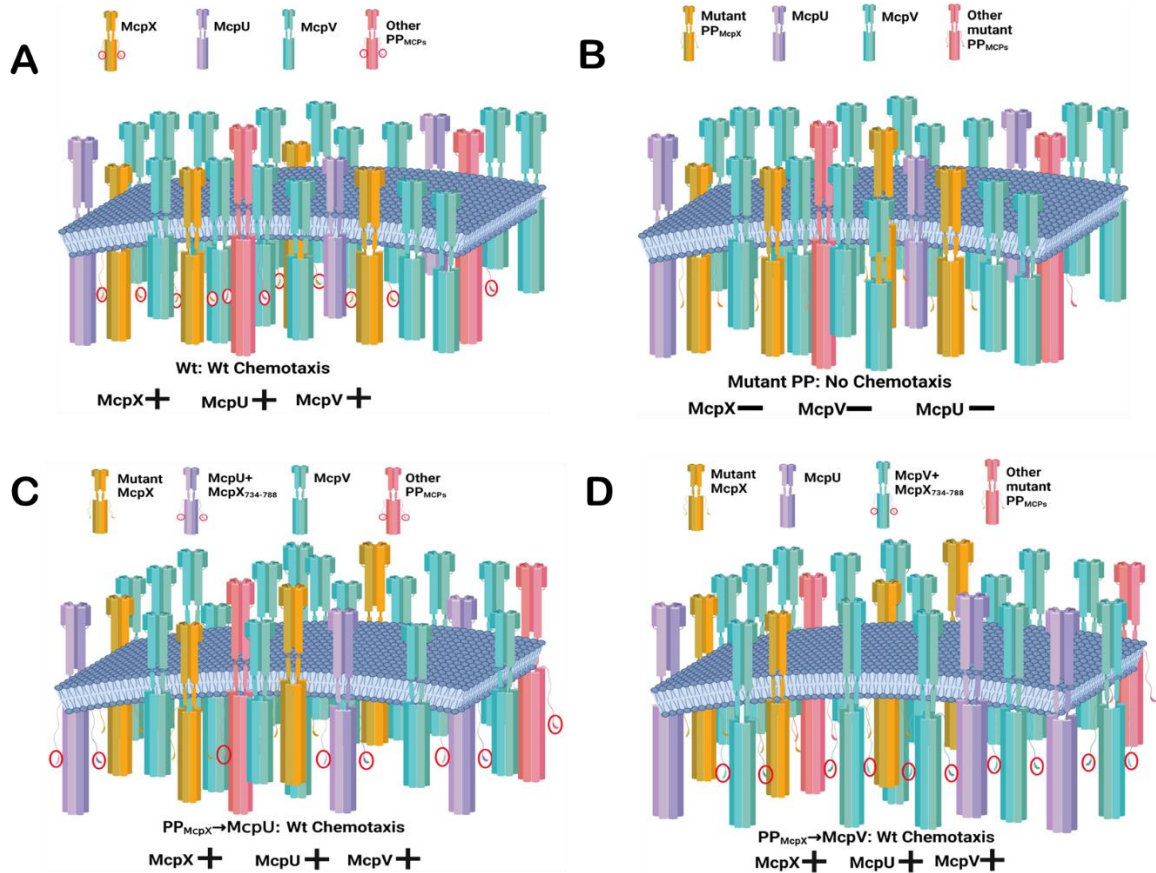


Fig. 2. 10 A summarized illustration of chemotaxis outcomes.

A. Wild type B. mutant strain with non-functional pentapeptides C. strain with a mutated McpX pentapeptide and a functional McpX pentapeptide added to McpU. D. strain with native pentapeptides mutated and a functional McpX pentapeptide added to McpV. With the exception of B, wild type chemotaxis was recorded in A, C, and D.

Supplementary Figure

	Signaling domain	Flexible linker	PP	
McpT	-----AAMVEEANAATHKLSAEADNLNLIAYFKVEREAVRTVVP	AKDASRPVSPARRMMGTVARAFGNGSAAVARD	DWEEF	665
McpW	-AAMVEQTNAASHTLAQDAEKLSEIVGQFRHGQARETAIRTAAI	QPPGRAGSATASAPARAATATAAAVPSLRKFAAAQSS	TRPAPSPAKALMGKLAGAFGNRPGSTPSVTASGE	NWEEF 689
McpX	-----AAMVEETTAASMLNDEARALSALVARFQIAPQAAQAS	AEMLRGTAERMRAAAPAENRPAQAPRSAAYSNSTQR	VLAKTSGANALAQD	NWEEF 788
McpY	-----AAMVEESTAASHRMSQEADALHALLRQFRIGRDAS	PA SDNRMEAPHSPTRLHATAKTLRSGTRSNLALAPAAD	DWENF	593
McpU	AAMVEQQTAAASHGLASEAAAALNALLAQFILGETQAASYQAT	SRRAA-----		707
McpV	AAMVEETTAASQTLAQESRELKALLEQFRLEERGAQPAYGRA	A-----		604
McpZ	ASMVEEATGTSRALANQADTLMMLVEQFRLEPVAAADHSYRA	A-----		841
IcpA	AALAGAALASTDDLHGVI VELGETIRRFLHLDQRARSAA SF	APRMRIEAPEDETTS PFGEVTSERHLAGWR		533

Fig. S1. Alignment of the C-terminal regions of *S. meliloti* chemoreceptors comprised of the C-terminal part of the signaling domain, the flexible linker, and the pentapeptide motif. The pentapeptides (PP) of McpT, McpW, McpX and McpY are highlighted in red.

Chapter 3— The novel *Sinorhizobium meliloti* chemotaxis protein CheT is a phosphatase for the sink response regulator and links signal termination and sensory adaptation.

ALFRED AGBEKUDZI¹, TIMOFEY D. ARAPOV¹, WING-CHEUNG LAI², GERALD L. HAZELBAUER², ANN M. STOCK³, AND BIRGIT E. SCHARF¹

¹ Department of Biological Sciences, Life Sciences I, Virginia Tech, Blacksburg, VA 24061, USA

² Department of Biochemistry, University of Missouri-Columbia, Columbia, MO 65211, USA

³ Department of Biochemistry and Molecular Biology, Robert Wood Johnson Medical School, Rutgers University, Piscataway, NJ 08854, USA

Running title: CheT, a novel *Sinorhizobium meliloti* chemotaxis protein

Key words: carboxyl methylation, sensory adaptation, speed-variable flagellar motor, transmembrane receptors, two-component system

*For correspondence:

E-mail bscharf@vt.edu

Tel (+1) 540 231 0757

Fax (+) 540 231 4043

Biological Sciences, Life Sciences I

Virginia Tech

Blacksburg, VA 24061, USA

Attribution: AA performed phosphorylation assays, Isothermal titration calorimetry experiments, Size-Exclusion Chromatography coupled with Multi-Angle Light Scattering (SEC-MALS), Swimming velocity analysis of *cheT* mutants. TDA performed methylation and crosslinking assays. The manuscript was written by AA, TDA, and BES.

ABSTRACT

Sinorhizobium meliloti senses nutrients and compounds exuded from its alfalfa host roots and coordinates an excitation, termination and adaptation pathway during chemotaxis. We investigated the role of the novel *S. meliloti* chemotaxis protein CheT. Although CheT and *Escherichia coli* CheZ share little sequence homology, CheT is predicted to possess an α -helix with a DXXXQ phosphatase motif. Phosphorylation assays demonstrated that CheT dephosphorylates the phosphate-sink response regulator, CheY1~P, but not the motor response regulator CheY2~P, by enhancing its decay two-fold. Isothermal Titration Calorimetry (ITC) experiments revealed that CheT binds to a phosphomimic of CheY1 with a K_D of 2.9 μ M, which is 25-fold stronger than its binding to CheY1. Dissimilar chemotaxis phenotypes of the Δ *cheT* mutant and *cheT* DXXXQ phosphatase mutants lead to the hypothesis that CheT exerts additional function(s). A screen for potential binding partners of CheT revealed that it forms a complex with the methyltransferase CheR. ITC experiments confirmed CheT/CheR binding with a K_D of 19 μ M, and a SEC-MALS analysis determined a 1:1 and 2:1 CheT/CheR complex formation. Although they did not affect each other's enzymatic activity, CheT binding to CheY1~P and CheR may serve as a link between signal termination and sensory adaptation.

INTRODUCTION

Motile bacteria have evolved diverse mechanisms for movement in the environment. They can swim to flee harm, reach an infection site, and facilitate host interactions [1]. This motility behavior is carried out by efficiently powered intracellular motors, intricately synthesized and assembled structures like flagella, and are controlled by a set of core and auxiliary chemosensory proteins. Flagellated bacteria are able to alternate between straight swimming paths or runs and random reorientations or tumbles to traverse a concentration gradient. This phenomenon known as a biased random walk [2] is mediated by a complex signal transduction system, which is best studied in the γ -proteobacterium, *Escherichia coli* (for reviews, see Wadhams *et al.* [3], Porter *et al.* [4], Sourjik *et al.* [5]).

Signalling in *E. coli* is initiated by a repertoire of chemoreceptors or Methyl Accepting Chemotaxis Proteins (MCPs) that are dimeric transmembrane proteins, which form a stable, ternary complex with two CheW adaptor protein monomers and a histidine kinase CheA dimer [3]. These complexes congregate into larger hexagonal arrays that allow for amplification of detected cues and cooperative signalling among different receptor types [6-8]. Chemoreceptors regulate the autokinase activity of CheA, which autophosphorylates by catalyzing the hydrolysis of ATP to form CheA~P and then transfers phosphoryl groups to a conserved aspartate residue of the response regulator CheY [9]. In *E. coli*, phosphorylated CheY (CheY~P) interacts with the flagellar motor protein FliM, altering flagellar rotation from counterclockwise (CCW) the default state of the flagellar motors, to clockwise (CW) resulting in a tumble reaction [10-12]. A phosphatase, CheZ, accelerates CheY~P dephosphorylation and therefore signal termination.

Through a mechanism known as adaptation cells that navigate a stimuli gradient maintain their sensitivity to a broad range of concentrations by modulating kinase activity (for recent reviews,

see Vladimirov *et al.* [13], Tu *et al.* [14]). The *E. coli* adaptation system is based on enzyme-catalyzed reversible addition of methyl group to conserved glutamate residues in the cytoplasmic signaling domain of MCPs [15-17]. Receptor methylation is generated by CheR, a constitutively active methyltransferase, while the CheA-dependent activated methylesterase CheB serves as an antagonist to CheR function [10, 13, 18, 19]. The adaptation enzymes are tethered to the chemoreceptor cluster via a canonical C-terminal pentapeptide motif [20]. Upon binding of an attractant to an MCP, the rate of CheA autophosphorylation is reduced. As a result, the amount of CheB~P is reduced, causing an increase in net level MCP methylation [21-23]. A second activity of CheB~P is the deamidation of conserved glutamyl residues in the cytoplasmic domain of MCPs, converting them into new glutamate sites receptive to methylation by CheR.

E. coli and *Bacillus subtilis* share the basic, two-component system architecture but also exhibit notable differences. Unlike *E. coli*, the attractant binding in *B. subtilis* activates the CheA kinase, increasing CheY~P levels, and thereby triggering counter-clockwise rotation of the motor and a run behavior [24]. Thus, counter-clockwise rotation causes runs and clockwise rotation promotes cell tumbles in both organisms [25, 26]. In addition to CheB and CheR being present in both organisms, *B. subtilis* expresses CheD, a deamidase, which positively regulates the autokinase activity of CheA when bound to the chemoreceptors [27, 28]. Furthermore, there are two phosphatases of CheY~P; a CheC protein that is localized with the receptors, and FliY, an integral part of the *B. subtilis* flagellar motor C-ring [29, 30]. A second function of CheD is regulated through CheC. The receptor-bound population of CheD is diminished through CheC-CheD interaction. This feedforward regulatory mechanism downregulates CheA activity and the cellular levels of CheY~P. As CheY~P is being dephosphorylated by FliY and CheC, dissociated CheD binds to the chemoreceptors, thus restoring CheA autokinase activity [31, 32]. Analyses of *B.*

subtilis and *E. coli* have revealed mechanistic differences in the way receptor methylation influences histidine kinase activity. *B. subtilis* maintains a steady level of methylated sites on MCPs, but changes in the methylation state of individual conserved glutamate residues dictate the activity of the kinase [32-34]. Thus, although CheB and CheR functions have been conserved in both species, their action promote different outcomes.

Sinorhizobium meliloti, a bacterium of global agricultural importance utilizes an elaborate chemosensory system to control its clockwise rotating peritrichous flagella to locate nutrients and germinating seeds and roots of its host *Medicago sativa* for establishing a nitrogen-fixing symbiotic relationship [35, 36]. Sensing of host phytochemicals by *S. meliloti* MCPs direct movement of bacteria towards roots hairs, where the exchange of chemicals results in the invasion of the host root by the symbiont and ultimately in the formation of root nodules. *S. meliloti* has six transmembrane and two cytosolic chemoreceptors controlling its flagellar-driven movement [37]. The main ligands of McpT, McpU, McpV, McpX have been identified as broad-range of carboxylates, amino acids, short chain carboxylic acids, and quaternary ammonium compounds, respectively [38-41].

S. meliloti and other related α -proteobacteria such as *Agrobacterium tumefaciens*, *Azospirillum brasilense*, and *Caulobacter crescentus* possess more than one response regulator species and have been known to lack a CheZ homologue [42, 43]. Hence, signal termination is mediated by phosphoryl group transfer from CheY2~P to CheA, which in turn transfers phosphate groups to a second response regulator, CheY1[43-47]. CheS, a small protein absent in *E. coli*, promotes interaction between CheA and CheY1, which allows for the drainage of the phosphate sink [47]. In *S. meliloti*, interaction of the phosphorylated motor response regulator (CheY2~P) with flagellar motors reduces flagellar rotary speed [43-45, 48].

S. meliloti possesses both adaptation proteins and their target MCP glutamate residues are mostly conserved projecting similar adaptational mechanisms [37, 49]. Our recent study of the adaptation system in *S. meliloti* revealed that CheR and CheB bind to the C-terminal chemoreceptor pentapeptide tether, a trait shared with the *E. coli* system (Agbekudzi & Scharf, under revision). On the other hand, the presence of a deamidase CheD may suggest an adaptation system that is closer to that of *B. subtilis*. These similarities and variations profoundly justify further studies of the *S. meliloti* adaptation module, and how it fits into its unique chemotaxis system. In this work, the role of the *S. meliloti* chemotaxis protein CheT, which is encoded by the last gene in the chemotaxis operon (*cheI*) downstream of *cheD*, was investigated [50]. We present evidence that CheT is involved in the adaptation and signal termination pathway of *S. meliloti*.

RESULTS

Bioinformatics analyses predicts CheT to be a structural homolog of *E. coli* CheZ.

The major chemotaxis operon *cheI* in *S. meliloti* contains a gene of unknown function, which is the last gene in the operon downstream of *cheD*. The deduced primary sequence of the gene product is a protein with 124 amino acid residues (13.4 kDa), which we named CheT. It has no apparent homologues in paradigm models of bacterial chemotaxis, but *cheT* is similar to genes found in other, closely related alphaproteobacteria such as *Sinorhizobium medicae*, *Agrobacterium tumefaciens*, *Caulobacter crescentus*, *Rhizobium leguminosarum* and *Hoeflea* sp. 108 (Fig. 1). Gene synteny of these orthologs is highly conserved, as they are the last gene in the major chemotaxis operons of each species, with the exception of *C. crescentus*, which has two additional chemotaxis genes in the operon preceding the *cheT* homologue. Their primary sequences exhibit varied identity of 81 % (*S. medicae*), 70 % (*A. tumefaciens*), 67 % (*R. leguminosarum*), 28 % (*Hoeflea* sp. 108) and 20 % (*C. crescentus*) (Fig. 1). PSIPRED predicts the secondary structure of CheT to contain four alpha helices accounting for 56 % of the primary sequence with the remainder of the sequence being composed of unstructured linkers [51]. Across all genomes surveyed, the position of and distance between two residues, Asp-57 and Gln-61, were highly conserved. The DXXXQ sequence has been previously implicated as a phosphatase motif on the catalytic surface of CheZ [52, 53] suggesting that CheT is a CheZ-like phosphatase.

AlphaFold predicts a monomeric structure for CheT consisting of two core alpha helices with mostly unstructured N- and C-terminal regions [54]. (Fig. 2A). Similarly, the crystal structure of the *E. coli* phosphatase CheZ exhibits two extended helical folds. Interestingly, the conserved Asp and Gln in the phosphatase motif in both *E. coli* CheZ and *S. meliloti* CheT are equally aligned on the helical coil. The position of their side chains in CheZ allows for efficient access to water and

the CheY active site to catalyze the rapid dephosphorylation of CheY~P [55]. Therefore, we hypothesize that, despite sequence differences, CheT is a functional homologue of *E. coli* CheZ.

CheT enhances dephosphorylation of CheY1~P but not CheY2~P

To experimentally corroborate the AlphaFold prediction that CheT is a CheZ phosphatase homolog, we performed time course phosphorylation assays using purified recombinant CheA, CheY2, and CheT in a molar ratio of 1:5:10. Following the autophosphorylation reaction of CheA with [γ - 32 P]-ATP (Fig. 3A lane 1), we initiated phosphotransfer by the addition of CheY2. Subsequently, an equal volume of buffer and CheT were simultaneously added to the reaction mixtures to determine the effect of CheT on CheY2~P. The reactions, with or without CheT, were terminated after 20, 40, 60 and 80 seconds (Fig. 3A lanes 2-9), separated by SDS-PAGE and exposed to a phosphoscreen. Autodephosphorylation of CheY2~P occurred over time; however, no differences in the CheY2~P band intensity were observed in the absence or presence of CheT (Fig. 3A). This result allows the conclusion that CheT does not enhance the dephosphorylation of CheY2~P.

Next, we performed the same time course experiment to analyze the effect of CheT on CheY1~P. However, no CheY1~P band was visible after the 20-sec time points (data not shown). Therefore, we limited the experiment to 10 and 20 seconds (Fig. 3B). After CheA autophosphorylation with [γ - 32 P]-ATP (Fig. 3B, lane 1), we observed phosphotransfer to CheY1 (lane 2). The addition of CheT (lane 3) resulted in the complete disappearance of the CheY1~P band after 10 seconds (lane 4). This experiment identified CheT as CheY1-specific phosphatase.

Kinetics of CheY1~P dephosphorylation by CheT

To determine the kinetics of CheY1~P dephosphorylation by CheT and identify the role of the phosphatase motif residues Asp-57 and Gln-61, we performed the assay with purified CheA~³²P. Reactions were carried out at molar CheA, CheY1 and CheT ratios of 10:1:0.1. Phosphotransfer reactions from purified CheA~³²P were initiated by the addition of CheY1. Subsequently, CheT, CheT-D57A, and CheT-Q61A were added to the individual phosphorylation reactions and terminated at times indicated. Samples were separated by SDS-PAGE and the gel exposed to a phosphor-storage screen. The exposed screen was scanned, a digital image obtained using an Amersham Typhoon scanner, and band intensities analyzed with ImageQuantTM TL 10.1 software. CheY1~P bands were significantly reduced in the presence CheT, however, the addition of CheT variants had no effect on CheY1~P band intensities (Figs. 4A & B). The deduced decay curve (Fig. 4C) revealed that CheT accelerated CheY1~P dephosphorylation two-fold, reducing its half-life from 26 to 13 seconds. In contrast, the half-life of CheY1~P in the presence of CheT-D57A and CheT-Q61A were 30 and 22 seconds, respectively. These results indicate a role for Asp-57 and Gln-61 in the catalysis of CheY1 dephosphorylation by CheT.

CheT binds strongly to CheY1~P

The enzymatic activity of CheT on CheY implies that both proteins closely interact with each other. To investigate their interaction, we employed Isothermal Titration Calorimetry (ITC) to determine the affinity of CheT to CheY1 and a phosphomimic of CheY1 (CheY1-BeF₃⁻). We observed exothermic heat changes for both protein pairs, producing dissociation constants (K_D) of 75 and 2.9 μ M, respectively (Figs. 5A & B). To test the contribution of the phosphatase DXXXQ motif in binding, we titrated CheT-D57A with CheY1 and CheY1-BeF₃⁻. The exothermic heats from the binding interaction resulted in K_D s of 48 and 11 μ M, respectively, inferring that the

mutation in the phosphatase motif does not disrupt binding to CheY1 or its phosphomimic form (Figs. 5C & D).

Phenotypic analysis of an *S. meliloti* strain lacking *cheT*

To gauge the function of CheT in chemotaxis, an in-frame deletion was introduced into the *S. meliloti* wild-type strain (RU11/001), and the chemotactic ability of the resulting mutant strain (RU11/319) was assessed and compared to six other chemotaxis deletion mutants (Fig. S1). The $\Delta cheT$ mutant strain exhibited a 50 % reduction in swim ring diameter on Bromfield soft agar plates compared to the wild type. This chemotaxis defect could be fully restored by complementation with a *cheT*-expressing plasmid. Deletions of *cheA*, *cheD*, *cheR*, and *cheY2* were more detrimental than that of *cheT*, while the deletion of *cheY1* was less severe. The *cheB* deletion strain displayed the most similar reduction in swim ring size to the $\Delta cheT$ strain.

To further assess how chemotaxis is affected by the deletion of *cheT*, we used computerized motion analysis to quantify the average free-swimming velocity of a population of cells. The swimming speed of *S. meliloti* is controlled by the levels of phosphorylated CheY2 [45]. A low swimming speed is indicative of high levels of CheY2~P, whereas a high swimming speed is the result of low levels of CheY2~P. Attractant stimulation inhibits CheA activation and subsequently reduces phosphorylation of CheY2 causing a 10 % increase in swimming speed in wild type (Fig. 6A) [37]. Consequently, deletion of *cheA* or *cheY2* resulted in an increased swimming speed that is not elevated when cells were stimulated with proline (Fig. 6A) [37, 56]. On the other hand, the swimming speeds of non-stimulated *cheB*, *cheY1*, and *cheS* deletion strains were decreased, because CheB and CheY1 compete with CheY2 in phosphoryl groups from CheA, and CheS enhances phosphotransfer to CheY1 [45] (Fig. 6A). Upon attractant stimulation, swimming speeds

of these strains increased due to decreasing CheY2~P levels. Strains lacking *cheD* or *cheR* exhibited a fast-swimming phenotype in the absence and presence of the attractant. This phenotype is shared with the *cheT* deletion strain suggestive of low CheY2~P levels (Fig. 6A & B). Bioinformatics analysis identified two conserved residues in CheT that are critical for phosphatase activity in *E. coli* CheZ and its homologues (Fig. 1) [52, 53]. To test whether these residues are important for CheT function, we created two mutant strains with Asp-57 and Gln-61 replaced with alanine residues. When this strain was subjected to swimming speed analysis, we recorded increased swimming velocity similar to the *cheT* strain. However, when stimulated with an attractant, the swimming speed further increased (Fig. 6B). In conclusion, deletion of *cheT* caused a chemotaxis defect in *S. meliloti* resulting in a fast-swimming phenotype and insensitivity to attractant stimulation, whereas mutations in the phosphatase motif also caused mutant cells to swim fast but they could be stimulated with an attractant. These differences in chemotactic behavior suggest that CheT has a function in addition to its phosphatase activity on CheY1~P.

CheT forms a complex with CheR.

Due to the differences in the *cheYI* deletion and phosphatase mutants, we hypothesized that CheT might have a dual role, which could explain the unexpected phenotype of the *cheT* mutants. To test the interaction of CheT with other *S. meliloti* chemotaxis proteins, we used an *in-vitro* chemical crosslinking assay. CheT and its putative target proteins were crosslinked with 1 % glutaraldehyde and separated electrophoretically via SDS-PAGE. Subsequent detection was achieved using an anti-CheT antibody. From the banding pattern on the immunoblot we inferred that CheT migrates according to its predicted molecular weight at 13.4 kDa and has a strong tendency to dimerize despite the presence of a reducing agent (Fig. 7A, lane 1). The crosslinking agent further promoted

dimerization and completely depleted the monomer pool (Fig. 7A, lane 2). Out of eight chemotaxis proteins tested, only the addition of CheR (34 kDa) to the crosslinking reaction resulted in a significant change in banding pattern. Two new major bands emerged, migrating at approximately 45 and 90 kDa, which concurred with a reduction in CheT-dimer band intensity (Fig. 7A, lane 6). Both bands are indicative of the formation of a 1:1 and a 2:2 CheR/CheT complex, respectively. In conclusion, data obtained from these crosslinking experiments revealed a putative interaction between CheT and CheR. It should be noted that a weak crosslinked band emerged in the reaction with CheY1, which is in line with the ITC data (Fig. 5A). To quantify the interaction of CheT and CheR, we subjected CheR to microcalorimetric titrations with CheT, which produced exothermic binding heats with a derived K_D of 19 μM (Fig. 7B). In summary, CheT binds to both *S. meliloti* CheY1 and CheR with similar binding affinities.

CheT exists as a homodimer and forms a heterooligomeric complexes with CheR.

E. coli CheZ is a homodimer with two core amphipathic helices from each monomer forming the interaction face [55, 57, 58]. Therefore, we sought to investigate whether CheT has a similar oligomeric state. To determine the molecular weight of CheT in solution we employed Size-Exclusion Chromatography coupled with Multi-Angle Light Scattering (SEC-MALS), which allows the molecular size determination of purified proteins and protein complexes [59]. CheT has a molecular weight of 13.4 kDa and produced an elution peak with a calculated molecular weight of 26 kDa (Fig. 8A). Thus, like CheZ, *S. meliloti* CheT forms a stable homodimer in solution. CheR produced a single peak suggestive of a monomer (Fig. 8B). To establish the stoichiometry of the CheT and CheR complex, an equimolar mixture of the two proteins was subjected to SEC-MALS analysis. We observed the emergence of three elution peaks with peak 1, 2, and 3

corresponding to a 34-kDa CheR monomer, a 47-kDa CheR/CheT (1:1) complex, and a 60-kDa CheR/CheT (1:2) complex (Fig. 8C). These results confirm the complex formation between CheT and CheR.

The complex formation between CheT and CheR does not affect CheT phosphatase activity.

Next, we performed a phosphorylation assay to test if the CheT/CheR complex formation affects dephosphorylation of CheY1~P by CheT. Experiments were performed similarly to those shown in Fig. 4, but in the presence of CheR. Phosphotransfer from CheA~P to CheY1 was initiated and CheY1~P band intensity measured over time following the addition of CheT and CheR in a 1:1 and 1:3 ratio (Fig. 9). No difference in CheT-mediated CheY1~P dephosphorylation was observed in the presence of CheR. This suggests that the presence of CheR had no effect on CheT phosphatase activity under these experimental conditions.

CheR methylation of McpX is unaltered by CheT

To test whether CheT affects methyltransferase activity of CheR, we applied a tritium-based *in-vitro* methylation assay as developed for *E. coli* chemoreceptors [60]. We chose McpX, which detects quaternary ammonium compounds, as substrate for methylation. McpX was overexpressed in *E. coli* strain Lemo21 (DE3), and McpX-containing membrane vesicles were isolated. These were then incubated with CheR in the presence of [³H]-S-adenosyl-L-methionine (SAM[³H]) and aliquots withdrawn at different time points. Samples were separated via SDS-gel electrophoresis and the release of [³H]-methanol from alkali-hydrolyzed gel fragments containing McpX was determined. Over a time-course of 15 min, McpX methylation increased linearly. Yet, the addition of CheT had no significant effect on CheR methylation activity (Fig. 10) Next, we analyzed

methylation of McpX in the presence of one of its ligands, choline [61, 62]. In analogy to *E. coli* MCPs, the addition of a ligand should increase receptor methylation *in vitro* [63]. Nonetheless, this was not the case for McpX (Fig. 11). We also tested whether divalent cations, reducing (DTT) or chelating (EDTA) agents were required for CheT function. However, no significant change in McpX methylation was observed, with one exception; the addition of 5 mM MgCl₂ slightly reduced activity (Fig. 11), although this effect was not consistently observed in all experimental variations. It has been reported that cyclic-di-GMP (c-di-GMP) is an activator for the CheR-binding protein MapZ in *Pseudomonas aeruginosa* [64, 65]. Therefore, we assayed McpX methylation by CheR in the presence of CheT and c-di-GMP but found no significant impact. Finally, the methyltransferase activity of copurified CheR/CheT was compared to that of CheR, again without observing any difference in McpX methylation (data not shown). To assay a different CheR substrate, we purified membrane vesicles containing McpU. Yet, we were unsuccessful in determining conditions at which McpU was methylated by CheR (data not shown). In conclusion, CheT had no effect on McpX methylation by CheR under these assay conditions.

DISCUSSION

Investigations of the *S. meliloti* chemotaxis signaling pathway had focused on chemoreceptor function, intracellular phosphotransfer reactions, and composition of the chemotactic signaling complex [43, 45-47, 61, 66-68]. This present work uncovered the role of CheT, encoded by the last gene in the chemotaxis operon, as a phosphatase specific for the phosphate sink response regulator, CheY1. Further studies revealed an additional role of CheT in adaptation that is not yet fully understood but sets apart the *S. meliloti* chemotaxis system only further from the enteric model.

Some information can be deduced through a comparison of chemotactic adaptation enzymes across species. The canonical adaptation system in *E. coli* employs CheR and CheB to modify conserved glutamate residues in the signaling domains of MCPs [69]. Both proteins bind to high-abundance MCPs in *E. coli* and low to moderately abundant MCPs in *S. meliloti* via a C-terminal pentapeptide motif that serves as a tether in the chemoreceptor array [20, 70]. In *S. meliloti*, four of the eight chemoreceptors (including McpX) possess a conserved pentapeptide motif [71]. However, different from *E. coli*, these MCPs are not present at high abundance, but only represent 13 % of the total receptor pool, compared to 93% in *E. coli* [72]. Furthermore, *S. meliloti* CheR varies from *E. coli* CheR in lacking all residues in the beta-subdomain required for pentapeptide binding, a characteristic shared with closely related alphaproteobacteria (Fig. 1) [73]. In addition, the CheR to pentapeptide-bearing receptor (PP_{MCPs}) ratio is particularly high in *S. meliloti* with approximately five CheR molecules per PP_{MCPs} monomer, compared to 0.01 in *E. coli* (Agbekudzi & Scharf, in revision). Lastly, the presence of CheD and our discovery of the interaction between the phosphatase CheT and the adaptation methyltransferase CheR sets the *S. meliloti* system apart from the enterobacterial paradigm.

Phosphorylation assays with CheA~³²P, CheY1, and CheT at molar ratios of 10:1:0.1 revealed a two-fold reduction of CheY1~P by CheT. CheT variant proteins with mutations in the phosphatase motif had no effect on CheY1 dephosphorylation (Fig. 4C). CheT binds CheY1-BeF₃⁻ 25-fold more strongly than unphosphorylated CheY1, and this binding is independent of mutations in the DXXXQ phosphatase motif (Figs. 5C & D). In comparison, *E. coli* CheZ binds to CheY~P with two orders of magnitude higher than to non-phosphorylated CheY [74]. The formation of homodimers is another characteristic CheT shares with CheZ [58] (Fig. 8A). These findings position CheT as a novel player in the signal termination pathway of *S. meliloti*, which was previously thought to lack a phosphatase and instead solely uses a phosphate sink for signal termination (Figs. 3B & 4) [66, 75, 76]. Since CheY1 serves as a sink towards the motor output response regulator, enhanced CheY1~P dephosphorylation should allow for a better drainage of the phosphoryl group pool [76, 77]. In this case, the expected motility phenotype of a strain lacking the CheY1 phosphatase would be a reduction in swimming speed, as CheY2~P levels would be increased. However, the deletion of *cheT* or the introduction of point mutations in the DXXXQ motif resulted in increased swimming velocity of these mutants pointing to a decreased cellular concentration of CheY2~P (Fig. 6B). The high swimming speeds in the *cheT* mutants relative to wild type appear to be a consequence of increased cellular levels of CheY1~P in the absence of CheT or its phosphatase activity. Since phosphotransfer from CheA~P to CheY2 is reversible and in equilibrium, the effectual CheY2~P levels are a consequence of an equilibrium shift toward the formation of CheY1~P. [66] Thus, high cellular levels of CheY1~P might have an inhibitory effect on kinase activity, which would reduce cellular levels of CheY2~P and lead to an increase in swimming speed. Alternatively, it is plausible that high levels of CheY1~P led to a redirection of

phosphoryl groups from CheA~P to CheB, thus increasing CheB~P levels and its inhibitory action on CheA kinase activity. Consequently, CheY2~P levels decrease and swimming speed increases. Interestingly, *cheT* phosphatase mutants increased their swimming velocity upon attractant stimulation, a phenotype that is not shared with the *cheT* deletion mutant (Fig. 6B). This implies that disruption of CheT's phosphatase activity only affects its function on CheY1 but not its other role(s) in *S. meliloti* chemotaxis. On the contrary, deletion of *cheT* disrupted sensitivity or response to the attractant proline, a feature that is also observed in the *cheR* deletion strain (Fig. 6B). Furthermore, both phosphatase motif mutants presented a swim ring diameter that was two-thirds of wild type and identical to that of the *cheY1* deletion strain. On the other hand, the swim ring diameter of the *cheT* deletion strain was half of wild type (Fig. S1). This further implies that CheT, in addition to its phosphatase activity on CheY1~P, exerts a second function in *S. meliloti* chemotaxis that likely is in regulating adaptation.

We discovered that CheT interacts with the methyltransferase CheR with a K_D of 19 μ M as monitored by ITC experiments (Figs. 7A, B). SEC-MALS experiments indicated that CheT monomers and dimers are able to form a complex with CheR monomers (Fig. 8C). The close interaction between CheT and CheR motivated us to investigate whether they affect each other's function. However, CheR had no effect on the phosphatase activity of CheT, and CheT had no effect on the methylation of McpX by CheR (Figs. 9-11). It remains to be seen whether CheT affects the methyltransferase activity of CheR with other MCPs. Meanwhile, evidence in this study indicates that CheT most likely also plays a role in chemotactic adaptation, as CheR and CheT form a stable complex and mutants lacking either *cheR* or *cheT* present similar characteristics in swim speed assays.

The *S. meliloti* CheT-CheR-CheY1~P interaction resembles the CheC–CheD–CheY~P adaptation system in *Bacillus subtilis* as both systems consist of a phosphatase, an adaptation protein, and a phosphorylated response regulator. The CheC phosphatase binds to both, CheD and CheY~P, which is analogous to CheT interaction with CheR and CheY1~P. While *S. meliloti* CheR has no enzymatic activity on CheT activity and vice versa, CheD binding to CheC increases its CheY~P phosphatase activity approximately fivefold [29, 78, 79]. Furthermore, the behavior of strains expressing CheC variants with disrupted CheY interaction or abolished phosphatase activity demonstrates that chemotaxis is largely dependent on CheC binding to CheY~P and CheD rather than on its CheY~P phosphatase activity [79]. Ongoing research aims to identify CheT residues required for CheR and CheY1~P binding, an important step to further characterize the role of CheT in *S. meliloti* chemotaxis.

Here, we have shown that CheT is part of the signal termination and adaptation system of *S. meliloti* chemotaxis, which was a rather unexpected result. More insights can be gained by investigating the unexplored functions of chemoreceptor methylation and demethylation by CheR and CheB, respectively, and the role of CheD in adaptation.

MATERIALS AND METHODS

Bacterial strains and plasmids

E. coli K12 and *S. meliloti* MV II-I derivatives used are listed in Table 1. The wild-type *S. meliloti* strain RU11/001, is a spontaneous streptomycin-resistant derivative of MVII-1 [80].

Genetic and DNA manipulations

S. meliloti mutants listed in Table 1 were created by allelic replacement essentially as laid out in Sourjik *et al.* and Zatakia *et al.* [45, 72].

Media and growth conditions

S. meliloti strains were grown in TYC (0.5 % tryptone, 0.3 % yeast extract, 0.13 % CaCl₂ x 6 H₂O [pH 7.0]) at 30 °C for 2 days. For motility and tracking experiments, cultures were subsequently diluted 1:100 in 10 ml RB minimal medium [6.1 mM K₂HPO₄, 3.9 mM KH₂PO₄, 1 mM MgSO₄, 1 mM (NH₄)₂SO₄, 0.1 mM CaCl₂, 0.1 mM NaCl, 0.01 mM Na₂MoO₄, 0.001 mM FeSO₄, 20 µg/l biotin, 100 µg/l thiamine], which was added as liquid layer on top of Bromfield medium (0.04 % tryptone, 0.01 % yeast extract, 0.01 % CaCl₂·2H₂O) agar plates and incubated at 30 °C to an optical density at 600 nm (OD₆₀₀) of 0.1. *E. coli* strains were grown at 37 °C in lysogeny broth (LB). Antibiotics were used at the following concentration: for *S. meliloti*, streptomycin at 600 µg/ml, neomycin 120 µg/ml, for *E. coli*, ampicillin at 100 µg/ml and chloramphenicol at 30 µg/ml.

Swim plate assays

Bromfield medium swim plates containing 0.3 % (wt/vol) Bacto agar were inoculated with 3 µl of *S. meliloti* cultures grown in TYC and incubated at 30 °C for 3 to 4 days.

Computerized motion analysis of free-swimming cells

Overnight cultures were grown to an OD₆₀₀ of 2.5 and diluted to OD₆₀₀ of 0.004 in an overlay broth that was prepared by incubating Bromfield plates with a 10-ml layer of RB at 30°C for 16 h. Motile cells between an OD₆₀₀ of 0.16 to 0.18 were harvested and suspended in RB to a final OD₆₀₀ of 0.05 [81]. To determine swimming velocities, bacteria were analyzed by phase-contrast microscopy using a Nikon Eclipse E600 microscope with a 40× objective and a custom Nikon CMOS camera from The Imaging Source or a Zeiss standard 14 phase-contrast microscope (magnification, × 400) (Charlotte, NC, USA). After addition of 10 mM proline to cultures on a slide, videos of the motile behavior of wild-type and mutant cell populations were taken within 20 seconds. Five-second videos were analyzed using the TumbleScore program to quantify swimming velocities [82] or swim tracks were analyzed using the computerized motion analysis of the Hobson BacTracker system (Hobson Tracking Systems, Sheffield, United Kingdom) as previously described in Meier *et al.*, 2007 [71]. Mean and standard deviation were calculated from three separate biological replicates. Statistical significance was determined by a two-tailed Student's *T*-test in relation to the wild-type strain speed.

Expression and purification of CheR and CheT

CheT and CheR were overexpressed in *E. coli* ER2566 from pBS359 and pBS450, respectively. Cells were grown at 37 °C in LB containing 100 µg/ml ampicillin to an OD₆₀₀ of 0.7-0.9 and gene expression was induced with 0.3 mM IPTG (isopropyl-β-d-thiogalactopyranoside). Cultivation of the cells continued for 16-20 h at 16 °C until cells harvest by centrifugation. The cells were suspended in IMPACT buffer (20 mM Tris/HCl [pH 8.0], 500 mM NaCl, 1 mM EDTA). Cells were then lysed by three passages through a French pressure cell (SLM Aminco, Silver Spring,

MD) at 20,000 psi and centrifuged 48,000 x g at 4 °C for 1 h to remove insoluble material and unlysed cells. The soluble fraction was passed through a 0.2 µm filter and loaded on a chitin agarose (NE Biolabs, Beverly MA, USA) column (2.6 x 5.0 cm) equilibrated with IMPACT buffer. The column was washed with 10-20 bed volumes of IMPACT buffer at 4 °C. Intein-mediated cleavage was induced by equilibration of the column with two bed volumes of IMPACT buffer containing 50 mM dithiothreitol, followed by 12-36 h incubation at 4 °C. The protein was eluted with IMPACT buffer and protein-containing fractions were collected. Fractions were pooled, concentrated to 10 ml and subjected to size exclusion chromatography (SEC) on a HiPrep™ 26/60 Sephacryl™ S-200 HR column (GE Healthcare Life Sciences). Cells were grown at 37 °C in lysogeny broth (LB) containing 100 µg/ml ampicillin to an OD₆₀₀ of 0.7- 0.9 and gene expression was induced with 0.5 mM IPTG. Cultivation of the cells continued for 4 h at 37° C until cells harvest by centrifugation. Cells were suspended in Ni-NTA binding buffer (500 mM NaCl, 20 mM imidazole, 1 mM PMSF, 20 mM NaPO₄ [pH 7.0]), lysed by three passages through a French pressure cell (SLM Aminco, Silver Spring, MD), and centrifuged for 1 h at 48,000 x g and 4 °C. The soluble fraction was passed through a 0.2 µm filter and loaded onto a charged 5-ml Ni-NTA column (GE Healthcare Life Sciences). Proteins were eluted using a linear gradient of elution buffer (500 mM NaCl, 500 mM imidazole, 1 mM PMSF, 20 mM NaPO₄ [pH 7.0]). Protein-containing elution fractions were pooled, concentrated and further purified through SEC on a HiPrep 26/60 Sephacryl™ S-200 HR column (Cytiva).

Expression and purification of other chemotaxis proteins

Expression and purification of CheA, CheA/CheS, CheY1, CheY2, and CheS was performed as described in Dogra *et al.*, 2012 [47]. Expression and purification of CheB, CheD, and CheW1 was accomplished essentially as described in Arapov *et al.* [83].

Size exclusion chromatography and multiangle light scattering.

The molecular masses of CheT, CheR, CheT/CheR, and CheY1 were determined by size exclusion chromatography with online absorbance, multiangle light scattering (MiniDawn, Wyatt Technology), and refractive index detectors (Optilab). One milligram of purified proteins and CheR and CheT mixture were incubated at room temperature for 30 mins before being subjected to Superdex 200 increase (10/300 GL) column (Cytiva), which was equilibrated in 25 mM Tris/HCl pH 7.5, 125 mM NaCl at 22 °C and a flow rate of 0.5 ml/min. The refractive index (RI) signal was used as a concentration source for analyzing the light scattering data with the ASTRA program (version 8.1.2.1; Wyatt Technology).

Isothermal titration calorimetry (ITC)

Direct binding analysis was performed with a MicroCal PEAQ-ITC (Malvern Panalytical Ltd). Three hundred microliters of 30-50 μ M CheR or CheY1/CheY1-BeF₃⁻ were loaded into the sample cell and titrated with 300-535 μ M of CheT from the syringe. To produce the CheY1-BeF₃⁻ complex, 7 mM MgCl₂, 5 mM BeSO₄, and 30 mM NaF were mixed with 30-50 μ M CheY1 for 5 min at room temperature. All ITC experiments were performed at 25 °C. Protein solutions were degassed at 24 °C before loading them into the MicroCal PEAQ-ITC. To obtain baseline titrations and for reference subtraction, proteins were titrated into buffer only. The dissociation constant

(K_D) was determined from heat changes during titration of the ligand with the protein using the MicroCal PEAQ-ITC analysis software “one binding sites” model.

***In-vitro* crosslinking assays**

Freshly prepared glutaraldehyde (Sigma-Aldrich) at a final concentration of 1 % (wt /vol) was used for protein crosslinking experiments essentially as previously described [46, 47]. Proteins were used at a concentration of 0.7 μ M in a buffer containing 20 mM NaCl, 1 mM EDTA, 20 mM NaPO₄, pH 7.5. Reactions were stopped after an incubation of 30 min at room temperature by the addition of an equal volume of 2x Laemmli buffer.

Immunoblots

Cross-linked samples were separated by gel electrophoresis on a 15% SDS polyacrylamide gel and transferred to a 0.45 μ m nitrocellulose membrane in transfer buffer (20 % methanol, 50 mM Tris, 40 mM glycine). Membranes were blocked overnight with 5 % non-fat dry milk with 0.1 % Tween 20 in phosphate buffered saline (PBS, 100 mM NaCl, 80 mM Na₂HPO₄, 20 mM NaH₂PO₄, pH 7.5). Blots were then probed with anti-CheT or anti-CheR affinity-purified antibodies at a 1:400 dilution for 1.5 h at room temperature. Blots were subsequently washed for 30 min with PBS/0.1 % Tween 20 with four buffer changes and probed with donkey anti-rabbit conjugated with horseradish peroxidase at a 1:1,500 dilution for 1.5 h. The blots were then washed for 30 min with PBS/0.1 % Tween 20 with four buffer changes. Detection was performed by chemiluminescence (Amersham ECL Western Blotting Detection Kit, GE Healthcare) using Hyperfilm ECL (GE Healthcare).

Autophosphorylation of CheA and phosphotransfer to CheY1 or CheY2 in the presence of CheT

Purified CheA was dialyzed against 20 mM Tris/HCl, pH 7.5, 0.5 mM EDTA, 2 mM DTT, 10 % (vol/vol) glycerol (TEDG₁₀) overnight at 4 °C. Autophosphorylation of CheA was initiated by the addition of 0.6 mM 10 µCi [γ -³²P] ATP. Reactions were performed in TEDG₁₀ containing 5 mM MgCl₂ and 50 mM KCl at a final CheA concentration of 5 µM at 22 °C. Phosphotransfer was initiated by the addition of 25 µM CheY2 or CheY1 and monitored in the presence of 50 µM of CheT or CheT variants. Phosphorylation was terminated at given time intervals by adding 10-µl aliquots of the reaction mixture to 10 µl of SDS gel-loading buffer containing 10 mM EDTA. Samples were separated by electrophoresis on a 4-20 % Criterion TGX gradient gel (Biorad). Gels were enclosed in plastic wrap and exposed to a storage phosphor screen which was excited with a 633-nm excitation laser and observed using a 390-nm band filter using Amersham Typhoon phosphorimager (Cytiva). Band intensities were quantified with ImageQuant TL software (Cytiva).

Purification of [³²P]-phospho-CheA.

Purified CheA (6.1 nmol) was phosphorylated in 500 µl TEDG₁₀ containing 5 mM MgCl₂ and 50 mM KCl using 100 µCi of 0.4 mM [γ -³²P]-ATP for 15 min at 22°C. The reaction mixture was subjected to gel filtration on a Sephadex G-50 column (16/20; Pharmacia Biotech) at a flow rate of 0.5 ml/min. The column was developed and equilibrated in TEDG₁₀, protein-containing fractions were combined after subjected to Liquid Scintillation Counting, and stored at -20 °C.

Kinetic assays of phosphotransfer from [³²P]phospho-CheA to CheY1 and phosphatase activity of CheT and CheT/CheT mixtures

Phosphotransfer reactions from purified [³²P]phospho-CheA (400 nM) were initiated by the addition of CheY1 or CheY2 (40 nM) in TEDG₁₀ containing 5 mM MgCl₂ and 50 mM KCl and phosphatase activity of CheT was assayed by adding 4 nM of CheT, CheT variants, and CheT/CheR mixtures after incubation for 30 mins at room temperature. Reactions were terminated at given time intervals by adding 10- μ l aliquots of the reaction mixture to 10 μ l of SDS gel loading buffer containing 10 mM EDTA. Samples were separated by electrophoresis on a 4-20 % Criterion TGX gradient gel (Biorad) and analyzed. Gels were enclosed in plastic wrap and exposed to a storage phosphor screen which was Amersham Typhoon phosphorimager (Cytiva). Band intensities were quantified with ImageQuant TL software (Cytiva), and time courses were plotted using Origin 8.1 software (OriginLab, Northampton, MA).

Isolation of McpX-containing membrane vesicles

Preparation of membrane vesicles was done essentially as previously described in Osborne and Munson [84] and Gegner *et al.* [85]. An overnight culture of *E. coli* Lemo21(DE3) with pBS1096 expressing McpX grown in LB containing ampicillin and chloramphenicol as well as 500 μ M L-rhamnose was diluted to a final OD₆₀₀ of 0.05. To ensure proper aeration, cultures were placed in flasks with the volume of the growth medium not exceeding 15 % of the maximum volume of each flask. Cells were grown at 37 °C to an OD₆₀₀ of 0.4-0.5, gene expression was induced by 0.4 mM IPTG and cultivation continued for 4 h at 37 °C. Cells were harvested by centrifugation and suspended in 10 mM Tris/HCl (pH 7.5), 20 % sucrose (wt/wt). Lysozyme and EDTA were subsequently added to a final concentration of 100 μ g/ml and 5mM, respectively. Cells were

incubated on ice for 5 min under gentle agitation. Two volumes of 5 mM EDTA, 1 mM PMSF and 1 mM 1,10 phenanthroline (Phe) were then slowly added with a glass pipette. Cells were lysed by the addition of four volumes of ice-cold H₂O and subsequent vigorous agitation for 1 min. DNase and MgCl₂ were added to a final concentration of 10 µg/ml and 3mM, respectively. The lysate was centrifuged for 1.5 h at 27,485 x g and 4 °C. The insoluble fraction was suspended in 50 mM Tris/HCl [pH 7.5], 5 mM MgCl₂, 50 mM KCl, 0.5 mM PMSF, 1 mM Phe, and subsequently dialyzed for 14 h at 4 °C against the same buffer.

***In-vitro* methylation assays**

In-vitro methylation assays were carried out essentially as described in Barnakov *et al.*, 1998 [60]. Isolated membrane vesicles with and without McpX, CheT, and CheR were dialyzed against TGD buffer (50 mM Tris/HCl [pH 7.5], 10 % glycerol, 5 mM dithiothreitol). McpX in membrane vesicles and CheR were used at 1.2 µM and 0.2 µM, respectively, in the absence and in the presence of 4.6 µM CheT, and reactions were initiated by addition of adenosyl-L-methionine S-[methyl-³H] (SAM) (PerkinElmer) (0.9 Ci/mmol) at a final concentration of 50 µM. At indicated time points, 20-µl samples were added to 20 µl 2x Laemmli buffer and boiled for 1 min to terminate the reactions. Twenty microliter aliquots were analyzed by electrophoresis on a 10 % acrylamide SDS-gel. Bands corresponding to McpX were excised from Coomassie-stained dry gels. The excised bands were subjected to alkali hydrolysis in 200 µl 1 M NaOH for 24 h. Quantification of released radiolabeled methanol was enabled by vapor-phase equilibrium of volatile methanol and ECONO-SAFE scintillation cocktail.

ACKNOWLEDGMENTS

This study was supported by NSF grants MCB-1253234 and MCB-1817652 to Birgit Scharf. We would like to thank Andrea Brücher for motility measurements, Victor Sourjik for constructing strains RU11/306, RU11/312, RU11/319, and Paul Muschler for constructing strain RU11/411 (Department of Genetics, University Regensburg, Germany).

TABLE

Table 3.1 Bacterial strains and plasmids

<u>Strain/Plasmid</u>	<u>Relevant Characteristics</u>	<u>Source or Reference</u>
<i>E. coli</i>		
BL21(DE3)	<i>F⁻ ompT hsdSB(rB⁻ mB⁻) gal dcm λ (DE3)</i>	Novagen
ER2566	<i>ion ompT lacZ::T7</i>	New England Biolabs
Lemo21(DE3)	<i>fhuA2 [lon] ompT gal (λDE3) dcm ΔhsdS/pLemo(Cm^r)</i>	New England Biolabs
M15/pREP4	<i>Ap^r Km^r; F- φ80ΔlacM15 thi lac- mtl- recA⁺</i>	Qiagen
S17-1	<i>Sm^r Tp^r; recA endA thi hsdR RP4-2 Tc::Mu::Tn7</i>	[86]
<i>S. meliloti</i>		
RU11/001	<i>Sm^r; Spontaneous streptomycin-resistant wild-type strain</i>	[87]
RU11/306	<i>ΔcheR</i>	Arapov <i>et al.</i> [83]
RU11/307	<i>ΔcheY2</i>	[45]
RU11/308	<i>ΔcheY1</i>	[45]
RU11/310	<i>ΔcheA</i>	[45]
RU11/312	<i>ΔcheB</i>	Arapov <i>et al.</i> [83]
RU11/319	<i>ΔcheT</i>	Arapov <i>et al.</i> [83]
RU11/411	<i>ΔcheD</i>	Arapov <i>et al.</i> [83]
BS170	<i>Sm^r; cheT with codon 61 changed from CAG to GCC (Q61A)</i>	This study
BS190	<i>Sm^r; cheT with codon 57 changed from GAC to GCC (D57A)</i>	This study
BS192	<i>Sm^r; cheT with codon 57 changed from GAC to GCC (D57A) & codon 61 changed from CAG to GCC (Q61A)</i>	This study
Plasmids		
pBBR1-MCS2	<i>Km^r; broad host-range vector</i>	[88]
pBS16 ^a	<i>Ap^r; pTYB1-cheY1</i>	[46]
pBS18 ^a	<i>Ap^r; pTYB1-cheY2</i>	[46]
pBS54	<i>Ap^r; pTYB11-motB</i>	[81]
pBS57 ^a	<i>Ap^r; pTYB1-cheA</i>	[46]
pBS93	<i>Ap^r; pTYB11-cheB</i>	This study
pBS173	<i>Km^r; 291-bp NcoI-BamHI fragment from pRU2804 containing cheS cloned into pET27bmod</i>	[47]
pBS189	<i>Km^r; pBBR1MCS2-lacI^q</i>	[67]
pBS295	<i>Km^r; pET27bmod-cheA-6Xhistag</i>	[76]
pBS331	<i>Ap^r; pTYB11-cheD</i>	This study
pBS359	<i>Ap^r; pTYB11-cheT</i>	This study
pBS445	<i>Km^r; pBS189-cheT</i>	This study
pBS450	<i>Ap^r; pTYB1-cheR</i>	This study
pBS567	<i>Ap^r; pQE60-cheW1</i>	This study

pBS639	Ap ^r ; pTYB11-CheTD57A	This study
pBS667	Ap ^r ; pTYB11-CheTQ61A	This study
pBS1095	Ap ^r ; pET22B(+)- <i>mcpU</i>	This study
pBS1096	Ap ^r ; pET22B(+)- <i>mcpX</i>	This study
pET27bmod	Km ^r ; expression vector	Novagen
pK18 <i>mobsacB</i>	Km ^r ; <i>mob sacB</i> , vector used for homologous allelic exchange	[89]
pQE60	Ap ^r ;	Qiagen
pTYB1	Ap ^r ; expression vector for Impact system	New England Biolabs
pTYB11	Ap ^r ; expression vector for Impact system	New England Biolabs

^aEquivalent to pRU2312, pRU2313, and pRU2326, respectively, as described in Riepl *et al.*, 2008 [46].

Figures

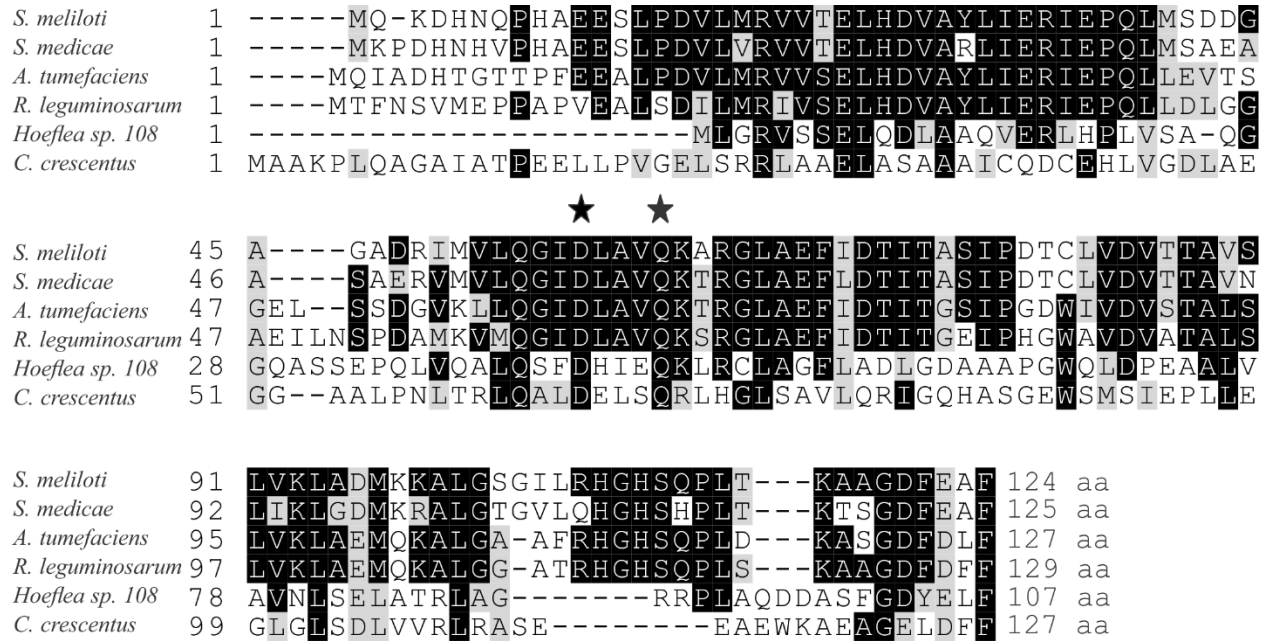


Fig. 3. 1 Alignment of the amino acid sequence of *S. meliloti* CheT (NP_384751.1) with five paralogues from related alphaproteobacteria.

Sinorhizobium medicae (YP_001325935.1), *Agrobacterium tumefaciens* (WP_003493786.1), *Rhizobium leguminosarum* (WP_003588573.1), *Hoeflea sp. 108* (WP_018430236.1), and *Caulobacter crescentus* CheU (NP_419258.1). GenBank accession numbers are given in parentheses. Sequences were aligned through ClustalOmega. Black shading indicates identical residues and grey shading indicates residues with similar side change properties. Stars indicate conserved residues indicative of a putative (DXXXQ) CheZ-like phosphatase motif.

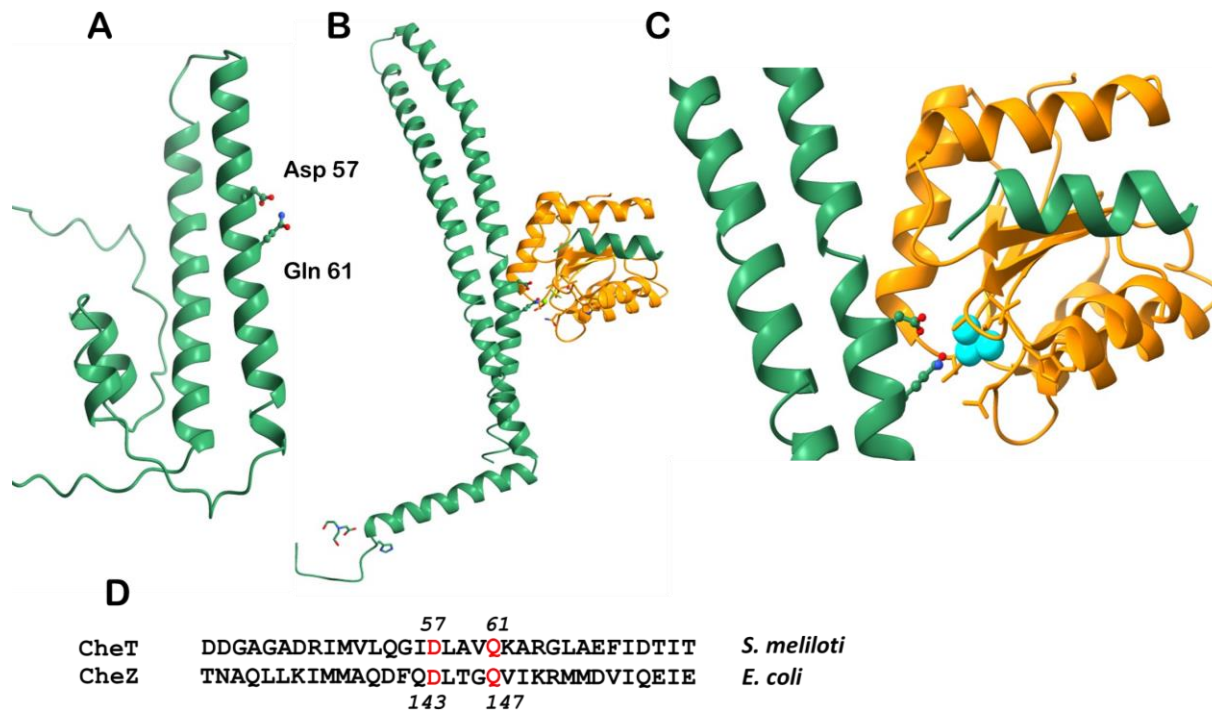


Fig. 3. 2 Structure prediction of *S. meliloti* CheT and comparison to *E. coli* CheZ.

A. Predicted AlphaFold structure of *S. meliloti* CheT. The side chains of the conserved Asp and Gln residues of the putative DXXXQ phosphatase motif are shown as ball and sticks with red and blue representing oxygen and nitrogen atoms, respectively. B. Crystal structure of *E. coli* CheZ bound to CheY (PDB# 1KMI) C. An enlarged ribbon image of B the active site of CheY (orange), BeF_3^- (cyan), and CheZ (green) with Asp and Gln residues of the DXXXQ phosphatase motif shown as ball and sticks with oxygen (red) and nitrogen atoms (blue). D. A sequence segment of amino acid residues bearing the DXXXQ phosphatase motif in *S. meliloti* CheT and *E. coli* CheZ.

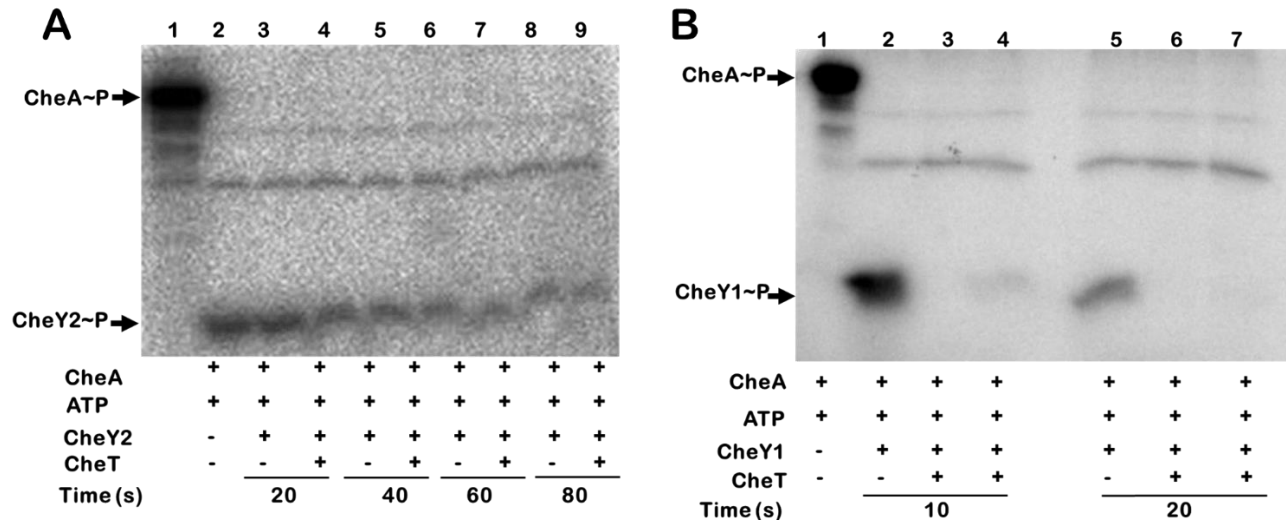


Fig. 3. 3 Dephosphorylation of CheY1 and CheY2 in the presence of CheT. Reactions contained 5 μ M CheA, 25 μ M CheY2 or CheY1, 50 μ M CheT, 25 μ M CheT and 10 μ Ci [γ - 32 P]-ATP in TEDG₁₀ buffer and were performed at room temperature. A. Time course of CheY2~P dephosphorylation B. Time course of CheY1~P dephosphorylation. Samples were separated using a 15% SDS-PAGE followed by overnight exposure of a storage phosphoscreen. A digital image was produced from laser-induced excitation of the phosphoscreen with the Amersham Typhoon FLA 950 imager. The lower molecular weight band with constant intensity seen in both images likely represents a phosphorylated CheA degradation product.

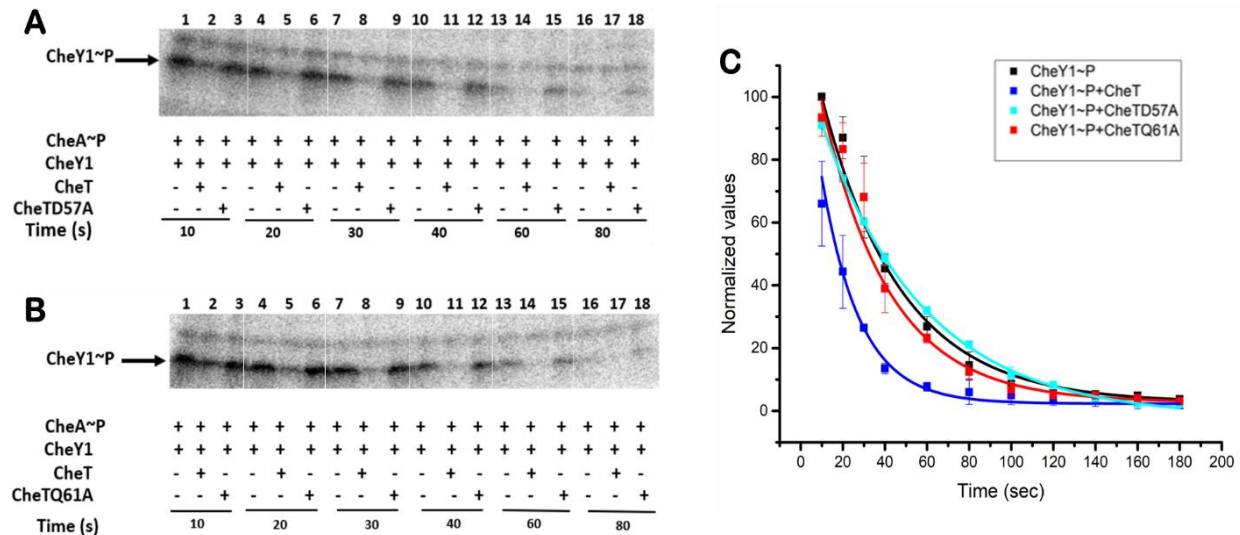


Fig. 3. 4 Kinetics of CheY1~P dephosphorylation in the presence of CheT and its variants. Reactions were carried out at molar CheA, CheY1 and CheT ratios of 10:1:0.1. A. Digital image of CheY1~P dephosphorylation in the presence of CheT and CheT-D57A. B. Digital image of CheY1~P dephosphorylation in the presence of CheT and CheT-Q61A. C. A decay curve of CheY1~P

dephosphorylation normalized to CheY1~P at 10 seconds. Data points are the means from three replicates of CheY1~P pixel intensity and error bars reflect standard deviation determined with Amersham Typhoon image analyzer software.

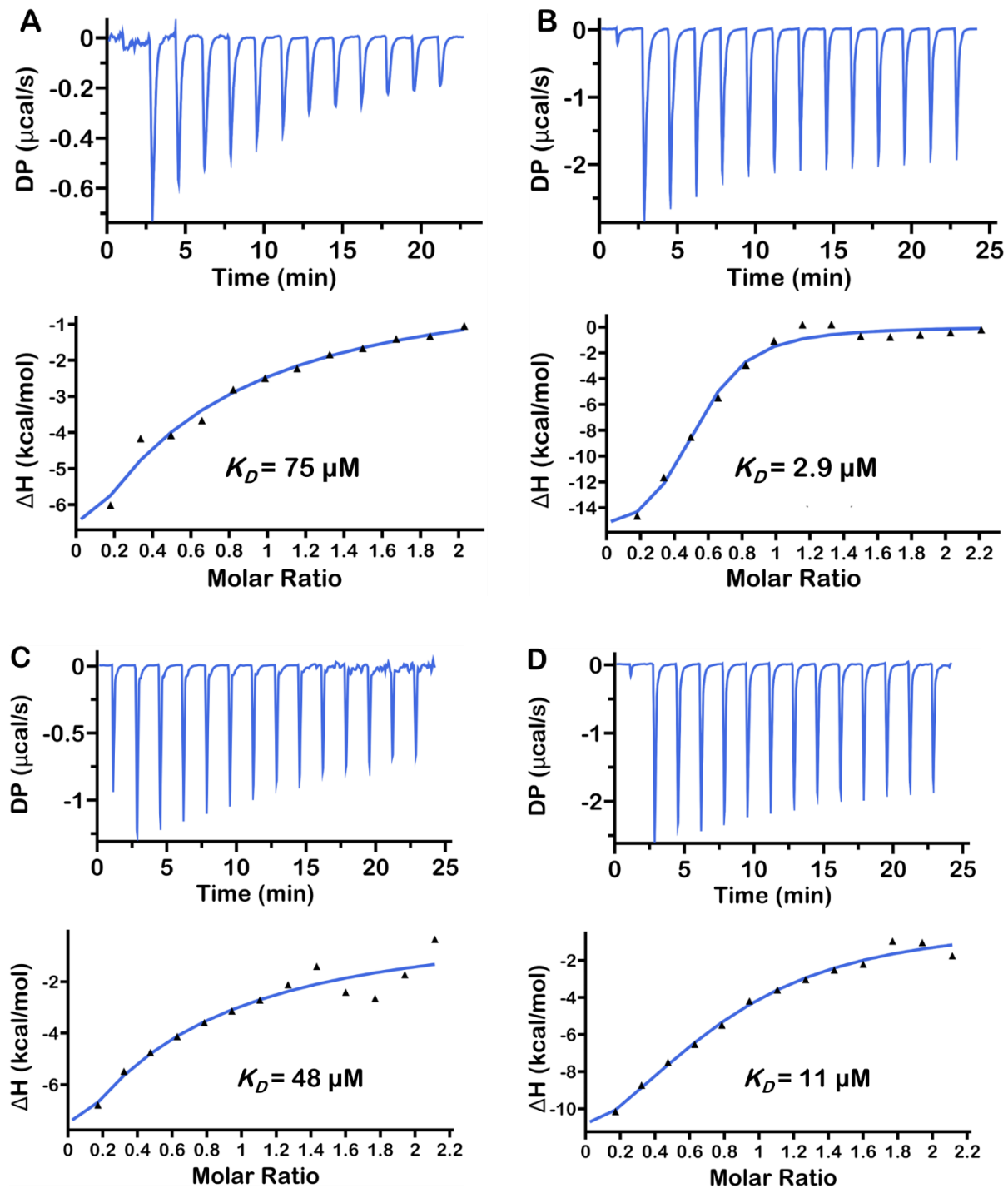


Fig. 3. 5 Isothermal titration calorimetry depicting the binding interaction.

(A) CheT and CheY1, (B) CheT and CheY1-BeF₃⁻, (C) CheTD57A and CheY1, (D) CheTD57A and CheY1-BeF₃⁻. Upper panels: Raw data for the titration of 535 μM CheT with 50 μM CheY1 for Fig. A & B and 300 μM CheTD57A with 300 μM CheY1 for Fig. C & D. Lower panels the dissociation constant, K_D generated from the normalized and dilution corrected integrated peak areas of the raw titration data.

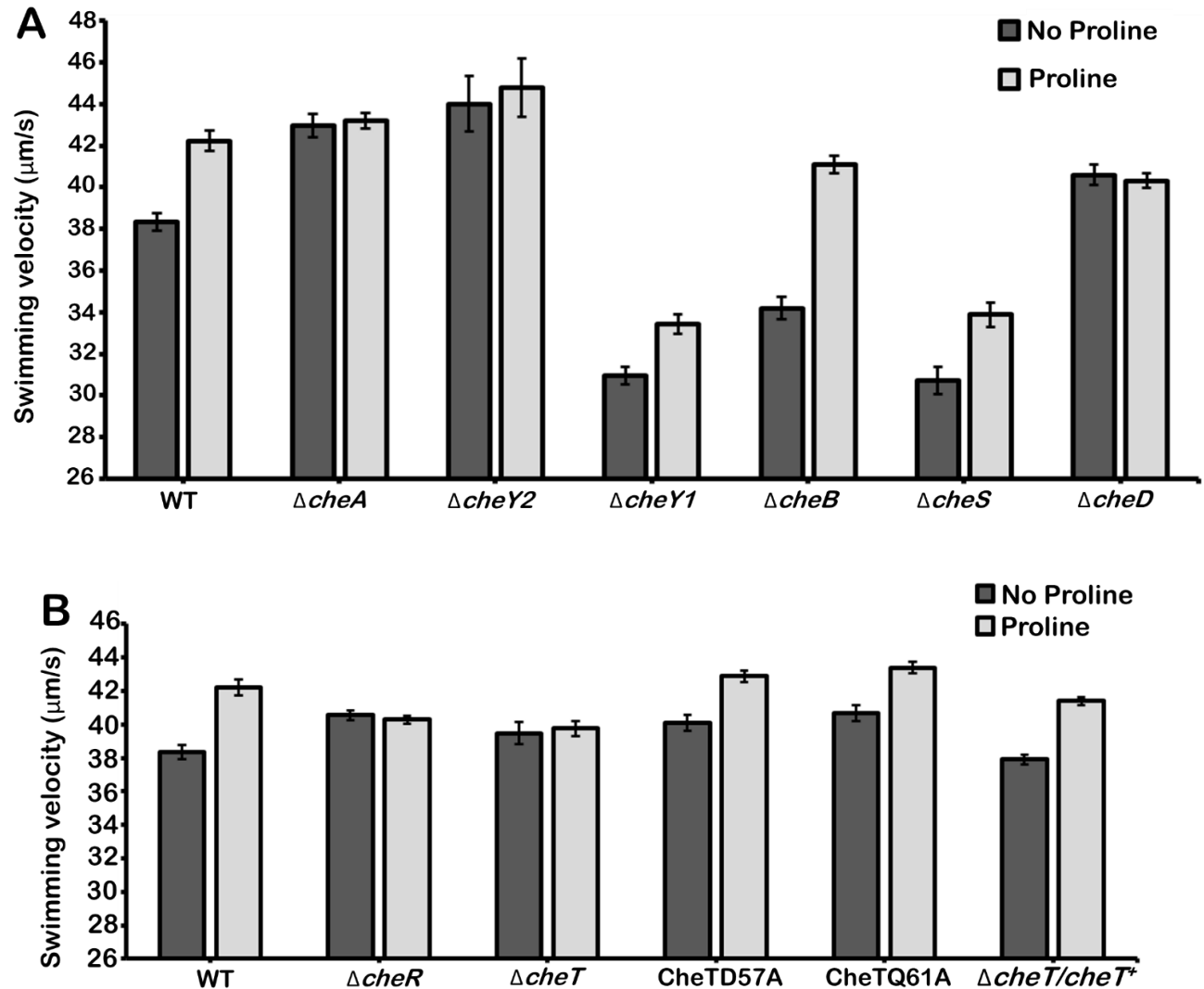


Fig. 3. 6 Free swimming speeds of *S. meliloti* strains before and after the addition of the attractant proline. Values are the means and standard deviations from at least three biological replicates. The dark and light gray bars represent swimming velocity of cells before and after stimulation with 10 mM proline, respectively. A. WT (RU11/001), $\Delta cheA$ (RU11/310), $\Delta cheY2$ (RU11/307), $\Delta cheY1$ (RU11/308), $\Delta cheB$ (RU11/312), $\Delta cheS$ (RU11/408) and $\Delta cheD$ (RU11/411) B. WT (RU11/001), $\Delta cheR$ (RU11/306), $\Delta cheT$, (RU11/319); CheTD57A (BS190), CheTQ61A (BS170), and $\Delta cheT/cheT^+$, $\Delta cheT$ (RU11/319) with pBBR1MCS-2-*cheT* (pBS445).

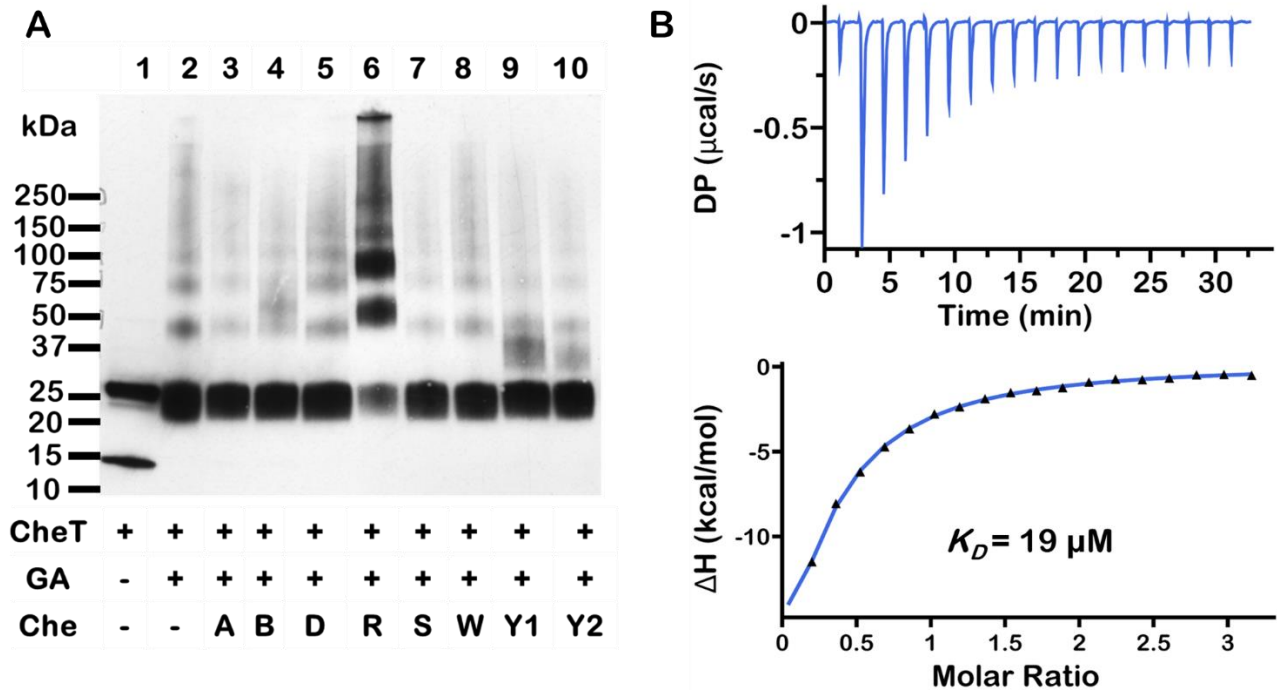


Fig. 3. 7 . Biochemical analyses to assess the binding of *S. meliloti* CheT and CheR.

A. Crosslinking studies of CheT ($0.7 \mu\text{M}$) with CheA, CheB, CheD, CheR, CheS, CheW1, CheY1, and CheY2 ($0.7 \mu\text{M}$) using glutaraldehyde (GA) for 45 min at room temperature. Products were separated by gradient gel electrophoresis and probed with an anti-CheT antibody. B. Isothermal titration calorimetry of recombinant CheR ($30 \mu\text{M}$) and CheT ($500 \mu\text{M}$). The upper panel shows the raw titration data while the lower panel depicts integrated raw data to obtain a K_D of $19 \mu\text{M}$. K_D generated from the normalized and dilution corrected integrated peak areas of the raw titration data.

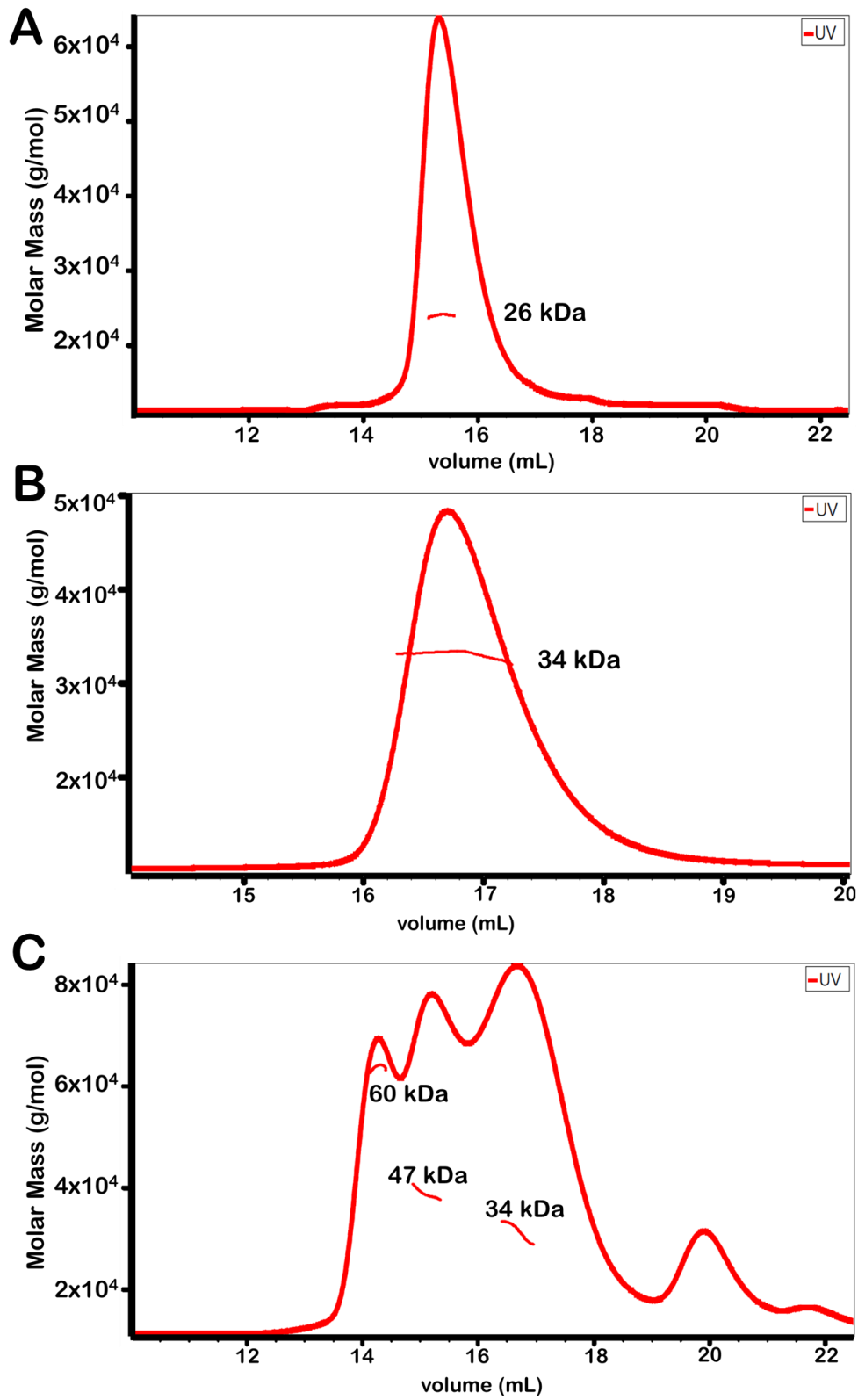


Fig. 3. 8 SEC-MALS analysis of CheT, CheR, CheT/CheR mixture and CheY1.

Molar masses were calculated using measurements taken from the UV detector, laser monitor correction modes, and RI (refractive index) signals as a function of elution volume. The molar mass measurement of 10,000 g/mol represents 10 kDa. A. CheT (13.4 kDa) elutes as dimer at approximately 26 kDa. B. CheR (34 kDa) elutes as monomer. C. Analysis of a CheR and CheT (1:1 molar ratio) mixture incubated for 30 minutes prior to loading on the column generated three significant peaks that presumably represent CheR (34 kDa), two heterodimers composed of a CheT dimer and a CheR monomer (47 kDa), and a CheT dimer and a CheR monomer (60 kDa), respectively.

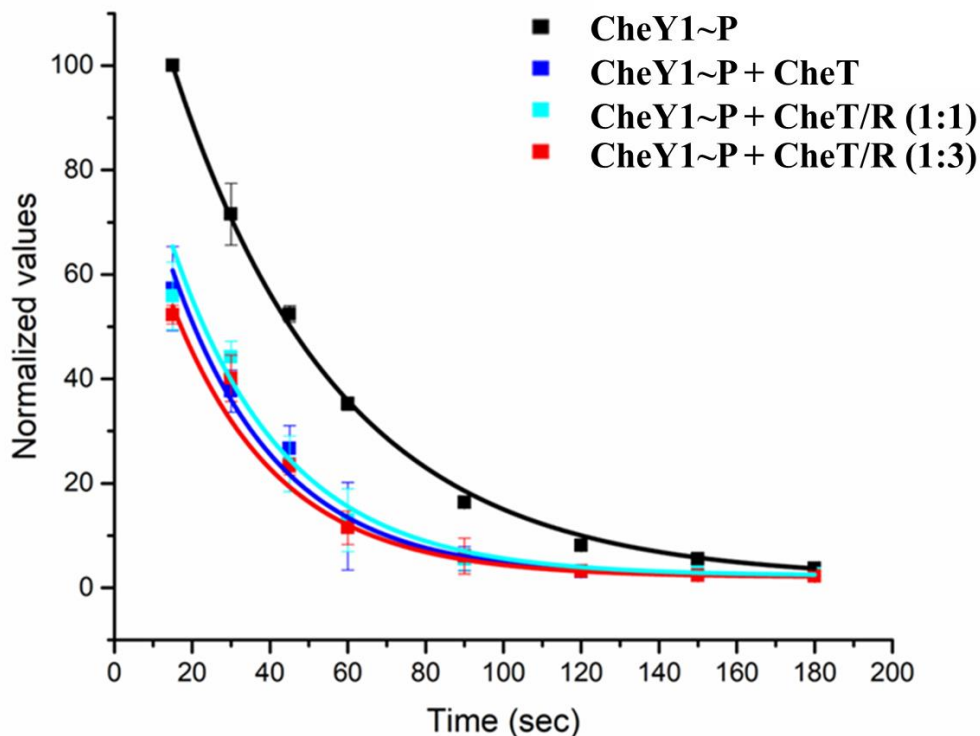


Fig. 3. 9 Kinetics of CheY1~P dephosphorylation in the presence of CheT and CheR in molar ratios of 1:1 and 1:3.

Data points are the means from three replicates measurements of CheY1~P pixel intensity and error bars reflect standard deviation determined with using Amersham Typhoon image analyzer software.

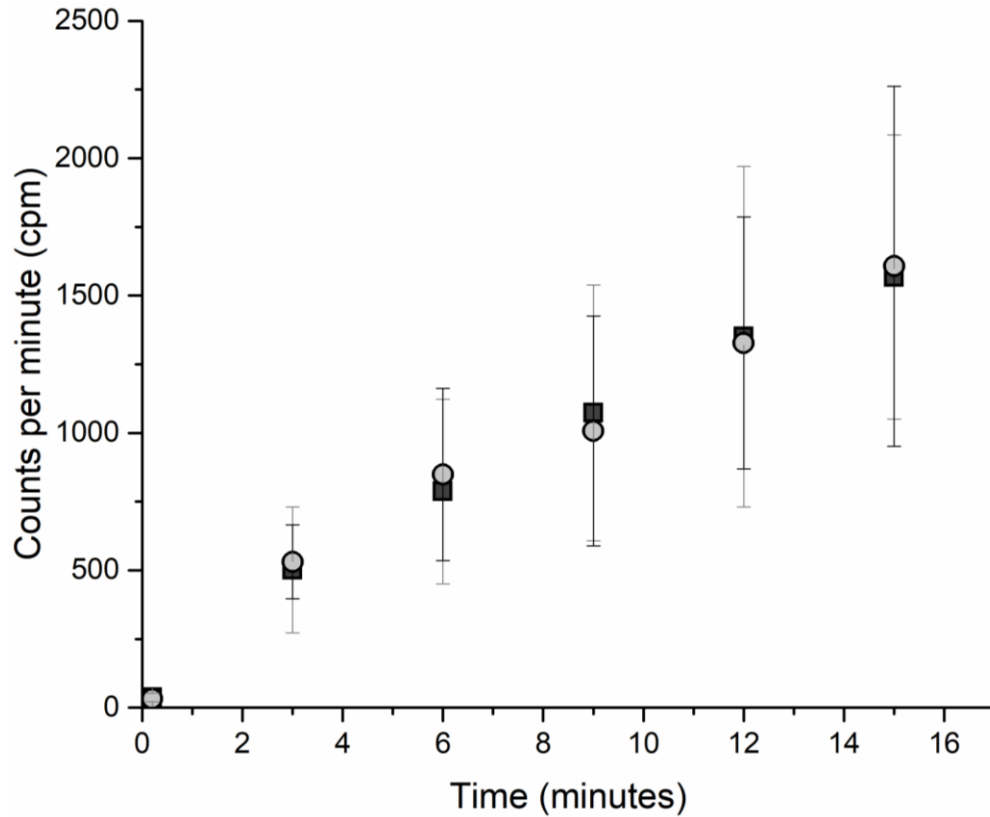


Fig. 3. 10 Time course of McpX methylation by CheR using [^3H]-S-adenosylmethionine (SAM[^3H]) as substrate.

Reactions of 1.2 μM McpX in membrane vesicles with 0.2 μM CheR and 50 μM SAM were incubated for 0.2, 3, 6, 9, 12, 15 min at room temperature and stopped by incubation at 100 $^\circ\text{C}$ in the presence of Laemmli buffer. Black squares and grey circles represent signals represent the mean derived from three replicates in the absence and presence of 4.6 μM CheT, respectively, error bars derived from the standard deviation of three replicates.

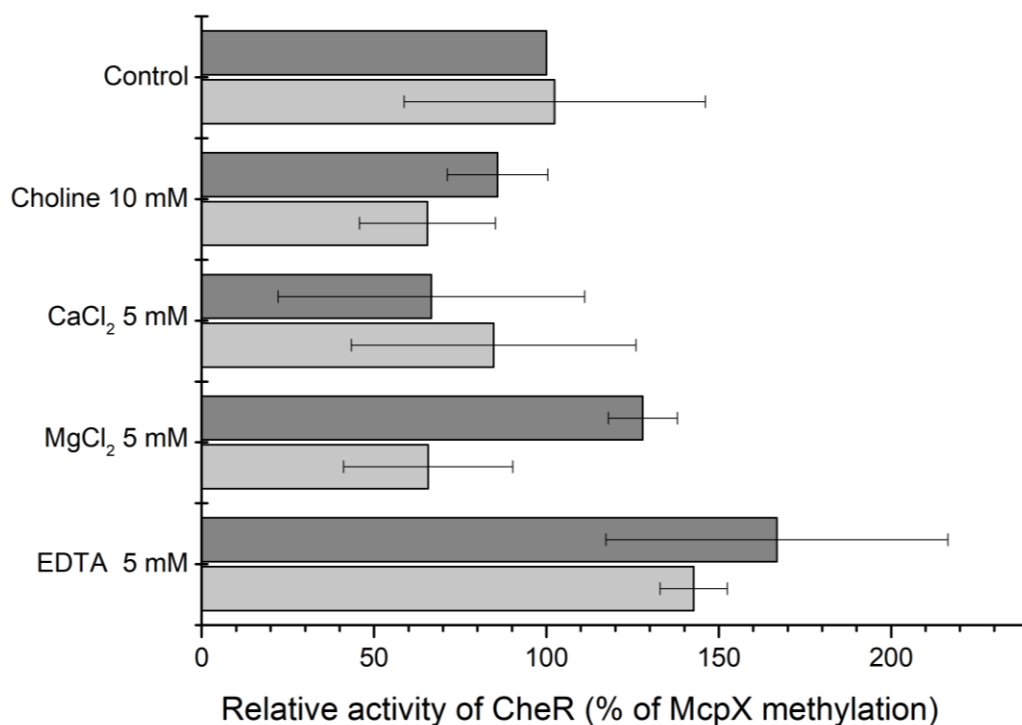


Fig. 3. 11 McpX methylation by CheR using [³H]-S-adenosylmethionine (SAM[³H]) as substrate with various supplements.

Reactions of 1.2 μM McpX in membrane vesicles with 0.2 μM CheR and 50 μM SAM[³H] were incubated for 15 min at room temperature and stopped by incubation at 100 °C in the presence of Laemmli buffer. All reactions were performed in TGD buffer with the specified additive for each condition. Dark and light grey bars represent the mean derived from three replicates in the absence and presence of 4.6 μM CheT.

Supplementary Figures

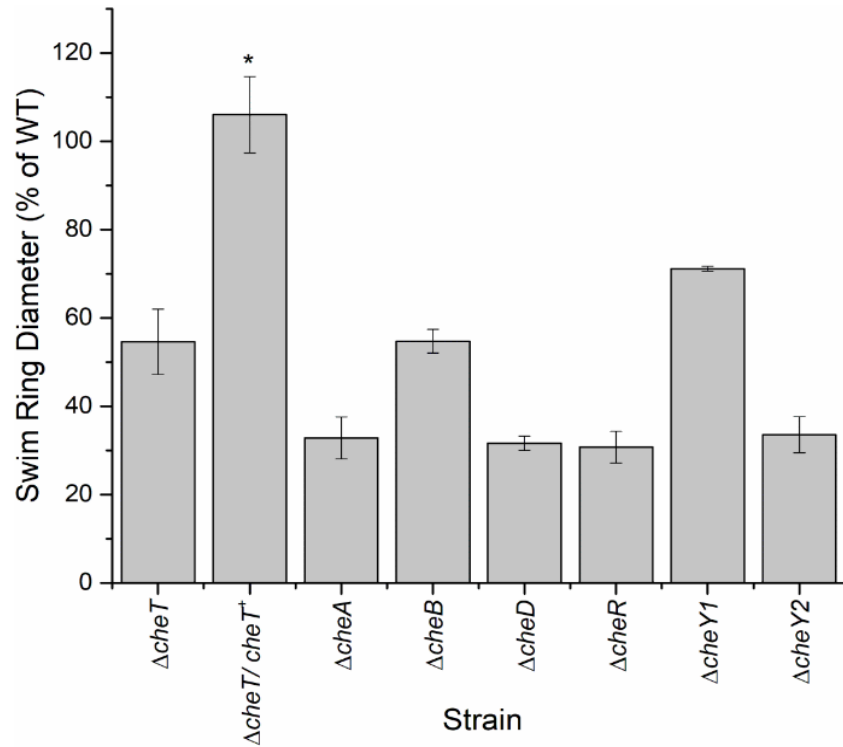


Fig. S1. Chemotactic responses of various *S. meliloti che* mutant strains in a quantitative swim plate assay compared to the wild-type strain (RU11/001). Strain designation: $\Delta cheT$, in-frame deletion of *cheT* (RU11/319), $\Delta cheT/cheT^+$, in-frame deletion of *cheT* (RU11/319) with pBBR1MCS-2-*cheT* (pBS445); $\Delta cheA$, in-frame deletion of *cheA* (RU11/310); $\Delta cheB$, in-frame deletion of *cheB* (RU11/312); $\Delta cheD$, in-frame deletion of *cheD* (RU11/411); $\Delta cheR$, in-frame deletion of *cheR* (RU11/306); $\Delta cheY1$, in frame deletion of *CheY1* (RU11/308); $\Delta cheY2$ in frame deletion of *cheY2* (RU11/307). Percentages of the wild-type swim diameter on 0.3% Bromfield agar are the means of seven replicates. Error bars represent the standard deviations from the mean. Statistical significance was determined by a two-tailed Student's T-test ($p < 0.05$). The asterisk symbol denotes no statistically significant difference from the wild type.

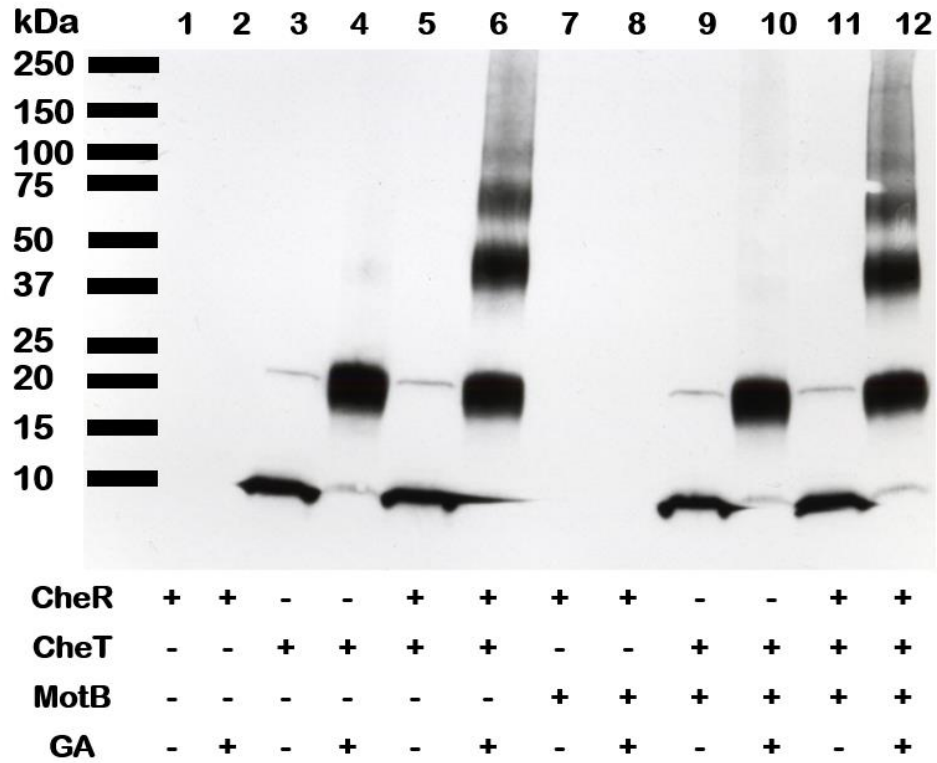


Fig. S2. Analysis of CheT and CheR binding with *S. meliloti* motor protein MotB. Crosslinking studies of *S. meliloti* CheT (0.7 μ M), CheR (0.7 μ M) and MotB (0.7 μ M) with glutaraldehyde (GA) for 45 min. Products were separated on a 4-20 % Criterion TGX gradient gel (Biorad) and probed with an anti-CheT antibody.

REFERENCES

1. Erhardt, M., 2016. Strategies to block bacterial pathogenesis by interference with motility and chemotaxis. How to overcome the antibiotic crisis: facts, challenges, technologies and future perspectives, 185-205.
2. Berg, H.C., 1993. Random walks in biology. Princeton University Press.
3. Wadhams, G.H. and Armitage, J.P., 2004. Making sense of it all: bacterial chemotaxis. *Nat Rev Mol Cell Biol*, 5(12): 1024-1037.
4. Porter, S.L., Wadhams, G.H., and Armitage, J.P., 2011. Signal processing in complex chemotaxis pathways. *Nat Rev Microbiol*. 9(3): 153-165.
5. Sourjik, V. and Wingreen, N.S., 2012. Responding to chemical gradients: bacterial chemotaxis. *Curr Opin Cell Biol*, 24(2): 262-268.
6. Yang, W. and Briegel, A., 2020. Diversity of bacterial chemosensory arrays. *Trends Microbiol*, 28(1): 68-80.
7. Briegel, A., Ladinsky, M.S., Oikonomou, C., Jones, C.W., Harris, M.J., Fowler, D.J., Chang, Y.W., Thompson, L.K., Armitage, J.P. and Jensen, G.J., 2014. Structure of bacterial cytoplasmic chemoreceptor arrays and implications for chemotactic signaling. *Elife*, 3, e02151.
8. Parkinson, J.S., Ames, P., and Studdert, C.A., 2005. Collaborative signaling by bacterial chemoreceptors. *Current Opinion in Microbiology*, 8(2): 116-121.
9. Levit, M.N., Liu, Y., and Stock, J.B., 1999. Mechanism of CheA protein kinase activation in receptor signaling complexes. *Biochemistry*, 38(20): 6651-6658.
10. Borkovich, K.A., Kaplan, N., Hess, J.F. and Simon, M.I., 1989. Transmembrane signal transduction in bacterial chemotaxis involves ligand-dependent activation of phosphate group transfer. *Proceedings of the National Academy of Sciences*, 86(4), 1208-1212.
11. Lukat, G.S., Lee, B.H., Mottonen, J.M., Stock, A.M. and Stock, J.B., 1991. Roles of the highly conserved aspartate and lysine residues in the response regulator of bacterial chemotaxis. *Journal of Biological Chemistry*, 266(13), 8348-8354.
12. Welch, M., Oosawa, K., Aizawa, S.L. and Eisenbach, M., 1993. Phosphorylation-dependent binding of a signal molecule to the flagellar switch of bacteria. *Proceedings of the National Academy of Sciences*, 90(19), 8787-8791.
13. Vladimirov, N. and Sourjik, V., 2009. Chemotaxis: how bacteria use memory. *Biol Chem*, 390(11): 1097-104.
14. Tu, Y., 2013. Quantitative modeling of bacterial chemotaxis: signal amplification and accurate adaptation. *Annual Review of Biophysics*, 42: 337-359.
15. Hazelbauer, G.L., Falke, J.J., and Parkinson, J.S., 2008. Bacterial chemoreceptors: high-performance signaling in networked arrays. *Trends Biochem Sci*, 33(1): 9-19.

16. Morgan, D.G., Baumgartner, J.W., and Hazelbauer, G.L., 1993. Proteins antigenically related to methyl-accepting chemotaxis proteins of *Escherichia coli* detected in a wide range of bacterial species. *J Bacteriol*, 175(1): 133-140.
17. Weis, R.M. and Koshland, D.E., 1988. Reversible receptor methylation is essential for normal chemotaxis of *Escherichia coli* in gradients of aspartic acid. *Proc Natl Acad Sci U S A*, 85(1): 83-87.
18. Hess, J.F., Oosawa, K., Kaplan, N., and Simon, M.I., 1988. Phosphorylation of three proteins in the signaling pathway of bacterial chemotaxis. *Cell*, 53(1), 79-87.
19. Lai, W.C., Barnakova, L.A., Barnakov, A.N. and Hazelbauer, G.L., 2006. Similarities and differences in interactions of the activity-enhancing chemoreceptor pentapeptide with the two enzymes of adaptational modification. *Journal of Bacteriology*, 188(15), 5646-5649.
20. Kehry, M.R., Bond, M.W., Hunkapiller, M.W. and Dahlquist, F.W., 1983. Enzymatic deamidation of methyl-accepting chemotaxis proteins in *Escherichia coli* catalyzed by the cheB gene product. *Proceedings of the National Academy of Sciences*, 80(12), 3599-3603.
21. Djordjevic, S., Goudreau, P.N., Xu, Q., Stock, A.M. and West, A.H., 1998. Structural basis for methylesterase CheB regulation by a phosphorylation-activated domain. *Proceedings of the National Academy of Sciences*, 95(4), 1381-1386.
22. Krembel, A., Colin, R. and Sourjik, V., 2015. Importance of multiple methylation sites in *Escherichia coli* chemotaxis. *PLoS One*, 10(12), e0145582.
23. Garrity, L.F. and Ordal, G.W., 1997. Activation of the CheA kinase by asparagine in *Bacillus subtilis* chemotaxis. *Microbiology*, 143(9): 2945-2951.
24. Bourret, R.B., Borkovich, K.A., and Simon, M.I., 1991. Signal transduction pathways involving protein phosphorylation in prokaryotes. *Annual Review of Biochemistry*, 60(1): 401-441.
25. Stock, J., Ninfa, A., and Stock, A., 1989. Protein phosphorylation and regulation of adaptive responses in bacteria. *Microbiological Reviews*, 53(4): 450-490.
26. Rao, C.V., Glekas, G.D., and Ordal, G.W., 2008. The three adaptation systems of *Bacillus subtilis* chemotaxis. *Trends in Microbiology*, 16(10): 480-487.
27. Kristich, C.J. and Ordal, G.W., 2002. *Bacillus subtilis* CheD is a chemoreceptor modification enzyme required for chemotaxis. *Journal of Biological Chemistry*, 277(28): 25356-25362.
28. Szurmant, H., Muff, T.J., and Ordal, G.W., 2004. *Bacillus subtilis* CheC and FliY are members of a novel class of CheY-P-hydrolyzing proteins in the chemotactic signal transduction cascade. *Journal of Biological Chemistry*, 279(21): 21787-21792.
29. Bischoff, D.S. and Ordal, G.W., 1992. Identification and characterization of FliY, a novel component of the *Bacillus subtilis* flagellar switch complex. *Molecular Microbiology*, 6(18): 2715-2723.

30. Rosario, M.L. and Ordal, G.W., 1996. CheC and CheD interact to regulate methylation of *Bacillus subtilis* methyl-accepting chemotaxis proteins. *Mol Microbiol*, 21(3): 511-518.
31. Rao, C.V., Glekas, G.D., and Ordal, G.W., 2008. The three adaptation systems of *Bacillus subtilis* chemotaxis. *Trends Microbiol*, 16(10): 480-7.
32. Glekas, G.D., Cates, J.R., Cohen, T.M., Rao, C.V. and Ordal, G.W., 2011. Site-specific methylation in *Bacillus subtilis* chemotaxis: effect of covalent modifications to the chemotaxis receptor McpB. *Microbiology*, 157, 56.
33. Walukiewicz, H.E., Tohidifar, P., Ordal, G.W. and Rao, C.V., 2014. Interactions among the three adaptation systems of *Bacillus subtilis* chemotaxis as revealed by an in vitro receptor-kinase assay. *Molecular Microbiology*, 93(6), 1104-1118.
34. Ashish, C., 2015. *Sinorhizobium meliloti* bacteria contributing to rehabilitate the toxic environment. *Journal of Bioremediation and Biodegradation*, 6(2).
35. Götz, R. and Schmitt, R., 1987. *Rhizobium meliloti* swims by unidirectional, intermittent rotation of right-handed flagellar helices. *Journal of Bacteriology*, 169(7): 3146-3150.
36. Meier, V.M., Muschler, P., and Scharf, B.E., 2007. Functional analysis of nine putative chemoreceptor proteins in *Sinorhizobium meliloti*. *Journal of Bacteriology*, 189(5): 1816-1826.
37. Baaziz, H., Compton, K.K., Hildreth, S.B., Helm, R.F. and Scharf, B.E., 2021. McpT, a broad-range carboxylate chemoreceptor in *Sinorhizobium meliloti*. *Journal of Bacteriology*, 203(17), 10-1128.
38. Compton, K.K., Hildreth, S.B., Helm, R.F. and Scharf, B.E., 2018. *Sinorhizobium meliloti* chemoreceptor McpV senses short-chain carboxylates via direct binding. *Journal of Bacteriology*, 200(23), 10-1128.
39. Webb, B.A., Compton, K.K., Del Campo, J.S.M., Taylor, D., Sobrado, P. and Scharf, B.E., 2017. *Sinorhizobium meliloti* chemotaxis to multiple amino acids is mediated by the chemoreceptor McpU. *Molecular Plant-Microbe Interactions*, 30(10), 770-777.
40. Webb, B.A., Karl Compton, K., Castañeda Saldaña, R., Arapov, T.D., Keith Ray, W., Helm, R.F., and Scharf, B.E., 2017. *Sinorhizobium meliloti* chemotaxis to quaternary ammonium compounds is mediated by the chemoreceptor McpX. *Molecular Microbiology*, 103(2), 333-346.
41. Miller, L.D., Russell, M.H. and Alexandre, G., 2009. Diversity in bacterial chemotactic responses and niche adaptation. *Advances in Applied Microbiology*, 66, 53-75.
42. Scharf, B.E. and R. Schmitt, 2002. Sensory transduction to the flagellar motor of *Sinorhizobium meliloti*. *J Mol Microbiol Biotechnol*, 4(3): 183-6.
43. Attmannspacher, U., Scharf, B., and Schmitt, R., 2005. Control of speed modulation (chemokinesis) in the unidirectional rotary motor of *Sinorhizobium meliloti*. *Mol Microbiol*, 56(3): 708-18.
44. Sourjik, V. and Schmitt, R., 1996. Different roles of CheY1 and CheY2 in the chemotaxis of *Rhizobium meliloti*. *Mol Microbiol*, 22(3): 427-36.

45. Riepl, H., Maurer, T., Kalbitzer, H.R., Meier, V.M., Haslbeck, M., Schmitt, R. and Scharf, B., 2008. Interaction of CheY2 and CheY2-P with the cognate CheA kinase in the chemosensory-signalling chain of *Sinorhizobium meliloti*. *Molecular Microbiology*, 69(6), 1373-1384.
46. Dogra, G., Purschke, F.G., Wagner, V., Haslbeck, M., Kriehuber, T., Hughes, J.G., Van Tassell, M.L., Gilbert, C., Niemeyer, M., Ray, W.K., and Helm, R.F., 2012. *Sinorhizobium meliloti* CheA complexed with CheS exhibits enhanced binding to CheY1, resulting in accelerated CheY1 dephosphorylation. *Journal of Bacteriology*, 194(5), 1075-1087.
47. Schmitt, R., 2002. *Sinorhizobial* chemotaxis: a departure from the enterobacterial paradigm. *Microbiology*, 148(3): 627-631.
48. Arapov, T.D., Saldaña, R.C., Sebastian, A.L., Ray, W.K., Helm, R.F. and Scharf, B.E., 2020. Cellular stoichiometry of chemotaxis proteins in *Sinorhizobium meliloti*. *Journal of Bacteriology*, 202(14), 10-1128.
49. Sourjik, V., Sterr, W., Platzer, J., Bos, I., Haslbeck, M. and Schmitt, R., 1998. Mapping of 41 chemotaxis, flagellar and motility genes to a single region of the *Sinorhizobium meliloti* chromosome. *Gene*, 223(1-2), 283-290.
50. Buchan, D.W. and Jones, D.T., 2019. The PSIPRED protein analysis workbench: 20 years on. *Nucleic Acids Res*, 47(W1): W402-W407.
51. Zhao, R., Collins, E.J., Bourret, R.B. and Silversmith, R.E., 2002. Structure and catalytic mechanism of the *E. coli* chemotaxis phosphatase CheZ. *Nature structural biology*, 9(8), 570-575.
52. Liu, X., Liu, W., Sun, Y., Xia, C., Elmerich, C. and Xie, Z., 2018. A cheZ-like gene in *Azorhizobium caulinodans* is a key gene in the control of chemotaxis and colonization of the host plant. *Applied and Environmental Microbiology*, 84(3), e01827-17.
53. Varadi, M. and Velankar, S., The impact of AlphaFold Protein Structure Database on the fields of life sciences. *Proteomics*, 2022: 2200128.
54. Sourjik, V. and Schmitt, R., 1996. Different roles of CheY1 and CheY2 in the chemotaxis of *Rhizobium meliloti*. *Molecular Microbiology*, 22(3), 427-436.
55. Blat, Y. and Eisenbach M., 1996. Mutants with Defective Phosphatase Activity Show No Phosphorylation-dependent Oligomerization of CheZ: The Phosphatase of Bacterial Chemotaxis. *Journal of Biological Chemistry*, 271(2): 1232-1236.
56. Blat, Y. and Eisenbach, M., 1996. Oligomerization of the Phosphatase CheZ Upon Interaction with the Phosphorylated Form of CheY: The Signal Protein of Bacterial Chemotaxis. *Journal of Biological Chemistry*, 271(2): 1226-1231.
57. Some, D., Amartely, H., Tsadok, A. and Lebendiker, M., 2019. Characterization of proteins by size-exclusion chromatography coupled to multi-angle light scattering (SEC-MALS). *JoVE (Journal of Visualized Experiments)*, (148), e59615.

58. Barnakov, A.N., Barnakova, L.A., and Hazelbauer, G.L., 1998. Comparison In Vitro of a high- and a low-abundance chemoreceptor of *Escherichia coli*: similar kinase activation but different methyl-accepting activities. *J Bacteriol*, 180(24): 6713-6718.
59. Webb, B.A., Compton, K., Castañeda Saldaña, R., Arapov, T.D., Keith Ray, W., Helm, R.F. and Scharf, B.E., 2017. *Sinorhizobium meliloti* chemotaxis to quaternary ammonium compounds is mediated by the chemoreceptor McpX. *Molecular microbiology*, 103(2), pp.333-346.
60. Shrestha, M., Compton, K.K., Mancl, J.M., Webb, B.A., Brown, A.M., Scharf, B.E. and Schubot, F.D., 2018. Structure of the sensory domain of McpX from *Sinorhizobium meliloti*, the first known bacterial chemotactic sensor for quaternary ammonium compounds. *Biochemical Journal*, 475(24), 3949-3962.
61. Spiro, P.A., Parkinson, J.S. and Othmer, H.G., 1997. A model of excitation and adaptation in bacterial chemotaxis. *Proceedings of the National Academy of Sciences*, 94(14), 7263-7268.
62. Yan, X.F., Xin, L., Yen, J.T., Zeng, Y., Jin, S., Cheang, Q.W., Fong, R.A.C.Y., Chiam, K.H., Liang, Z.X. and Gao, Y.G., 2018. Structural analyses unravel the molecular mechanism of cyclic di-GMP regulation of bacterial chemotaxis via a PilZ adaptor protein. *Journal of Biological Chemistry*, 293(1), 100-111.
63. Orr, M.W. and Lee, V.T., 2016. A PilZ domain protein for chemotaxis adds another layer to c-di-GMP-mediated regulation of flagellar motility. *Science signaling*, 9(450), fs16-fs16.
64. Sourjik, V. and Schmitt R., Phosphotransfer between CheA, CheY1, and CheY2 in the chemotaxis signal transduction chain of *Rhizobium meliloti*. *Biochemistry*, 1998. 37(8): 2327-2335.
65. Webb, B.A., Hildreth, S., Helm, R.F. and Scharf, B.E., 2014. *Sinorhizobium meliloti* chemoreceptor McpU mediates chemotaxis toward host plant exudates through direct proline sensing. *Applied and Environmental Microbiology*, 80(11), 3404-3415.
66. Compton, K.K., Hildreth, S.B., Helm, R.F. and Scharf, B.E., 2018. *Sinorhizobium meliloti* chemoreceptor McpV senses short-chain carboxylates via direct binding. *Journal of Bacteriology*, 200(23), 10-1128.
67. Simms, S.A., Stock, A.M., and Stock, J.B., 1987. Purification and characterization of the S-adenosylmethionine:glutamyl methyltransferase that modifies membrane chemoreceptor proteins in bacteria. *J Biol Chem*, 262(18): 8537-43.
68. Wu, J., Li, J., Li, G., Long, D.G. and Weis, R.M., 1996. The receptor binding site for the methyltransferase of bacterial chemotaxis is distinct from the sites of methylation. *Biochemistry*, 35(15), 4984-4993.
69. Meier, V.M., Muschler, P., and Scharf, B.E., 2007. Functional analysis of nine putative chemoreceptor proteins in *Sinorhizobium meliloti*. *J Bacteriol*, 189(5): 1816-1826.
70. Zatakia, H.M., Arapov, T.D., Meier, V.M. and Scharf, B.E., 2018. Cellular stoichiometry of methyl-accepting chemotaxis proteins in *Sinorhizobium meliloti*. *Journal of Bacteriology*, 200(6), 10-1128.

71. Perez, E. and Stock, A.M., 2007. Characterization of the *Thermotoga maritima* chemotaxis methylation system that lacks pentapeptide-dependent methyltransferase CheR:MCP tethering. *Mol Microbiol*, 63(2): 363-78.
72. Blat, Y. and Eisenbach, M., 1994. Phosphorylation-dependent binding of the chemotaxis signal molecule CheY to its phosphatase, CheZ. *Biochemistry*, 33(4): 902-906.
73. Schmitt, R.D., 2002. *Sinorhizobial* chemotaxis: a departure from the enterobacterial paradigm. *Microbiology*, 148(3): 627-631.
74. Dogra, G., Purschke, F.G., Wagner, V., Haslbeck, M., Kriehuber, T., Hughes, J.G., Van Tassell, M.L., Gilbert, C., Niemeyer, M., Ray, W.K. and Helm, R.F., 2012. *Sinorhizobium meliloti* CheA complexed with CheS exhibits enhanced binding to CheY1, resulting in accelerated CheY1 dephosphorylation. *Journal of Bacteriology*, 194(5), 1075-1087.
75. Amin, M., Kothamachu, V.B., Feliu, E., Scharf, B.E., Porter, S.L., and Soyer, O.S., 2014. Phosphate sink containing two-component signaling systems as tunable threshold devices. *PLoS computational biology*, 10(10), 1003890.
76. Chao, X., Muff, T.J., Park, S.Y., Zhang, S., Pollard, A.M., Ordal, G.W., Bilwes, A.M. and Crane, B.R., 2006. A receptor-modifying deamidase in complex with a signaling phosphatase reveals reciprocal regulation. *Cell*, 124(3), 561-571.
77. Muff, T.J. and Ordal, G.W., 2007. The CheC phosphatase regulates chemotactic adaptation through CheD. *Journal of Biological Chemistry*, 282(47): 34120-34128.
78. Krupski, G., Götz, R., Ober, K., Pleier, E., and Schmitt, R., 1985. Structure of complex flagellar filaments in *Rhizobium meliloti*. *Journal of Bacteriology*, 162(1), 361-366.
79. Sobe, R.C., Gilbert, C., Vo, L., Alexandre, G. and Scharf, B.E., 2022. FliL and its paralog MotF have distinct roles in the stator activity of the *Sinorhizobium meliloti* flagellar motor. *Molecular Microbiology*, 118(3), 223-243.
80. Pottash, A.E., McKay, R., Virgile, C.R., Ueda, H. and Bentley, W.E., 2017. TumbleScore: Run and tumble analysis for low frame-rate motility videos. *Biotechniques*, 62(1), 31-36.
81. Arapov, T.D., Saldaña, R.C., Sebastian, A.L., Ray, W.K., Helm, R.F. and Scharf, B.E., 2020. Cellular stoichiometry of chemotaxis proteins in *Sinorhizobium meliloti*. *Journal of Bacteriology*, 202(14), 10-1128.
82. Osborn, M. and Munson, R., 1974. Separation of the inner (cytoplasmic) and outer membranes of gram-negative bacteria. *Methods Enzymol*, Elsevier. 642-653.
83. Gegner, J.A., Graham, D.R., Roth, A.F. and Dahlquist, F.W., 1992. Assembly of an MCP receptor, CheW, and kinase CheA complex in the bacterial chemotaxis signal transduction pathway. *Cell*, 70(6), 975-982.
84. Simon, R., O'connell, M., Labes, M. and Pühler, A., 1986. Plasmid vectors for the genetic analysis and manipulation of rhizobia and other gram-negative bacteria. *Methods in Enzymology*, 118, 640-659.

85. Pleier, E. and Schmitt, R., 1991. Expression of two *Rhizobium meliloti* flagellin genes and their contribution to the complex filament structure. *J Bacteriol*, 173(6): 2077-85.
86. Kovach, M.E., Elzer, P.H., Hill, D.S., Robertson, G.T., Farris, M.A., Roop II, R.M. and Peterson, K.M., 1995. Four new derivatives of the broad-host-range cloning vector pBBR1MCS, carrying different antibiotic-resistance cassettes. *Gene*, 166(1), 175-176.
87. Schäfer, A., Tauch, A., Jäger, W., Kalinowski, J., Thierbach, G. and Pühler, A., 1994. Small mobilizable multi-purpose cloning vectors derived from the *Escherichia coli* plasmids pK18 and pK19: selection of defined deletions in the chromosome of *Corynebacterium glutamicum*. *Gene*, 145(1), 69-73.

Chapter 4— GENERAL DISCUSSION

The advent of the 20th century ushered in an era of extraordinary growth in the human population. This has been attributed to the advancement in modern medicine and sanitation leading to a steady decline in mortality rates [1] and the increase in agricultural output, marked by the “green revolution”. The “green revolution” enabled high yielding varieties of wheat, rice, and corn to be produced [2] and averted the expected mass starvation of humans but created unforeseen problems [3]. First, the human population doubled twice; from 1900 - 1957, and again by 1995. Current United Nations projections indicate that, the global population will increase to 9.6 billion people by 2050, and then peak at about 10.9 billion people by 2100 [4]. Meeting the dietary needs of such an unprecedented population boom has warranted encroachment into forests for more agricultural land and the extensive use of environmentally unfriendly fertilizers. Furthermore, rising incomes especially in the developed world and decline in global poverty has correlated with dietary shift to the consumption of more animal products like meat, eggs, and milk [5]. However, raising these animals for food is highly inefficient, as cattle and poultry need to consume 20 kg and 4.4 kg of plant nutrition to make 1 kg of edible protein, respectively [6]. Thus, it is estimated that greater than 50 % of arable land is used in rich nations for feeding livestock and 80 % of the world’s agricultural land is grazed by animals [4]. In summary, there is a case to be made that agriculture, as currently practiced, is massively unsustainable and is in discord with ensuring a secure food production and simultaneously living in a healthy environment.

Agriculture and food production contributes to at least a quarter of total global greenhouse gas emissions. The demands of feeding billions of people using nitrogen fertilizers deposits into the environment excesses that the natural ecosystems cannot handle. The surplus leach into water

systems and lead to eutrophication [7, 8]. Another consequence is nutrient runoffs into the ocean, which cause low-oxygen “dead zones” that destabilize aquatic life. [9].

Among the many solutions put forward by experts to make agricultural practices more environmentally friendly include reliance on biological nitrogen fixation, the use of biofertilizers, and the application of diazotrophs as seed inoculant to meet human and animal nutritional needs [10-12]. More importantly, the fixed nitrogen by legumes can be transferred to adjacent non-fixing crops by means of nitrogen transfer [13]. While agronomic use biofertilizers and bioinoculants is on the rise, major constraint persist that make their effect in field and lab conditions vary [14]. This includes limited knowledge in understanding the lifestyle of bacteria that culminate in biological nitrogen fixation in both symbiotic and free living diazotrophs. One critical behavior exhibited by symbiotic bacteria is the directed movement towards plant roots to initiate nodulation and nitrogen fixation via chemotaxis. For example, *Azorhizobium caulinodans* ORS571, a diazotroph that is a motile and chemotactically active rhizobial symbiont of *Sesbania rostrata*, has been implicated in the establishment of various plant-microbe associations [15]. Chemotaxis is also important for the competition of *Sinorhizobium meliloti* strains in nodulating the plant host [16]. Since alfalfa is the third most widely grown crop in the US, it has the potential of improving nitrogen content of soils when incorporated in crop rotation programs and is a great source of animal feed with minimal destruction to the environment [16]. Thus, the translational goal of this study is to understand the molecular underpinnings of *S. meliloti* chemotaxis to make bio-inoculants that establish thriving symbiotic relationships with the alfalfa host.

The enterobacterial model has served as the basis for understanding chemotaxis, however, it is increasingly becoming apparent that the niches occupied by different bacterial species over evolutionary time period has influenced differences in the metabolic requirements, motile

behavior, and chemotaxis [17-19]. Therefore, to meet our translational goal, there is a need for a holistic appreciation of the chemotaxis system in *S. meliloti*.

In chapter 2, we investigated the role of the C-terminal pentapeptides in *S. meliloti* chemoreceptors in chemotaxis [20, 21]. Other systems efficiently perform chemotaxis in the absence of pentapeptide-bearing chemoreceptors, while *E. coli* greatly depends on its high abundance pentapeptide-bearing receptors to mediate and assist adjacent chemoreceptors to achieve chemotaxis [22]. *S. meliloti* is unique in that most of its chemoreceptor population lacks the pentapeptide motif. Also, it was previously reported that domains in CheR responsible for binding the pentapeptide were absent in *S. meliloti* CheR [23]. Therefore, it was predicted that *S. meliloti* employs a pentapeptide-independent chemotaxis system. However, this study demonstrated that CheR binds to the pentapeptides of McpT, McpW, McpX, and McpY, which contribute to 13 % of the total chemoreceptor population [24]. While binding was not observed between CheB and the pentapeptides, activated CheB bound to these pentapeptides. The low number of pentapeptide-bearing receptors begs the question how *S. meliloti* achieves a sufficient number of CheR and CheB molecules for adaptation on all chemoreceptors. Cellular stoichiometries of *S. meliloti* chemotaxis proteins showed that a ratio of pentapeptide-bearing chemoreceptor monomers to CheR to CheB equals 1 : 3.8 : 1.6, which could provide sufficient tethering sites for the adaptation proteins [25]. We investigated the effects of fusing the linker and pentapeptide of McpX to McpU and McpV, receptors that naturally lack the pentapeptide and observed wild-type responses to the cognate ligands of McpU, McpV, and McpX, indicating that the pentapeptides mediate chemotaxis irrespective of the chemoreceptor type. It will be interesting to see whether mutants with an increased number of pentapeptide-bearing receptors can outperform the wild type in competition and nodulation assays. In addition, characterizing the composition of the chemosensory array will

be critical in understanding the basis of the differential chemotaxis responses in the McpT/W/Y-PP_{W-A} strain to glycine betaine and lysine. In conclusion, our work provides evidence that, although the pentapeptide motif occupies the last position on chemoreceptors, it is by no means the least in importance, as it is a potential site for engineering strains to enhance the *S. meliloti* chemotaxis system.

In chapter 3, the role of the chemotaxis protein CheT was determined as a phosphatase of the sink response regulator CheY1. This was particularly unexpected as the chemotaxis system in *S. meliloti* already employs retrophosphorylation from CheY2~P to CheA and the rapid spontaneous dephosphorylation of CheY1~P to dissipate phosphoryl groups in signal termination [26, 27]. Interestingly, CheT is not a redundant signal termination protein since deletion of *cheT* or mutations in the phosphatase motif affect swimming behavior of the mutant cells. This raises the question of what the need for a phosphatase enhancing-dephosphorylation of CheY1~P is. Since efficient chemotaxis depends on timely termination of the signal transduction pathway, mathematical models may shed more light on the purpose of a CheT-mediated dephosphorylation of CheY1~P. In the meantime, we have evidence that CheT has additional roles based on the phenotypic variation in phosphatase motif mutants and the *cheT* deletion mutant. Moreover, interaction of CheT with the adaptation protein CheR suggests a second function, which links signal termination and sensory adaptation. Although the methyltransferase and phosphatase activities of CheR and CheT are unaltered by the formation of this protein complex under examined conditions, both deletion mutants exhibit insensitivity to attractant stimulation in swim velocity assays. The role of this CheT/CheR interaction is not yet understood, however, ongoing research to characterize the residues required for CheT and CheR binding may provide these answers.

The chemotaxis system of *S. meliloti* mirrors *E. coli* in utilizing pentapeptide-dependent CheR and CheB proteins for chemotaxis [22, 28]. It also uses a protein with a CheZ-like DXXXQ motif to dephosphorylate a response regulator protein [29, 30]. Nevertheless, some deviations between the two bacteria species are notable. The C-terminal pentapeptides of *S. meliloti* chemoreceptors reside on low to moderately expressed chemoreceptors that make up only 13 % of MCP population but 93 % of the *E. coli* MCP population [24, 31]. As a consequence, the relatively high abundance of CheR and CheB proteins in *S. meliloti* may ensure that ample adaptation proteins are available at the receptor clusters. In addition, CheZ in *E. coli* is a phosphatase of CheY, the motor response regulator, while *S. meliloti* CheT is a phosphatase of the sink response regulator but not the flagellar motor response regulator. The phosphatase CheT binds to the adaptation protein CheR in *S. meliloti* and CheY1~P but CheZ only binds to CheY in *E. coli*.

Overall, this work has provided novel insight into the *S. meliloti* chemotaxis system that will be vital in creating robust bio-inoculants that can outcompete native strains to establish an effective symbiosis with their host plants to increase crop yields without compromising environmental sustainability.

REFERENCES

1. Kirk, D., 1996. Demographic transition theory. *Population studies*, 50(3): 361-387.
2. Tilman, D. and Clark, M., 2015. Food, agriculture & the environment: Can we feed the world & save the earth? *Daedalus*, 144(4): 8-23.
3. Ehrlich, P., 1968. *The Population Bomb* (New York: Ballantine). Friends of the Earth,
4. FAO, F., 2017. Agriculture Organization of the Nations. Food and Agriculture Organization of the United Nations Statistics Division (FAOSTAT).[En línea].
5. Drewnowski, A. and Popkin, B.M., 1997. The nutrition transition: new trends in the global diet. *Nutrition Reviews*, 55(2): 31-43.
6. Kearney, J., 2010. Food consumption trends and drivers. *Philosophical transactions of the royal society B: biological sciences*, 365(1554), 2793-2807.
7. Smith, K., McTaggart, I.P., and Tsuruta, H., 1997. Emissions of N₂O and NO associated with nitrogen fertilization in intensive agriculture, and the potential for mitigation. *Soil Use and Management*. 13: 296-304.
8. Carpenter, S.R., Caraco, N.F., Correll, D.L., Howarth, R.W., Sharpley, A.N. and Smith, V.H., 1998. Nonpoint pollution of surface waters with phosphorus and nitrogen. *Ecological Applications*, 8(3), 559-568.
9. Rabalais, N.N., Turner, R.E., and Wiseman Jr, W.J., 2002. Gulf of Mexico hypoxia, aka “The dead zone”. *Annual Review of Ecology and Systematics*, 33(1): 235-263.
10. Fatima, P., Mishra, A., Om, H., Saha, B. and Kumar, P., 2019. Free living nitrogen fixation and their response to agricultural crops. *Biofertilizers and Biopesticides in Sustainable Agriculture*, 173-200.
11. Nirala, R., Kumar, M., Kumar, R.R., Prasad, B.D., Pal, A.K., Kumar, V., Jha, V.K. and Ranjan, T., 2019. Symbiotic Nitrogen Fixation and Pulses Yield. In *Biofertilizers and Biopesticides in Sustainable Agriculture* CRC Press, 159-172.
12. Farrar, K., Bryant, D., and Cope-Selby, N, 2014. Understanding and engineering beneficial plant–microbe interactions: plant growth promotion in energy crops. *Plant Biotechnology Journal*. 12(9): 1193-1206.
13. Fustec, J., Lesuffleur, F., Mahieu, S. and Cliquet, J.B., 2010. Nitrogen rhizodeposition of legumes. A review. *Agronomy for Sustainable Development*, 30, 57-66.
14. Vandana, U.K., Chopra, A., Bhattacharjee, S. and Mazumder, P.B., 2017. Microbial biofertilizer: A potential tool for sustainable agriculture. *Microorganisms for Green Revolution: Volume 1: Microbes for Sustainable Crop Production*, 25-52.
15. Jiang, N., Liu, W., Li, Y., Wu, H., Zhang, Z., Alexandre, G., Elmerich, C. and Xie, Z., 2016. A chemotaxis receptor modulates nodulation during the *Azorhizobium caulinodans-Sesbania rostrata* symbiosis. *Applied and Environmental Microbiology*, 82(11), 3174-3184.
16. Caetano-Anollés, G., Wall, L.G., De Micheli, A.T., Macchi, E.M., Bauer, W.D. and Favelukes, G., 1988. Role of motility and chemotaxis in efficiency of nodulation by *Rhizobium meliloti*. *Plant physiology*, 86(4), 1228-1235.
17. Krell, T., Lacal, J., Muñoz-Martínez, F., Reyes-Darias, J.A., Cadirci, B.H., García-Fontana, C. and Ramos, J.L., 2011. Diversity at its best: bacterial taxis. *Environmental microbiology*, 13(5), 1115-1124..
18. Miller, L.D., Russell, M.H., and Alexandre, G., 2009. Diversity in bacterial chemotactic responses and niche adaptation. *Advances in Applied Microbiology*, 66: 53-75.
19. Colin, R., Ni, B., Laganenka, L. and Sourjik, V., 2021. Multiple functions of flagellar motility and chemotaxis in bacterial physiology. *FEMS Microbiology Reviews*, 45(6), fuab038.

20. Velando, F., Gavira, J.A., Rico-Jiménez, M., Matilla, M.A. and Krell, T., 2020. Evidence for pentapeptide-dependent and independent CheB methylesterases. *International Journal of Molecular Sciences*, 21(22), 8459.
21. Ortega, Á. and Krell, T., 2020. Chemoreceptors with C-terminal pentapeptides for CheR and CheB binding are abundant in bacteria that maintain host interactions. *Computational and Structural Biotechnology Journal*, 18, 1947-1955.
22. Li, M. and Hazelbauer, G.L., 2005. Adaptational assistance in clusters of bacterial chemoreceptors. *Molecular Microbiology*, 56(6): 1617-1626.
23. Perez, E. and Stock, A.M., 2007. Characterization of the *Thermotoga maritima* chemotaxis methylation system that lacks pentapeptide-dependent methyltransferase CheR: MCP tethering. *Molecular Microbiology*, 63(2): 363-378.
24. Zatakia, H.M., Arapov, T.D., Meier, V.M. and Scharf, B.E., 2018. Cellular stoichiometry of methyl-accepting chemotaxis proteins in *Sinorhizobium meliloti*. *Journal of Bacteriology*, 200(6), 10-1128.
25. Arapov, T.D., Saldaña, R.C., Sebastian, A.L., Ray, W.K., Helm, R.F. and Scharf, B.E., 2020. Cellular stoichiometry of chemotaxis proteins in *Sinorhizobium meliloti*. *Journal of Bacteriology*, 202(14), 10-1128.
26. Sourjik, V. and Schmitt, R., 1996. Different roles of CheY1 and CheY2 in the chemotaxis of *Rhizobium meliloti*. *Molecular Microbiology*, 22(3): 427-436.
27. Sourjik, V. and Schmitt, R., 1998. Phosphotransfer between CheA, CheY1, and CheY2 in the chemotaxis signal transduction chain of *Rhizobium meliloti*. *Biochemistry*, 37(8): 2327-2335.
28. Yonekawa, H., Hayashi, H., and Parkinson, J., 1983. Requirement of the cheB function for sensory adaptation in *Escherichia coli*. *Journal of bacteriology*, 156(3): p. 1228-1235.
29. Zhao, R., Collins, E.J., Bourret, R.B. and Silversmith, R.E., 2002. Structure and catalytic mechanism of the *E. coli* chemotaxis phosphatase CheZ. *Nature Structural Biology*, 9(8), 570-575.
30. Silversmith, R.E., 2010. Auxiliary phosphatases in two-component signal transduction. *Current Opinion in Microbiology*, 13(2): 177-183.
31. Li, M. and Hazelbauer, G.L., 2004. Cellular stoichiometry of the components of the chemotaxis signaling complex. *Journal of Bacteriology*, 186(12): 3687-3694.